THE UNIVERSITY OF OKLAHOMA

GRADUATE COLLEGE

APPLICATION OF THE METHOD OF TIGHT BINDING TO THE ELECTRONIC STRUCTURE OF SOLIDS

A DISSERTATION

SUBMITTED TO THE GRADUATE FACULTY

in partial fulfillment of the requirements for the

degree of

DOCTOR OF PHILOSOPHY

BY

ROY C. CHANEY

Norman, Oklahoma

1970

APPLICATION OF THE METHOD OF TIGHT BINDING

TO THE ELECTRONIC STRUCTURE OF SOLIDS

APPROVED BY

Chun C. Lin

J. M. Canfield

Robert M. St. John

Sylvand Bergerson

Earl La Ron

DISSERTATION COMMITTEE

Acknowledgement

The author wishes to express his sincere appreciation to Professor Chun C. Lin for suggesting the problem and for aid and assistance in doing the research which is reported in this thesis.

The author would also like to thank Dr. Earl E. Lafon for much advice and assistance both in the theoretical and the computational aspects of the calculations.

The author is also appreciative to his father, Mr. Preston E. Chaney for much help in computational work.

The author is especially grateful to the Sun Oil Company for making their computor facilities available to him.

It is also a pleasure for the author to express his appreciation to his wife for her constant encouragement and aid.

Table of Contents

List of Tables

List of Illustrations

CHAPTER I

Crystal Lattice

This work is primarily concerned with the calculation of the energy band structure of lithium, sodium, silicon and lithium fluoride using the method of tight binding and with an extension of the method of tight binding to the calculation of the electronic structure of impurities. We will first consider the crystalline structure of each of these four solids.

The lithium and sodium atoms form body-centered cubic structures. The body-centered cubic lattice can be constructed by putting an atom at each of the four corners of a cube and putting an atom at the center of the cube. This cube repeats itself all over the crystal. A mathematical description of the location of the atoms in a body-centered cubic crystal can be made by defining the primitive translation vector,

$$\vec{R}_n = n_1 \vec{a}_1 + n_2 \vec{a}_2 + n_3 \vec{a}_3 , \qquad (1.1)$$

where n_1, n_2 and n_3 are integers,

$$\vec{a}_1 = \frac{a_o}{2} (-1, 1, 1)$$
$$\vec{a}_2 = \frac{a_o}{2} (1, -1, 1)$$
$$\vec{a}_3 = \frac{a_o}{2} (1, 1, -1)$$

and a_o is the lattice constant. By picking different values of n_1, n_2, and n_3, a different value of the primitive translation vector $\vec{R}_n$ will be generated which will give the location of another atom in the crystal. If all combinations of n_1, n_2, and n_3 are used, the entire crystal will be mapped out. It is convenient to imagine that we have divided the crystal into many small sections which repeat themselves as we move from point to point in the crystal. The parallelepiped defined by the vectors $\vec{a}_1$, $\vec{a}_2$, and $\vec{a}_3$ is one way of defining the primitive unit cell. If we have a function which is periodic throughout the crystal, we can obtain all of the information about this function by specifying its value inside the parallelepiped since we know that the function repeats itself for the same relative point in all other parallelepipeds in the crystal. An alternative choice of the primitive unit cell would be the Wigner-Seitz cell which is pictured in Fig. 1. It is generally used because it shows the rotational symmetry of the crystal.

Since the crystaline lattice has a periodic structure, it is many times useful to expand periodic functions (such as the crystal potential) in a Fourier expansion. If we have a periodic function $f(\vec{r})$, it can be expanded in a Fourier series as

$$f(\vec{r}) = \sum_{\nu} a_{\nu} e^{i\vec{K}_{\nu}\cdot\vec{r}} , \tag{1.2}$$

where a_ν is the Fourier coefficient. The vector $\vec{K}_\nu$ is defined such that

$$\vec{K}_{\nu}\cdot\vec{R}_n = 2p\pi , \tag{1.3}$$

I) Wigner Seitz cell for body-centered cubic lattice

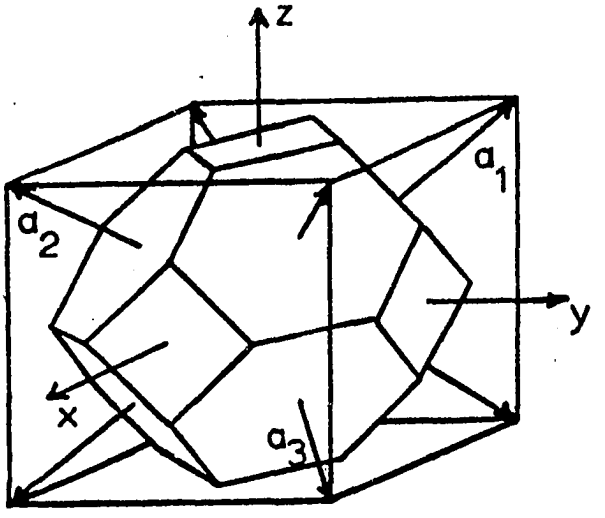

II) Brillouin zone for body-centered cubic lattice

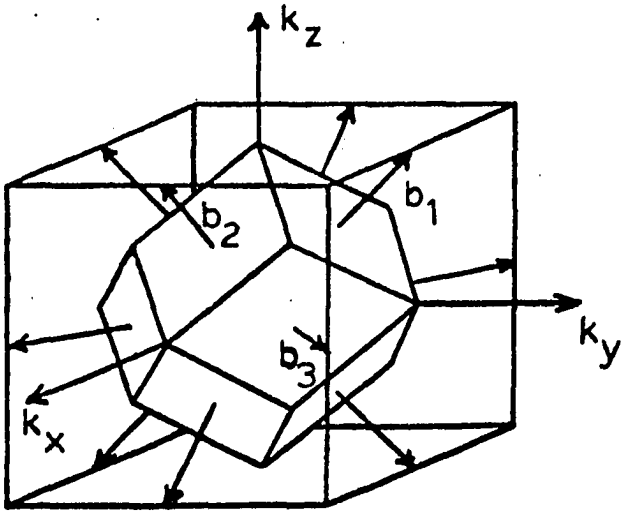

Figure 1. Unit cells for body-centered cubic crystals

where p is an integer which is dependent on $\vec{K}_\nu$ and $\vec{R}_n$. Just as the $\vec{R}_n$ vectors were defined in terms of the vectors $\vec{a}_1$, $\vec{a}_2$, and $\vec{a}_3$ the $\vec{K}_\nu$ vector can be defined in terms of the vectors $\vec{b}_1$, $\vec{b}_2$, and $\vec{b}_3$;

$$\vec{K}_\nu = m_1\vec{b}_1 + m_2\vec{b}_2 + m_3\vec{b}_3 , \tag{1.4}$$

where m_1, m_2, and m_3 are integers. The vectors $\vec{b}_1$, $\vec{b}_2$, and $\vec{b}_3$ can be defined in terms of $\vec{a}_1$, $\vec{a}_2$, and $\vec{a}_3$ as

$$\begin{aligned} \vec{b}_1 &= C[\vec{a}_2 \times \vec{a}_3] \\ \vec{b}_2 &= C[\vec{a}_3 \times \vec{a}_1] \\ \vec{b}_3 &= C[\vec{a}_1 \times \vec{a}_2] \end{aligned} \tag{1.5}$$

where $C = 2\pi/\{\vec{a}_1 \cdot [\vec{a}_2 \times \vec{a}_3]\}$. The three dimensional space defined by $\vec{b}_1$, $\vec{b}_2$, and $\vec{b}_3$ is known as reciprocal space. If we were to construct a Wigner-Seitz unit cell in this reciprocal space, it would have the shape shown in Fig. 1 for a body-centered cubic structure. The volume enclosed within this reciprocal space Wigner-Seitz cell is known as the first Brillouin zone, although many times the word first is dropped and it is called the Brillouin zone.

The silicon and lithium fluoride crystals can be constructed from two interpenetrating sublattices of face-centered cubic (f.c.c.) structure. Each lattice site of one sublattice is separated from the corresponding member of the other sublattice by a non-primitive translation $\vec{T}$($\vec{T} \neq \vec{R}_n$ for any n) directed along the body diagonal of the face centered cube of the first sublattice. The magnitude of $\vec{T}$ is

$\sqrt{3}\, a_o/4$ for the case of silicon and $\sqrt{3}\, a_o'/2$ for the case of lithium fluoride, where a_o and a_o' are the lattice constants of silicon and lithium fluoride respectively.

The face-centered cubic lattice can be constructed by placing atoms at each of the corners of a cube and by also placing atoms at the midpoint of each of the faces of the cube. This cube repeats itself all over the crystal. The location of the atoms in the crystal can be described mathematically by defining the vector $\vec{R}_n$ in terms of $\vec{a}_1$, $\vec{a}_2$, and $\vec{a}_3$ as was done in Eq. (1.1). However, for the case of a face-centered cubic lattice the vectors $\vec{a}_1$, $\vec{a}_2$, and $\vec{a}_3$ are defined as

$$\vec{a}_1 = \frac{a_o}{2}\,(1,\ 1,\ 0)$$
$$\vec{a}_2 = \frac{a_o}{2}\,(1,\ 0,\ 1)$$
$$\vec{a}_3 = \frac{a_o}{2}\,(0,\ 1,\ 1)\ .$$

The Wigner-Seitz cell can then be constructed as before and one finds that it has the shape shown in Fig. 2. The vectors $\vec{b}_1$, $\vec{b}_2$, and $\vec{b}_3$ can now be evaluated by using Eq. (1.5) and the Brillouin zone constructed for the face-centered cubic lattice. It has the form shown in Fig. 2.

Now that we have a physical and mathematical description of the crystal lattice for the b.c.c. (body-centered cubic) and f.c.c. (face-centered cubic) structures, we are ready to formulate the band-structure problem.

I) Wigner seitz cell for face-centered cubic lattice

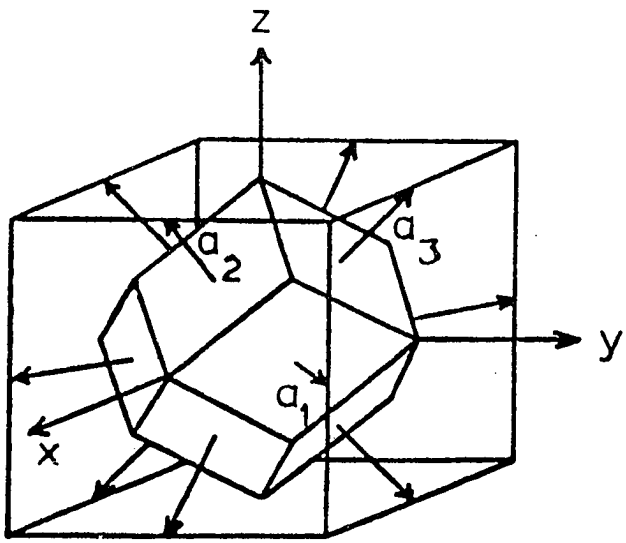

II) Brillouin zone for face-centered cubic lattice

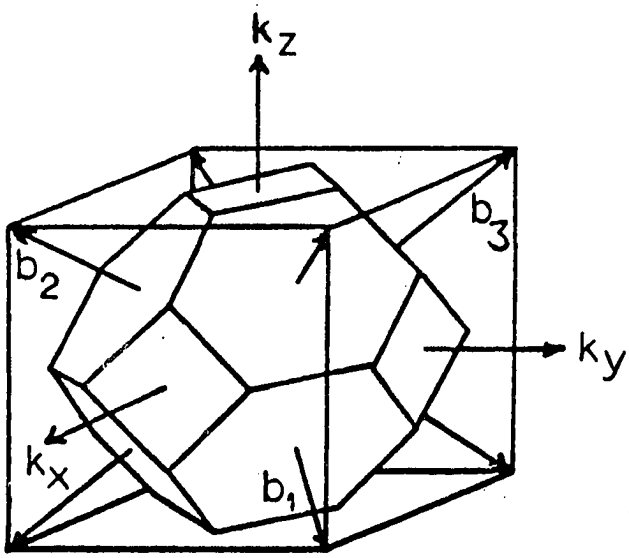

Figure 2. Unit cells for face-centered cubic crystals

CHAPTER II

Band-Structure Formulation

A brief description of the band-structure formulation is contained in the following chapter. For a more complete description see one of the publications listed under Ref. 1, 2 or 3.

Several approximations are generally made in the band-structure formulation in order to reduce the calculation of the electronic states in a crystal into a manageable form for solution on the computer. The first approximation is to assume that the nuclei are held fixed in the positions characteristic of a perfect crystal at absolute zero temperature and only consider the wavefunctions and energy levels of the electrons moving about these nuclei. Under this approximation the N-electron crystal Hamiltonian will have the form of

$$H = \sum_i \left(-\frac{\nabla_i^2}{2}\right) - \sum_i \sum_n \left(\frac{z_n}{|\vec{r}_i - \vec{R}_n|}\right) + \sum_i \sum_{j \neq i} \left(\frac{1}{|\vec{r}_i - \vec{r}_j|}\right) \quad (2.1)$$

where the i summation is over all of the electrons, the j summation is over all electrons in the crystal except for the i'th electron, $\vec{r}_i$ is a vector from the origin to the i'th electron, the n summation is over all of the nuclei in the crystal, $\vec{R}_n$ is a vector from the origin to the n'th nucleus, z_n is the charge on the n'th nucleus and the units of measure are atomic units. Under these approximations the

will become a function. Our one electron Hamiltonian can then be written as

$$H = -\tfrac{1}{2}\nabla^2 + V_{crys}(\vec{r}) \ , \qquad (2.5)$$

where we have used the notation $V_{crys}(\vec{r})$ to imply that $V_{crys}(\vec{r})$ is the effect upon the electron due to the rest of the crystal. The one-electron Hartree-Fock equation can be carried to self consistency by using the crystal wave function ψ which is obtained from the first calculation to generate a new potential $V_{crys}(\vec{r})$, performing a second calculation using this new potential and generating a new set of crystal wave functions ψ'. The alternate calculation of the wave function and the crystal potential can then be continued until there is little change in the crystal potential between successive calculations. However, one must have a starting potential for the initial calculation. Two different types of starting potentials will be used in this work: the muffin-tin potential and the overlapping atomic potential. The muffin-tin approximation consists of imagining that the Wigner-Seitz cell (which was described in chapter I) has been divided into two regions by a sphere which is centered about the atom. Within this inscribed sphere the spherically averaged crystal potential is used and outside of the inscribed sphere a constant value is used for the potential. Although this type of potential was chosen primarily for the simplification which it gives to certain methods of band structure calculation, there is some justification for using it for metals. Since the metal is a good conductor, one might expect the electrons to behave somewhat like free particles and not to be tightly bound to any one of the nuclei.

Putting the constant potential in the region outside of the inscribed sphere insures that the electrons behave as free particles in this region. The good agreement of the results using this potential with experiment bears out the adequacy of this model for application to metals. However, since the techniques which we used to perform band-structure calculations were not limited as to the choice of crystal potential, it seemed more physical to use a different type of potential for non-metals. For the non-metals we used the overlapping atomic potential model. This consists of approximating the crystal potential as a superposition of atomic potentials centered about each of the atomic sites in the crystal.

Assuming that we have chosen one of the two methods outlined above for calculating the crystal potential we must now decide on a one-electron crystal wave function to use in our calculation. Since the periodicity of the crystal and, therefore, the crystal Hamiltonian of the Hartree-Fock Slater equations has such a profound effect on the one-electron crystal wave function, it is instructive to examine this symmetry. The symmetry of a crystal can be defined by specifying the three primitive translational vectors $\vec{a}_1$, $\vec{a}_2$, and $\vec{a}_3$ and by defining the vector $\vec{R}_n$ which from Eq. (1.1) is:

$$\vec{R}_n = n_1 \vec{a}_1 + n_2 \vec{a}_2 + n_3 \vec{a}_3 ,$$

where n_1, n_2, n_3 are integers. The vector $\vec{R}_n$ for some value of n_1, n_2 and n_3 will take the radius vector $\vec{r}$ to any other equivalent point in the crystal. By equivalent point in the crystal we mean that the

Hamiltonian

$$H(\vec{r}) = H(\vec{r} + \vec{R}_n) \ . \tag{2.6}$$

If we were to define the translational operator T_n so that T_n operating on the general function $f(\vec{r})$ gives $f(\vec{r} + \vec{R}_n)$

$$T_n f(\vec{r}) = f(\vec{r} + \vec{R}_n) \ ,$$

we would see that there are two important properties to this translational operator. The first property is that it commutes with the Hamiltonian. This can be proven by the following equation

$$T_n \ H(\vec{r}) \ \psi(\vec{r}) = H(\vec{r} + \vec{R}_n) \ T_n \psi(\vec{r}) = H(\vec{r}) \ T_n \psi(\vec{r}) \ .$$

The second property is due to the fact that successive translations can be carried out in any order. It says that the T_n operator commutes with itself, i.e.

$$T_n T_{n'} f(\vec{r}) = T_n f(\vec{r} + \vec{R}_{n'}) = f(\vec{r} + \vec{R}_{n'} + \vec{R}_n)$$

$$= f(\vec{r} + \vec{R}_n + \vec{R}_{n'}) = T_{n'} f(\vec{r} + \vec{R}_n)$$

$$= T_{n'} T_n \ f(\vec{r}) \ .$$

However, there is a theorem in quantum mechanics which states that if more than one operator commutes with the Hamiltonian and they all commute with each other, that we can simultaneously diagonalize the Hamiltonian and the operators. Thus, we can set up solutions to

Schrodinger's equation which diagonalize all of these operators; that is, solutions such that when we increase the radius vector by $n_1\vec{a}_1 + n_2\vec{a}_2 + n_3\vec{a}_3$ we multiply the solution by a constant.

Since the original and the transformed wave functions must both be normalized, the absolute value of this constant must be unity. We can, therefore, find a real vector $\vec{k}$ such that the constant by which the wave function is multiplied when we make the translation $\vec{a}_1$ is $\exp(i\vec{k}\cdot\vec{a}_1)$; if we make the translation $\vec{a}_2$ the constant is $\exp(i\vec{k}\cdot\vec{a}_2)$; and for the translation $\vec{a}_3$ the constant is $\exp(i\vec{k}\cdot\vec{a}_3)$. Then if we make the translation $\vec{R}_n$, we multiply the wave function by the factor $\exp(i\vec{k}\cdot\vec{R}_n)$. In this case if the wave function is $\psi(r)$ then the quantity $\psi(r)e^{-i\vec{k}\cdot\vec{r}}$ must be unchanged when we make the translation $\vec{R}_n$ or must be a periodic function of $\vec{r}$ repeating its value in each unit cell. We then have the result

$$\psi_{\vec{k}}(\vec{r}) = u(\vec{r}) \exp(i\vec{k}\cdot\vec{r}) , \tag{2.7}$$

where $u(\vec{r})$ is a periodic function of $\vec{r}$ such that

$$u(\vec{r} + \vec{R}_n) = u(\vec{r}) .$$

This requirement on the functional form of the wave function is known as the Bloch theorem. Another important consequence of the Bloch theorem is that there are no matrix elements connecting the wave functions $(\psi_{\vec{k}}(\vec{r}))$ with different values of $\vec{k}$. The proof of this is a direct consequence of the fact that the Hamiltonian and translational operators commute. We see, therefore, that our infinite secular equation has been reduced into block structure (a single block for each

distinct value of $\vec{k}$).

The development of each of the different methods which are used in band-structure calculations is essentially the same up to this point. The methods differ, however, in the choice of the periodic function $u(\vec{r})$. The method of tight binding (or the method of linear combinations of atomic orbitals) consists of approximating the one-electron crystal wave function as a superposition of atomic wave functions situated about each of the atomic sites. The crystal wave function then has the form of

$$\psi(\vec{r}) = \sum_{R_\nu} a_\nu \, \phi_{n\ell m}(\vec{r} - \vec{R}_\nu) \tag{2.8}$$

where the summation over R_ν implies a summation over all of the atomic sites in the crystal, and the $\phi_{n\ell m}$ is the free atomic wave function of the atoms which make up the crystal. In order to satisfy the Bloch theorem, however

$$a_\nu = e^{i\vec{k}\cdot\vec{R}_\nu}.$$

Therefore, the Bloch sum functions which we use in the method of tight binding are

$$b_{n\ell m}(\vec{k},\vec{r}) = \psi(\vec{r}) = [N\Omega_{n\ell m}(\vec{k})]^{-1/2} \sum_{R_\nu} e^{i\vec{k}\cdot\vec{R}_\nu} \phi_{n\ell m}(\vec{r} - \vec{R}_\nu) \, , \tag{2.9}$$

where N is the number of atoms in the crystal, $\Omega_{n\ell m}(\vec{k})$ is a normalization constant. We use the notation $b_{n\ell m}(\vec{k},\vec{r})$ to denote that this is a Bloch function constructed from atomic wave functions of the form $\phi_{n\ell m}$ and that k is a good quantum number (the secular equation has block structure as a function of $\vec{k}$) specifying the translational symmetry of

the one-electron wave function.

The use of these Bloch sum functions has been called the method of tight binding because it was previously thought that the construction of the crystal wave function from linear combinations of atomic orbitals could only be used when the crystal electrons were tightly bound to their respective nuclei. However, it has been recently shown in a previous calculation on lithium[4] and will be verified by our results on the lithium and sodium crystals that the method of tight binding even works for metalic crystals for which the electrons cannot be considered to be tightly bound to their nuclei. This point will be discussed further in chapters III and VI.

Another way of constructing the crystal wave function is to expand $u(\vec{r})$ in a Fourier series. Since $u(\vec{r})$ is a periodic function, a Fourier expansion can be determined which is also periodic and will adequately represent $u(\vec{r})$. That is to say that the Fourier expansion

$$u(\vec{r}) \approx \sum_{\vec{K}_h} F(\vec{K}_h) \exp (i\vec{K}_h \cdot \vec{r}) \tag{2.10}$$

can adequately represent $u(\vec{r})$ if enough terms are included in the expansion. This expansion is known as the plane wave expansion of the crystal wave function. The total wave function is:

$$\psi_{\vec{k}}(\vec{r}) = \sum_{\vec{K}_h} v(\vec{k} + \vec{K}_h) \exp \{i(\vec{k} + \vec{K}_h)\cdot\vec{r}\} , \tag{2.11}$$

where the $\vec{k}$ vector gives the translational symmetry and the coefficient $v(\vec{k} + \vec{K}_h)$ is determined from the solution to the secular equation.

There are, however, problems involved in making band structure calculations using this type of crystal wave function. They are concerned with the determination of where to truncate this infinite Fourier expansion. Since the size of the secular equation goes up linearly with the number of terms (plane waves) in the Fourier expansion, the addition of many terms makes the diagonalization of the secular equation increasingly more difficult. Metals can be expected to be the best case for an expansion of this sort. They are good conductors and their electrons can be expected to behave as free particles. Therefore, a free particle (plane wave) expansion should represent the crystal wave function adequately. It has been found, however, that even for a metalic crystal the number of plane waves required is prohibitively large. The difficulty seems to be that in the region near the nuclei of the atoms the crystal wave functions oscillate so rapidly that many plane waves are required to represent them. Several techniques have been used to improve the plane wave expansion in this region. (Notably the Augmented Plane-Wave and the Orthogonalized-Plane-Wave methods). However, one method of solution for the crystal problem might be to use combinations of Bloch functions and plane waves to describe the crystal wave function. This technique has been investigated for the case of silicon and it was found that though many plane waves were required to represent the crystal wave function, the number of terms was small enough to make band-structure calculations using this technique practical. Another difficulty involved in the plane wave expansion technique is in deciding when convergence has been obtained. There is no physical justification

for truncating the Fourier expansion at any particular point. The only test for convergence is to do the same calculation with more terms.

Now that we have decided upon the Hamiltonian and the basis functions we are ready to calculate the matrix elements. Since most of the results which are presented in the following chapters involve band-structure calculations which were made using the Bloch function basis set, we will present a detailed description of the calculation of the matrix elements which involve this basis set.

The Bloch functions are used as basis for the secular equation

$$\left|H_{n\ell m,\, n'\ell'm'}(\vec{k}) - E\, S_{n\ell m,\, n'\ell'm'}(\vec{k})\right| = 0 \ . \tag{2.12}$$

The matrix elements are composed of the overlap, kinetic energy and potential integrals;

$$\begin{aligned}
S_{i,j}(\vec{k}) &= \int b_i^*(\vec{k},\vec{r})\, b_j(\vec{k},\vec{r})\, d\tau \\
&= [\Omega_i(\vec{k})\, \Omega_j(\vec{k})]^{-\frac{1}{2}} \sum_\nu e^{i\vec{k}\cdot\vec{R}_\nu} \int \phi_i^*(\vec{r})\, \phi_j(\vec{r}-\vec{R}_\nu)\, d\tau \\
&= [\Omega_i(\vec{k})\, \Omega_j(\vec{k})]^{-\frac{1}{2}} \sum_\nu e^{i\vec{k}\cdot\vec{R}_\nu} \langle \phi_i(\vec{0}) |\, \phi_j(\vec{R}_\nu)\rangle \ , \\
T_{i,j}(\vec{k}) &= \int b_i^*(\vec{k},\vec{r})\, (-\tfrac{1}{2}\nabla^2)\, b_j(\vec{k},\vec{r})\, d\tau \\
&= [\Omega_i(\vec{k})\, \Omega_j(\vec{k})]^{-\frac{1}{2}} \sum_\nu e^{i\vec{k}\cdot\vec{R}_\nu} \langle \phi_i(\vec{0}) \,|-\tfrac{1}{2}\nabla^2|\, \phi_j(\vec{R}_\nu)\rangle \ , \\
V_{i,j}(\vec{k}) &= \int b_i^*(\vec{k},\vec{r})\, V_{crys}(\vec{r})\, b_j(\vec{k},\vec{r})\, d\tau \\
&= [\Omega_i(\vec{k})\, \Omega_j(\vec{k})]^{-\frac{1}{2}} \sum_\nu e^{i\vec{k}\cdot\vec{R}_\nu} \langle \phi_i(\vec{0}) \,|V_{crys}|\, \phi_j(\vec{R}_\nu)\rangle \ .
\end{aligned} \tag{2.13}$$

The overlap and kinetic energy integrals occur frequently in molecular physics and many efficient methods have been devised to calculate them. Following a procedure developed by Lafon and Lin[4] the potential integral is evaluated by first expanding the crystal potential in a Fourier series,

$$V_{crys}(\vec{r}) = \sum_{\nu} V(\vec{K}_{\nu}) \cos(\vec{K}_{\nu} \cdot \vec{r}_c) , \qquad (2.14)$$

where $\vec{r}_c = \vec{r} - \vec{c}$ and $\vec{c}$ is the coordinate system for the Fourier expansion. The potential integral between a wave function ϕ_i centered about the point A and a wave function ϕ_j centered about B would be

$$\langle \phi_i(\vec{A}) | V_{crys}(\vec{r}_c) | \phi_j(\vec{B}) \rangle = \sum_{\nu} V(\vec{K}_{\nu}) \langle \phi_i(\vec{A}) | \cos(\vec{K}_{\nu} \cdot \vec{r}_c) | \phi_j(B) \rangle , \qquad (2.15)$$

It was shown by Lafon and Lin that if the atomic Hartree-Fock functions ϕ_i were expressed in terms of Slater-type orbitals ($e^{-\alpha r}$), i.e.

$$\phi_{1s}(\vec{r}) = a_1 e^{-\alpha_1 r} + a_2 e^{-\alpha_2 r} ,$$

then the multicenter integrals for the overlap, kinetic and potential could be reduced to a single numerical integration. The form of the numerical integrals was tabulated in their paper[4] for all combinations of the 1s, 2s and 2p Slater-type orbitals. The form of the numerical integrals for the 3s, 3p, and 3d Slater-type orbitals ($3s(r^2 e^{-\alpha r})$, $3p_x(x r e^{-\alpha r})$, $3d_{xy}(xy e^{-\alpha r})$, and $3d_{x^2}$ $(x^2 e^{-\alpha r})$) are found in Appendix I.

It has recently been shown[5] that if the atomic Hartree-Fock functions ϕ_h were constructed in terms of Gaussian type orbitals ($e^{-\alpha r^2}$) instead of the Slater-type orbitals, that the numerical integration is no longer necessary as all of the integrals appearing in the energy matrix can be expressed analytically. This point will be investigated in Chapter VI.

Now that we have the necessary tools for doing a band structure calculation we are ready to apply these techniques to the crystals of sodium, silicon, lithium and lithium fluoride.

CHAPTER III

Band Structure of Sodium

The crystal potential was constructed for sodium using the muffin-tin model which was described in chapter II. Since the crystal is periodic, the potential can be expanded in a Fourier series as

$$V_{crys}(\vec{r}) = \sum_{\nu} V_{K_\nu} \cos(\vec{K}_\nu \cdot \vec{r}_A) \ , \tag{3.1}$$

where the potential is expanded about the coordinate system $\vec{A}$ so that $\vec{r}_c = \vec{r}_A$. Using the standard methods of Fourier analysis we obtained

$$V_{K_\nu} = 1/\Omega \int_{\substack{\text{unit} \\ \text{cell}}} V_{crys}(\vec{r}) \cos(\vec{K}_\nu \cdot \vec{r}_A) d\tau \ , \tag{3.2}$$

where Ω is the volume of the Wigner-Seitz cell and the integration is to be over this volume. The volume of the Wigner-Seitz cell for a body-centered cubic crystal of sodium is $a_o^3/2$ where a_o is the lattice constant.

As we said in chapter II, the muffin-tin potential consists of using a spherical average of the crystal potential within an inscribed sphere about each of the lattice sites and using a constant value between the inscribed spheres.

We, therefore, approximate the crystal potential as

$$V_{crys}(\vec{r}) = \begin{cases} V(r) , & \text{inside the inscribed sphere,} \\ \overline{V} , & \text{between the inscribed sphere and the boundary of the Wigner-Seitz cell,} \end{cases}$$

where $V(r)$ is a spherical average of the crystal potential. If we write

$$V(r) = V'(r) + \overline{V} , \tag{3.3}$$

then the crystal potential can be split into two parts.

$$V'(\vec{r}) = \begin{cases} V(r) - \overline{V} , & \text{inside inscribed sphere,} \\ 0 , & \text{outside of inscribed sphere} \end{cases} \tag{3.4}$$

and

$\overline{V}$ - constant over the entire crystal.

Since the constant $\overline{V}$ will contribute only to the first Fourier coefficient ($\vec{K}_\nu = \frac{2\pi}{a_o}(0,0,0)$), we know that:

$$V_{\vec{K}_\nu \neq \vec{0}} = 1/\Omega \int_{\text{unit cell}} V'(r_A) \cos(\vec{K}_\nu \cdot \vec{r}_A) \, d\tau$$

$$= 1/\Omega \int_{\text{inscribed sphere}} V'(r_A) \cos(\vec{K}_\nu \cdot \vec{r}_A) \, d\tau ,$$

and

$$V_{\vec{K}_\nu = \vec{0}} = 1/\Omega \int_{\text{inscribed sphere}} V'(r_A) \, d\tau + \overline{V}. \tag{3.5}$$

However, before we can evaluate the integrals necessary for the Fourier expansion we must choose the potential to use within the inscribed sphere, the value of the lattice constant (a_o) and the value of $\overline{V}$ to use outside of the inscribed sphere. We used the Prokofjew[6] potential within the inscribed sphere and used a lattice constant of $a_o = 8.0426$ so that a direct comparison could be made with the composite wave work done by Schlosser and Marcus.[7] The average value of the Prokofjew potential in the region between the inscribed sphere and the boundary of the Wigner-Seitz cell was used as $\overline{V}$. In order to simplify the calculation of this average value ($\overline{V}$), we replaced the cell boundary by the boundary of a sphere of equivalent volume to the Wigner-Seitz cell. We obtained a value of $\overline{V} = -0.2686$ from this calculation. A comparison of the Fourier coefficients which we obtained by the evaluation of Eqs. (3.5) with the ones obtained by Schlosser and Marcus can be found in Table 1.

We curve fit the tabulated Hartree-Fock wave functions of Fock and Petrashen[8] using Slater-type orbitals for the 1s, 2s, 2p, 3s, 3p states. The results were:

$$\phi_{1s} = 7.1801\, S_1 + 12.6244\, S_2 + 0.038007\, r\, S_3 ,$$

$$\phi_{2s} = -1.115789\, S_1 + 5.7947\, S_2 - 6.4714\, r\, S_3 - 1.47257\, r\, S_4 - 0.011826\, r^2\, S_5 + 0.00158\, r^2\, S_6 ,$$

$$\phi_{3s} = -0.2416\, S_1 + 1.04212\, S_2 - 1.19055\, r\, S_3 - 0.285416\, r\, S_4 + 0.0750607\, r^2\, S_5 + 0.034495\, r^2\, S_6 ,$$

TABLE 1

Comparison of the Fourier coefficients of the Muffin-tin Prokofjew crystal potential of sodium with the calculation by Schlosser and Marcus. (potential in a.u.)

$\frac{2\pi}{a_o}(k_x, k_y, k_z)$	Present work	Schlosser and Marcus
0, 0, 0	-0.47031578	-0.47031599
1, 1, 0	-0.12250513	-0.12390902
2, 0, 0	-0.08424625	-0.08309317
2, 1, 1	-0.06563751	-0.06487826
2, 2, 0	-0.05578553	-0.05578832
3, 1, 0	-0.04950802	-0.04989783
2, 2, 2	-0.04459968	-0.04498674
3, 2, 1[a.]	-0.04028545	-0.04467628
4, 0, 0	-0.03639228	-0.03634278
3, 3, 0	-0.03293990	-0.03273291
4, 1, 1	-0.03293990	-0.03273291
4, 2, 0	-0.02996401	-0.02970388
3, 3, 2	-0.02745908	-0.02723443
4, 2, 2	-0.02537612	-0.02523942
4, 3, 1	-0.02364001	-0.02360569
5, 1, 0	-0.02364001	-0.02360569
5, 2, 1	-0.02088968	-0.02099840
4, 4, 0	-0.01974441	-0.01987185
4, 3, 3	-0.01869423	-0.01880754
5, 3, 0	-0.01869423	-0.01880754

TABLE 1 Continued

a. A larger discrepancy was found between the two sets of Fourier coefficients for $\vec{K}_\nu = \frac{2\pi}{a_0}(3, 2, 1)$. We felt that our value was correct since it gave a smooth curve for $V(K_\nu)$ as a function of the magnitude of $|K_\nu|$.

$$\phi_{2p_x} = \times(7.1376\ S_1 - 5.2863\ S_2 + 0.14702\ S_3 + 4.44533\ S_4 + 14.0496\ S_7)\ ,$$

$$\phi_{3p_x} = \times(-1.85643\ S_1 + 2.0223\ S_2 + 0.72637\ S_3 - 0.56913\ S_4 + 0.026238\ r\ S_5 + 0.014757\ r\ S_6 - 2.37233\ S_7 + 0.019099\ r\ S_8)\ , \qquad (3.6)$$

where

$$S_i = \exp(-\rho_i r)$$

and ρ_1 to ρ_8 are respectively 13.1474, 9.71542, 3.90983, 2.60387, 1.25944, 0.75485, 5.49636, 0.541733. We determined the atomic wave function of the 3d state by the Hartree-Fock-Slater method and curve fit the radial part of it using linear combinations of S_5, S_6, S_7, and S_8. Using this radial function we generated the five 3d functions corresponding to the symmetries xy, yz, zx, x^2-y^2, r^2-3z^2. The coefficients were:

$$\phi_{3d_{xy}} = xy(0.071688\ S_5 - 0.075850\ S_6 + 0.091190\ S_7 + 0.052076\ S_8)\ . \qquad (3.7)$$

We then constructed the Bloch functions:

$$b_{ns}(\vec{k}, \vec{r}) = \{N\ \Omega_{ns}(\vec{k})\}^{-\frac{1}{2}} \sum_\nu e^{i\vec{k}\cdot\vec{R}_\nu}\ \phi_{ns}(\vec{r} - \vec{R}_\nu)$$

$$b_{np}(\vec{k}, \vec{r}) = i\{N\ \Omega_{np}(\vec{k})\}^{-\frac{1}{2}} \sum_\nu e^{i\vec{k}\cdot\vec{R}_\nu}\ \phi_{np}(\vec{r} - \vec{R}_\nu)$$

$$b_{3d}(\vec{k}, \vec{r}) = \{N\Omega_{3d}(\vec{k})\}^{-\frac{1}{2}} \sum_{\nu} e^{i\vec{k}\cdot\vec{R}_\nu} \phi_{3d}(\vec{r} - \vec{R}_\nu) \ . \tag{3.8}$$

We used this set of 14 basis functions b_{1s}, b_{2s}, b_{3s}, b_{2p_x}, b_{2p_y}, b_{2p_z} b_{3p_x}, b_{3p_y}, b_{3p_z}, $b_{3d_{xy}}$, $b_{3d_{yz}}$, $b_{3d_{zx}}$, $b_{3d_{(x^2-y^2)}}$, $b_{3d_{(r^2-3z^2)}}$ to set up the secular equation and solved it for several different values of $\vec{k}$. The results are contained in Table 2 along with a comparison of the results of Schlosser and Marcus.[7] The agreement can be seen to be quite good (within 0.01 a.u.) except at the Γ point ($\vec{k}$ = [0,0,0]) where the tight binding value is 0.015 a.u. above that of Schlosser and Marcus. For k = 0 the crystal wave function for this energy is made up of only Bloch sums of s type symmetry atomic orbitals. Therefore, since the only s type symmetry functions in our secular equation were Bloch sums of 1s, 2s, 3s atomic orbitals, we have only two degrees of freedom in performing the linear variation calculation. The lack of sufficient flexibility in the trial function may be responsible for the discrepancy of 0.015 a.u. at the Γ point. To pursue this point, we generated a Bloch sum from an s-type atomic function composed of Slater-type orbitals with the same weighting as in the Hartree-Fock-Slater 3d wave function, i.e.,

$$\Phi_s = r^2(0.071688\ S_5 - 0.075850\ S_6 + 0.091190\ S_7 + 0.052076\ S_8) \tag{3.9}$$

and included this Bloch sum along with the 1s-2s-3s basis to recalculate the Γ point energy. This gives -0.2974 a.u. which is only 0.0064 a.u. higher than the Schlosser and Marcus value. The good agreement between

TABLE 2

Comparison of the energy band structure of sodium using the method of tight binding and the method of composite waves (energy in atomic units).

$a_o k_x/2\pi$	Tight Binding without 3d	Tight Binding with 3d	Composite waves[a]
[0,0,0] Γ_1	-0.2886	-0.2886	-0.3038
[1,0,0] Δ_1			
0.2	-0.2805	-0.2829	-0.2908
0.5	-0.2127	-0.2133	-0.2240
0.8	-0.0951	-0.0992	-0.1052
0.9	-0.0401	-0.0534	-0.0561
1.0	-0.0033 H_{15}	-0.0097 H_{12}	-0.0099 H_{12}
[1,1,0] Σ_1			
0.1	-0.2867	-0.2884	-0.2973
0.3	-0.2337	-0.2354	-0.2461
0.5	-0.1474	-0.1474	-0.1472
[1,1,1] Λ_1			
0.1	-0.2833	-0.2866	-0.2941
0.3	-0.2063	-0.2074	-0.2178
0.5	-0.0754	-0.0775	-0.0773

[a]See Ref. 7.

the two methods indicates that the method of tight binding gives an adequate representation of the crystal wave function even for a metal for which the electrons are not tightly bound to their respective nuclei. It might be instructive to investigate the crystal wave function to see why the method of tight binding can give such good results. The crystal wave function for the Γ point $\vec{k} = [0,0,0]$ is plotted in Fig. 3. This figure shows that the crystal wave function is flat over a large portion of the graph. If we have one free sodium atom, the wave function tends to decrease exponentially. Apparently if one adds together the exponential decay of each of these wave functions at the proper sites, then they will overlap with each other in a manner to give a flat charge distribution. The free electron has a completely flat charge distribution so one can see that the crystal wave function constructed by the method of tight binding automatically has free electron characteristics. This is the reason why it can give good values for the energy band structure of metals.

We have repeated the tight-binding calculation using only the 1s, 2s, 2p, 3s, 3p Bloch functions in the secular equations. The effect of removing the 3d Bloch functions from the secular equation is also given in Table 2. The effects of the 3d orbitals are most noticeable near the H point, $\vec{k} = \frac{2\pi}{a_o}[1,0,0]$. The Δ_1 band curve terminates at H_{12} which has the symmetry of d-type orbitals. If the 3d Bloch sums were omitted from the basis set, it is no longer possible to produce a crystal wave function of H_{12} symmetry, thus the Δ_1 line joins to H_{15} (p-type symmetry) at the H point. Aside from the H point

Figure 3. Crystal wavefunction and Bloch Sums at the Γ point of sodium along the [100] line of the crystal. The solid line is the crystal wavefunction, and the 3s and 4s Bloch sums are presented by uniform dashes and long-short dashes respectively

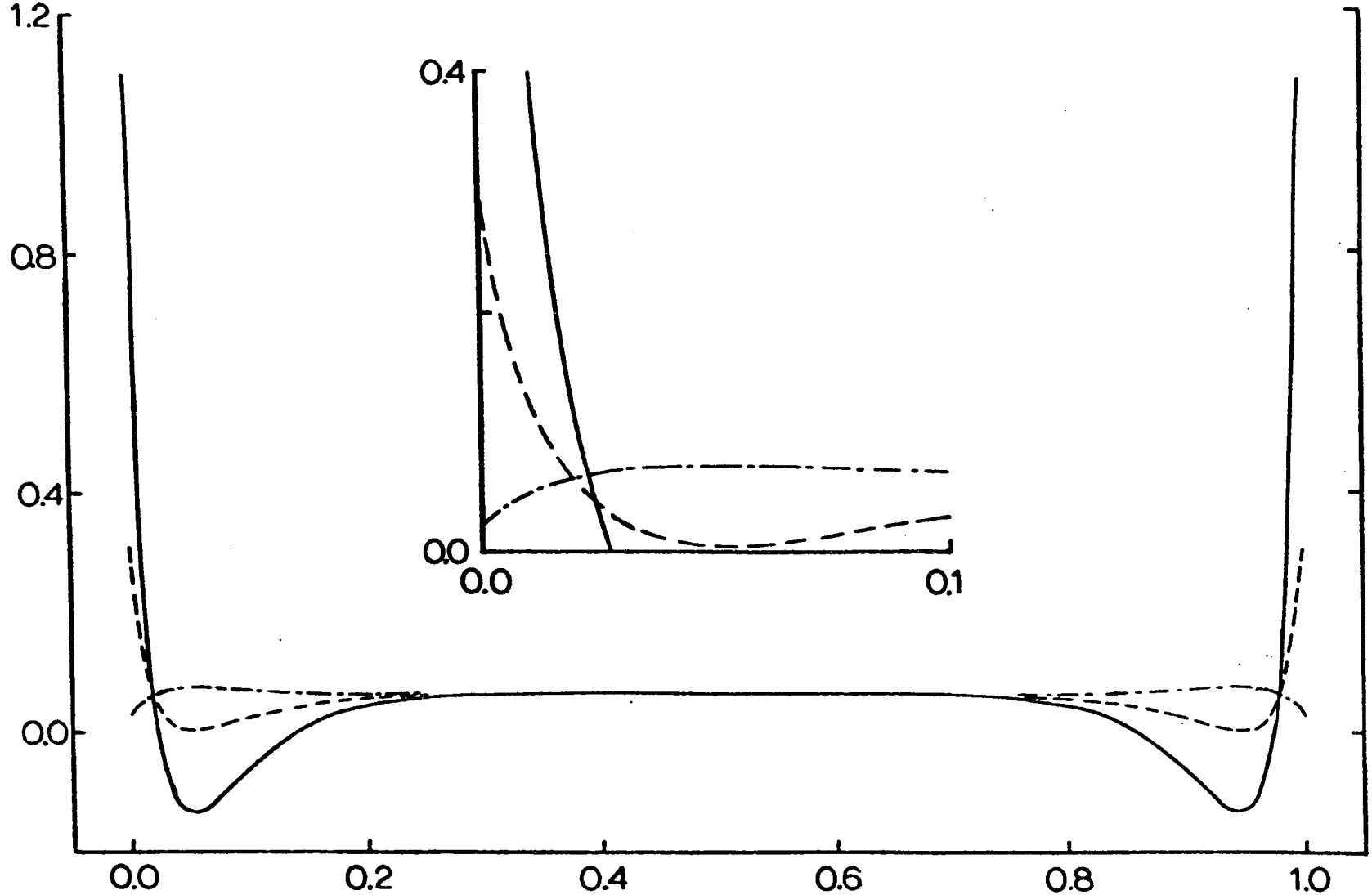

the conduction band energies calculated by the 1s, 2s, 2p, 3s, 3p basis set do not differ significantly from those using the more extended set.

Another point which needs to be cleared up is the question of convergence. That is to say, can we expect the Bloch functions for the atomic states up to n = 3 to give the secular equation enough variational freedom to give good values for the energy bands. To investigate this point we plotted a Bloch function which was constructed from a 4s sodium atomic orbital. The graph in Fig. 3 shows the 4s Bloch function plotted in comparison with the 3s Bloch function for $\vec{k}$=[0,0,0]. The normalized Bloch function is found to be virtually identical to the 3s function at all points except the region near the sodium nuclei. This region is represented adequately by the inclusion of the 1s and 2s Bloch functions. This shows that the inclusion of the 4s orbital in the basis set would not introduce any more variational freedom and would leave the energy practically unchanged.

Since the method of tight binding gives quantitative energy bands for the metals, it can be expected to give even better results for a non-conductor. We have, therefore, extended the method to the case of the silicon crystal.

CHAPTER IV

Band Structure of Silicon

The silicon lattice can be thought of as being constructed from two interpenetrating sublattices of face-centered cubic (fcc) structure which we will designate as sublattices 1 and 2. Each lattice site of the second sublattice is separated from the corresponding member of the first by a non-primitive translation $\vec{T}$ directed along the body diagonal of the face-centered cube of the first sublattice and of magnitude $\sqrt{3}\, a_o/4$ where a_o is the lattice constant of the sublattice. We will place the origin of our coordinate system at a point midway between these sublattices and with axes parallel to the edges of the face-centered cubes. The Wigner-Seitz cell situated about this origin has a volume $\Omega = (1/4)a_o^3$ and contains two atoms at locations given by

$$\vec{t}_1 = -\tfrac{1}{2}\vec{T} = -\frac{1}{8}\, a_o\, (1,1,1) = -\vec{t}_2 \qquad (4.1)$$

for sublattices 1 and 2 respectively. The atoms in the adjacent cells are given by $\vec{R}_\nu \pm \tfrac{1}{2}\vec{T}$ respectively. The overlapping atomic potential model[9] was used as the starting potential in this particular calculation.

Since the crystal has a periodic structure, the potential can be represented as a Fourier expansion. This Fourier expansion will only contain cosine terms since the crystal potential of silicon is invariant under inversion about the origin of our coordinate system. We then have:

$$V_{crys}(\vec{r}) = \Sigma_{\nu} V_{crys}(\vec{K}_{\nu}) \cos(\vec{K}_{\nu} \cdot \vec{r}) \ . \tag{4.2}$$

The crystal potential could also be expressed as a superposition of functions $V(\vec{r})$ centered about the atomic sites of the crystal, i.e.,

$$V_{crys}(\vec{r}) = \Sigma_{\mu} \{V[\vec{r} - (\vec{R}_{\mu} + \vec{t}_1)] + V[-\vec{r} + (\vec{R}_{\mu} + \vec{t}_2)]\} \ . \tag{4.3}$$

It is convenient to introduce the free atom charge density $\rho(\vec{r})$ which is obtained from the Hartree-Fock-Roothan calculations of Clementi[10] for the $(1s)^2(2s)^2(2p)^6(3s)^2(3p)^2$ ground state of silicon by the relation

$$4\pi\rho(r) = 2[R_{1s}(r)]^2 + 2[R_{2s}(r)]^2 + 6[R_{2p}(r)]^2 + 2[R_{3s}(r)]^2 + 2[R_{3p}(r)]^2 \ , \tag{4.4}$$

where the $R_{n\ell m}(r)$ are the radial parts of the solution to the self consistent field calculation. We can decompose $V(r)$ into the part due to the coulomb interaction of the nucleus and the electrons plus the exchange contribution which is approximated by $-3/2\ [3\rho(r)/\pi]^{1/3}$ in

Hartree atomic units. The Fourier coefficients then become

$$V_{crys}(\vec{K}_\nu) = -8\pi K_\nu^{-2}\Omega^{-1} \cos(\vec{K}_\nu \cdot \vec{t}_1) \{Z-K_\nu^{-1} \int_0^\infty 4\pi r\rho(r) \sin(K_\nu r)dr + K_\nu \int_0^\infty (\tfrac{3}{2}) r [3\rho(r)/\pi]^{1/3} \sin(K_\nu r)\, dr\}, \quad (4.5)$$

where Z is the atomic number. To facilitate the above integration, we curve fit $4\pi r\rho(r)$ and $(3/2)r[3\rho(r)/\pi]^{1/3}$ by a non-linear least square process. The analytic form which we obtained for these two functions from this curve fit is contained in Appendix II. The value of a_o for this calculation was chosen to be $a_o = 10.26$ a.u. in order to facilitate comparison with the calculation of Bassani and Yoshimine[11] by the method of orthogonalized plane waves, [OPW]. A comparison of our Fourier coefficients with those of Bassani and Yoshimine can be found in Table 3.

We used the analytic Slater-type orbital functions generated by Clementi[10] for the 1s, 2s, 3s, $2p_x$, $2p_y$, $2p_z$, $3p_x$, $3p_y$, $3p_z$ states of the silicon atom to construct the Bloch functions. We also curve fit the atomic wave function of the 3d state which had been calculated by the Hartree-Fock-Slater[12] method and generated the five 3d functions xy, yz, zx, x^2-y^2, r^2-3z^2. The coefficients were:

$$\begin{aligned} \phi_{3d_{xy}} = xy\{ & 0.818899 \exp(-4.08524\, r) \\ & + 0.374280 \exp(-7.81297\, r) \\ & + 0.208879 \exp(-1.09340\, r) \\ & + 0.197731 \exp(-1.86255\, r)\} . \end{aligned} \quad (4.6)$$

The 14 Bloch sums corresponding to 1s, 2s, 3s, $2p_x$, $2p_y$, $2p_z$, $3p_x$, $3p_y$, $3p_z$, $3d_{xy}$, $3d_{yz}$, $3d_{zx}$, $3d_{(x^2-y^2)}$, $3d_{(r^2-3z^2)}$ can then be constructed for each of the two sublattices making a total of 28 basis functions in all. However, we found that secular equation was real and was much easier to diagonalize for the Γ point if we formed the following "bonding" and "antibonding" combinations:

$$b_{\alpha,\Delta}(\vec{k},\vec{r}) = I(\alpha,\Delta)\ [N\ \Omega_\alpha^\Delta(\vec{k})]^{-1/2}$$
$$\Sigma_\nu\ [\exp(i\vec{k}\cdot\{\vec{R}_\nu+\vec{t}_1\})\phi_\alpha(\vec{r}-\vec{R}_\nu-\vec{t}_1) \tag{4.7}$$
$$+\ \Delta\ \exp(i\vec{k}\cdot\{\vec{R}_\nu+t_2\})\phi_\alpha(\vec{r}-\vec{R}_\nu-\vec{t}_2)]\ ,$$

where

$\Delta = \pm 1$

$\alpha = 1s, 2s, 3s, 2p_x, 2p_y, 2p_z, 3p_x, 3p_y, 3p_z, 3d_{xy}, 3d_{yz}, 3d_{zx}, 3d_{(x^2-y^2)}, 3d_{(r^2-3z^2)}$

$$I(\alpha,1) = iI(\alpha,-1) = \begin{cases} 1 \text{ for } \alpha = ns,\ nd \\ i \text{ for } \alpha = np_x \end{cases}$$

and $\Omega_\alpha^\Delta(\vec{k})$ are the normalization constants. The $I(\alpha,\Delta)$ are chosen so that the matrix elements will be real. The matrix elements corresponding to the overlap, kinetic and potential energy can then be calculated and the secular equation solved for the band structure. It is instructive to examine the effect that the inclusion of the Bloch sums of the 3d states has upon the silicon band structure. Bloch sums of the 1s, 2s, 2p, 3s, and 3p atomic orbitals can be considered to be a "minimal set"

TABLE 3

Comparison of the Fourier coefficients for the overlapping atomic crystal potential of silicon with the calculation by Bassani and Yoshimine.[11] (Potential in a.u.)

$\frac{2\pi}{a_o}(k_x, k_y, k_z)$	Present work	Bassani and Yoshimine
0, 0, 0	-1.0000	-1.000
1, 1, 1	-0.3635	-0.363
2, 2, 0	-0.1901	-0.190
3, 1, 1	-0.1532	-0.153
4, 0, 0	-0.1187	-0.118
3, 3, 1	-0.1055	-0.105
4, 2, 2	-0.0896	-0.089

for a tight-binding calculation since this many basis function are required to represent the different symmetries of the crystal wave function for different values of the $\vec{k}$ vector. The inclusion of the 3d state might be expected to change the energies some however, since the energy spacing between a 3p and 3d atomic state is small. The effect of the inclusion of the 3d states is presented in Table 4. The results of the diagonalization of the secular equation which includes the 3d states are presented in Fig. 4 along with a plot of the results obtained by Bassani and Yoshimine.[11] As can be seen, the tight-binding results lie considerably below those of the OPW calculation. Since the tight-binding scheme is a strict application of linear variation of parameters, we judge the tight-binding calculations to be considerably more accurate than the OPW calculation of Bassani and Yoshimine using some 90 basis functions. (The OPW method is a variation of the Fourier expansion (Plane Wave) technique which was described in chapter II).

The results from our tight-binding calculation for the relative positions of Γ'_2 and Γ_{15} were in disagreement with all the previous theoretical calculations. It was thought that a very accurate "OPW like" calculation might shed some light on the reasons for this discrepancy.

TABLE 4

Comparison of the energy band structure of silicon calculated without the 3d atomic states being included in the secular equation and with the inclusion of the 3d states (Energy in a.u.)

	with 3d	without 3d
[0, 0, 0]		
Γ_1	- 0.829	- 0.829
Γ_2'	- 0.325	- 0.325
Γ_{25}'	- 0.414	- 0.400
Γ_{15}	- 0.294	- 0.281
[.2, 0, 0]		
$\Delta_1(1)$	- 0.823	- 0.823
$\Delta_2'(1)$	- 0.454	- 0.443
$\Delta_2'(2)$	- 0.288	- 0.285
$\Delta_1(2)$	- 0.304	- 0.290
$\Delta_5(1)$	- 0.430	- 0.419
$\Delta_5(2)$	- 0.271	- 0.251
[.5, 0, 0]		
$\Delta_1(1)$	- 0.793	- 0.793
$\Delta_2'(1)$	- 0.547	- 0.541
$\Delta_2'(2)$	- 0.266	- 0.231
$\Delta_1(2)$	- 0.334	- 0.313

TABLE 4 Continued

	with 3d	without 3d
$\Delta_5(1)$	- 0.469	- 0.464
$\Delta_5(2)$	- 0.192	- 0.151
[.7, 0, 0]		
$\Delta_1(1)$	- 0.760	- 0.758
$\Delta_2'(1)$	- 0.608	- 0.604
$\Delta_2'(2)$	- 0.304	- 0.243
$\Delta_1(2)$	- 0.346	- 0.318
$\Delta_5(1)$	- 0.489	- 0.483
$\Delta_5(2)$	- 0.127	- 0.081
[1, 0, 0]		
$\chi_1(1)$	- 0.692	- 0.689
χ_4	- 0.501	- 0.495
$\chi_1(2)$	- 0.342	- 0.294
χ_3	- 0.048	- 0.030
[.4,.4, 0]		
$\Sigma_1(1)$	- 0.785	- 0.784
$\Sigma_3(1)$	- 0.574	- 0.569
$\Sigma_1(2)$	- 0.498	- 0.492
Σ_2	- 0.441	- 0.432
$\Sigma_3(2)$	- 0.291	- 0.277
Σ_4	- 0.245	- 0.220

TABLE 4 Continued

	with 3d	without 3d
$\Sigma_1(3)$	- 0.238	- 0.183
$\Sigma_3(3)$	- 0.184	- 0.123
[.75,.75,0]		
$\Sigma_1(1)$	- 0.709	- 0.708
$\Sigma_2(1)$	- 0.671	- 0.668
$\Sigma_1(2)$	- 0.536	- 0.531
Σ_2	- 0.488	- 0.482
$\Sigma_3(2)$	- 0.328	- 0.283
Σ_4	- 0.126	- 0.086
$\Sigma_1(3)$	- 0.233	- 0.171
$\Sigma_3(3)$	- 0.108	- 0.059
[.2,.2, .2]		
$\lambda_1(1)$	- 0.812	- 0.812
$\lambda_1(2)$	- 0.517	- 0.511
$\lambda_3(1)$	- 0.432	- 0.422
$\lambda_1(3)$	- 0.323	- 0.314
$\lambda_1(4)$	- 0.203	- 0.179
$\lambda_3(2)$	- 0.268	- 0.245
[.5, .5, .5]		
$L_2'(1)$	- 0.757	- 0.757
$L_1(1)$	- 0.643	- 0.636

TABLE 4 Continued

	with 3d	without 3d
L_4	- 0.453	- 0.445
$L_1(2)$	- 0.346	- 0.330
$L_2'(2)$	- 0.040	- 0.002
L_3	- 0.257	- 0.203

Figure 4. Energy band structure of silicon with overlapping atomic potential. The solid curves were calculated using the method of tight binding with the 1s-to-3d basis set. The dashed curves are the OPW results of Ref. 11.

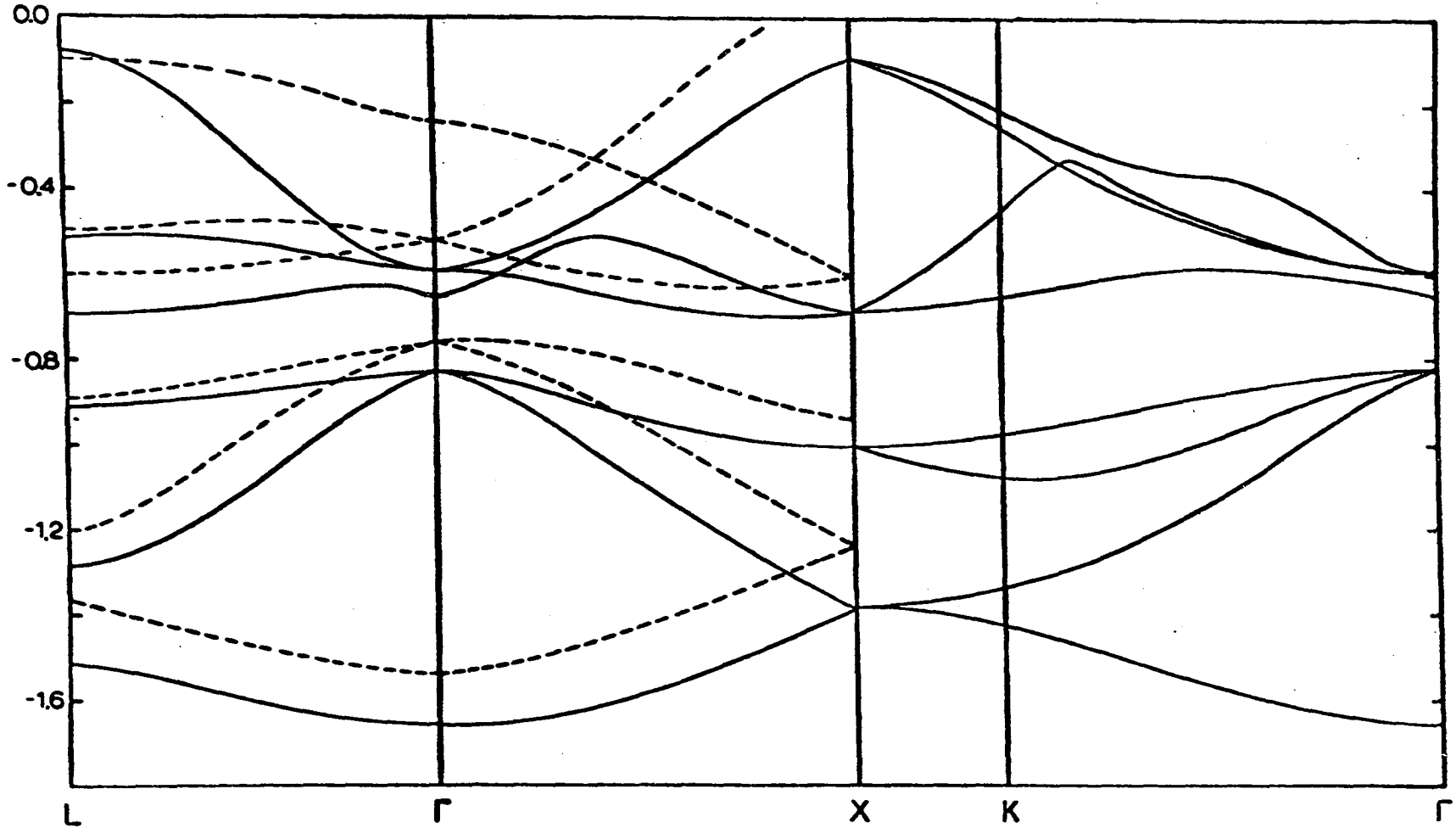

CHAPTER V

Silicon by Orthogonalized Plane Waves

We performed an orthogonalized plane wave calculation for the Γ point ($\vec{k}=[0,0,0]$) of silicon which was very similar in form to the OPW calculation of Bassani and Yoshimine.[11] However, several approximations which are generally used in an OPW calculation were not made in this work due to the fact that we could use some of the matrix elements from our previous tight-binding calculation. The difference between the OPW technique and the method of tight binding is in the choice of the $u(r)$ in Eq. (2.7). In chapter II it was stated that the truncated Fourier (plane wave) expansion provided a very adequate representation of the crystal wave function except in the region near the nuclei of the atoms which make up the crystal. The OPW technique is based on the assumption that the fast oscillation of the crystal wave function near the nuclei of the crystal is due to the fact that the crystal wave function must be orthogonal to the crystal core state levels (fully occupied levels). If one were to orthogonalize the plane waves to the Bloch sum functions which correspond to the crystal core states, one might be able to obtain faster convergence in the plane wave expansion. However, one does not have the Bloch sum functions for the crystal core states until after one has done the tight-binding calculation since the eigenvectors from the tight-binding secular equation

give the proper mixing between the Bloch sums of the atomic core state functions and those of the valence state to give the crystal core state function. The approximation that is generally made is that the atomic core state wave function is not changed very much when the atoms come together to form the crystal. Therefore, Bloch sums of atomic wave functions are used to approximate the crystal core state wave function.

The basis functions for the OPW band structure calculation for silicon can then be formed as

$$\Psi_h(\vec{k},\vec{r}) = (N\Omega)^{-\frac{1}{2}} e^{i(\vec{k}+\vec{K}_h)\cdot\vec{r}} - \sum_{\alpha,\Delta} \beta(h,\alpha,\Delta)\, b_{\alpha,\Delta}(\vec{k},\vec{r}) \quad , \tag{5.1}$$

where the $b_{\alpha,\Delta}(\vec{k},\vec{r})$ are those Bloch sum functions defined in Eq. (4.7), the α summation is over $b_{1s,\Delta}$, $b_{2s,\Delta}$, $b_{2p_x,\Delta}$, $b_{2p_y,\Delta}$, $b_{2p_z,\Delta}$, the Δ summation is over $\Delta = \pm 1$, h determines which plane wave we are working with and Ω is the volume of the Wigner-Seitz cell. The $\beta(h,\alpha,\Delta)$ are determined by the conditions that

$$\int \Psi_h^*(\vec{k},\vec{r})\, b_{\alpha,\Delta}(\vec{k},\vec{r})\, d\tau = 0 \tag{5.2}$$

for $\alpha = 1s, 2s, 2p_x, 2p_y, 2p_z$, $\Delta = \pm 1$. The terms in Eq. (5.2) involve integrals between plane waves and Bloch functions as well as integrals between one Bloch function and another Bloch function. The integrals between the plane wave and the Bloch function are handled in a rigorous fashion. However, the integrals between two Bloch functions involve the multicenter integrals between atomic wave functions centered about two different lattice sites. Since the core state atomic wave functions can be expected not to extend very far out into the crystal, there is

some justification for neglecting all of the multicenter integrals in Eq. (5.2) and for only retaining the integrals when the atomic wave functions are centered about the same lattice site. This approximation is generally made in an OPW calculation. However, since we had these multicenter integrals from our previous tight-binding calculation, it was not necessary for us to make this approximation. We used these basis functions to set up the matrix elements for the overlap and Hamiltonian matrices. These matrix elements have the form

$$
\begin{aligned}
S_{i,j} &= (N\Omega)^{-1} \int \exp\{-i(\vec{k}+\vec{K}_{h_i}) \cdot \vec{r}\} \exp\{i(\vec{k}+\vec{K}_{h_j}) \cdot \vec{r}\}\, d\tau \\
&- (N\Omega)^{-\frac{1}{2}} \sum_{\alpha,\Delta} \beta(h_i,\alpha,\Delta)^* \int b^*_{\alpha,\Delta}(\vec{k},\vec{r}) \exp\{i(\vec{k}+\vec{K}_{h_j}) \cdot r\} d\tau \\
&- (N\Omega)^{-\frac{1}{2}} \sum_{\alpha',\Delta'} \beta(h_j,\alpha',\Delta') \int \exp\{-i(\vec{k}+\vec{K}_{h_i}) \cdot \vec{r}\} b_{\alpha',\Delta'}(\vec{k},\vec{r}) d\tau \\
&+ \sum_{\alpha,\Delta} \sum_{\alpha',\Delta'} \beta^*(h_i,\alpha,\Delta)\beta(h_j,\alpha',\Delta') \int b^*_{\alpha,\Delta}(\vec{k},\vec{r})\, b_{\alpha',\Delta'}(\vec{k},\vec{r})\, d\tau ,
\end{aligned}
\tag{5.3}
$$

and

$$
\begin{aligned}
H_{i,j} &= (N\Omega)^{-1} \int \exp\{-i(\vec{k}+\vec{K}_{h_i}) \cdot \vec{r}\} \mathcal{H} \exp\{i(\vec{k}+\vec{K}_{h_j}) \cdot \vec{r}\}\, d\tau \\
&- (N\Omega)^{-\frac{1}{2}} \sum_{\alpha,\Delta} \beta(h_i,\alpha,\Delta)^* \int b^*_{\alpha,\Delta}(\vec{k},\vec{r}) \mathcal{H} \exp\{i(\vec{k}+\vec{K}_{h_j}) \cdot \vec{r}\}\, d\tau \\
&- (N\Omega)^{-\frac{1}{2}} \sum_{\alpha',\Delta'} \beta(h_j,\alpha',\Delta') \int \exp\{-i(\vec{k}+\vec{K}_{h_i}) \cdot \vec{r}\} \mathcal{H} b_{\alpha',\Delta'}(\vec{k},\vec{r}) d\tau \\
&+ \sum_{\alpha,\Delta} \sum_{\alpha',\Delta'} \beta(h_i,\alpha,\Delta)^* \beta(h_j,\alpha',\Delta') \int b^*_{\alpha,\Delta}(\vec{k},\vec{r}) \mathcal{H} b_{\alpha',\Delta'}(\vec{k},\vec{r})\, d\tau ,
\end{aligned}
\tag{5.4}
$$

where $\mathcal{H}$ is the one electron Hamiltonian. By substituting in for the Bloch functions of the core states and using the definition of $\beta^*(h_i,\alpha,\Delta)$ and $\beta(h_j,\alpha',\Delta')$, these equations can be further reduced to: (Details of this are worked out in Appendix III).

$$S_{i,j} = \delta_{\vec{K}_{h_i},\vec{K}_{h_j}} - I^*(\alpha,\Delta)\,[\Omega\Omega_\alpha^\Delta(\vec{k})]^{-\frac{1}{2}}\sum_{\alpha,\Delta}\beta(h_i,\alpha,\Delta)^*$$
$$[\exp(i\vec{K}_{h_j}\cdot\vec{t}_1) + \Delta\exp(i\vec{K}_{h_j}\cdot\vec{t}_2)]\int\phi_\alpha(\vec{r})\exp\{i(\vec{k}+\vec{K}_{h_j})\cdot\vec{r}\}\,d\tau \tag{5.5}$$

and

$$H_{i,j} = (N\Omega)^{-1}\int\exp\{-i(\vec{k}+\vec{K}_{h_i})\cdot\vec{r}\}\,\mathcal{H}\exp\{i(\vec{k}+\vec{K}_{h_j})\cdot\vec{r}\}\,d\tau$$
$$- I(\alpha,\Delta)^*[\Omega\Omega_\alpha^\Delta(\vec{k})]^{-\frac{1}{2}}\sum_{\alpha,\Delta}\beta(h_i,\alpha,\Delta)^*\int\exp\{-i(\vec{k}+\vec{K}_{h_j})\cdot\vec{r}\}\,\mathcal{H}$$
$$[e^{i\vec{k}\cdot\vec{t}_1}\phi_\alpha(\vec{r}-\vec{t}_1) + \Delta e^{i\vec{k}\cdot\vec{t}_2}\phi_\alpha(\vec{r}-\vec{t}_2)]\,d\tau$$
$$- I(\alpha',\Delta')\,[\Omega\Omega_\alpha^{\Delta'}(\vec{k})]^{-\frac{1}{2}}\sum_{\alpha',\Delta'}\beta(h_j,\alpha',\Delta')\int\exp\{-i(\vec{k}+\vec{K}_{h_i})\cdot\vec{r}\}\,\mathcal{H} \tag{5.6}$$
$$[e^{i\vec{k}\cdot\vec{t}_1}\phi_\alpha'(\vec{r}-\vec{t}_1) + \Delta e^{i\vec{k}\cdot\vec{t}_2}\phi_\alpha'(\vec{r}-\vec{t}_2)]\,d\tau$$
$$+\sum_{\alpha,\Delta}\sum_{\alpha'\Delta'}\beta(h_i,\alpha,\Delta)^*\beta(h_j,\alpha'\Delta')\int b^*_{\alpha,\Delta}(\vec{k},\vec{r})\,\mathcal{H}\,b_{\alpha',\Delta'}(\vec{k},\vec{r})\,d\tau\,,$$

Several approximations are made on the Hamiltonian matrix element (Eq. (5.6)) in many OPW calculations. The first approximation is to neglect the multicenter integrals involved in the fourth term of Eq. (5.6). The justification for this is the same as that used for

neglecting the multicenter nature of the integrals from Eq. (5.2) in that the core state atomic wave functions cannot be expected to extend very far out into the crystal. The second approximation is to say that in the region near the nuclei of the atoms which make up the crystal, the crystal Hamiltonian is nearly equal to the atomic Hamiltonian and, therefore, if ϕ_α is the solution to an atomic Hartree-Fock calculation,

$$\mathcal{H}_{\text{atomic}}\ \phi_\alpha = E_\alpha\ \phi_\alpha \tag{5.7}$$

we have that

$$\mathcal{H}_{\text{crys}}\ \phi_\alpha \tilde{=} E_\alpha\ \phi_\alpha. \tag{5.8}$$

The approximation of Eq. (5.8) is even worse if the core state functions ϕ_α are solutions to a variational Hartree-Fock calculation instead of a direct solution to the Hartree-Fock equation for then we can only say that

$$\int \phi_\alpha \mathcal{H}_{\text{atomic}}\ \phi_\alpha d\tau = E_\alpha \tag{5.9}$$

instead of Eq. (5.7). This approximation greatly simplifies the Hamiltonian matrix for it means that the second and third terms in Eq. (5.6) can be written as a constant multiplying the overlap between a plane wave and an atomic function and the fourth term can be written as a constant multiplying the overlap between two atomic wave functions. It was thought, however, that this approximation might not be justified for band structure calculation. In order to test this approximation we performed two calculations of the Γ point ($\vec{k} = [0,0,0]$) energy

levels for the case where ϕ_α has been obtained by the variational Hartree-Fock-Roothan procedure. (as was done by Bassani and Yoshimine). In the first calculation we rigorously computed the matrix elements except that we made the approximation that the crystal Hamiltonian could be replaced by the atomic Hamiltonian for the core state atomic wave functions and compared this result with that of a completely rigorous calculation of the matrix elements. The energies for various numbers of basis functions can be found in Table 5. The large difference between the Γ point eigenvalues calculated with and without this approximation is indicative of the fact that the approximation $\mathcal{H}_{crys}\ \phi_\alpha \simeq \mathcal{H}_{atom}\ \phi_\alpha$ is not justified. This is thought to be part of the reason behind the discrepancy between the tight-binding results and the results of Bassani and Yoshimine for silicon. We also tested the effect of orthogonalizing the Bloch sums of the atomic core states instead of the crystal core states by putting the atomic core states back into the secular equation. The linear variational theorem guarantees that when this is done that the energies obtained will be upper bounds on the energy of the bands in the crystal while if we just orthogonalize to the atomic core states, we cannot be sure that the energies which we calculate are above the energy bands of the crystal. The effect of augmenting the secular equation by putting in the core states can be seen in Table 6.

As can be expected, the energy levels rise when the secular equation is augmented (since previously there was no lower bound on the energy); however, the effect is rather small for the case of silicon,

TABLE 5

Comparison of the Γ point energies with the approximation that $\mathcal{H}_{crys}\phi_\alpha \approx \mathcal{H}_{atom}\phi_\alpha$ and without this approximation.

	113 OPW with approx	113 OPW no approx	609 OPW* with approx	609 OPW* no approx
Γ_1	- 0.768	- 0.837	- 0.815	- 0.856
Γ'_{25}	- 0.358	- 0.448		
Γ_{15}	- 0.257	- 0.323		
Γ'_2	- 0.160	- 0.292	- 0.250	- 0.340

*The plane waves are symmetrized in practice so that the largest matrix which must be diagonalized is a 45 x 45.

TABLE 6

Effect of putting the crystal core states into the secular equation.

	113 OPW	113 OPW + Atomic core	609 OPW	609 OPW + Atomic core
Γ_1	- 0.837	- 0.836	- 0.856	- 0.855
Γ'_{25}	- 0.448	- 0.442		- 0.457
Γ_{15}	- 0.323	- 0.319		- 0.335
Γ'_2	- 0.292	- 0.292	- 0.340	- 0.339

so this seems to be a good approximation for this particular crystal. It is worth noting that the augmentation of the secular equation is formally equivalent to including Bloch sums of atomic core states and plane waves in the secular equation without bothering to orthogonalize these plane waves to the Bloch sums of the atomic core states. This might be a good technique for calculating the excited energies in the crystal bands.

The answer to the question of why the relative positions of Γ_2' and Γ_{15} had not been predicted previously by plane wave type techniques becomes apparent when one looks at Fig. 5. This figure gives a plot of the Γ point energies using various numbers of plane wave basis functions plus the Bloch sums of the atomic core state functions in the secular equation. The Γ_2' energy level converges very slowly as a function of the number of basis functions. If one had performed the calculation with 113 or less orthogonalized plane waves (as had been done in the past), one would get the Γ_2' energy level to be above the Γ_{15} energy level. However, when one includes more OPW's the Γ_2' level continues to go down until at 609 OPW's the Γ point energy levels agree well with the tight-binding results for silicon (plotted on the right for comparison).

We have, therefore, shown that the tight-binding results for silicon are correct. The ordering of Γ_2' and Γ_{15} predicted by tight binding has also been recently confirmed independently by another orthogonalized plane wave calculation done by Stukel and Euwema.[13]

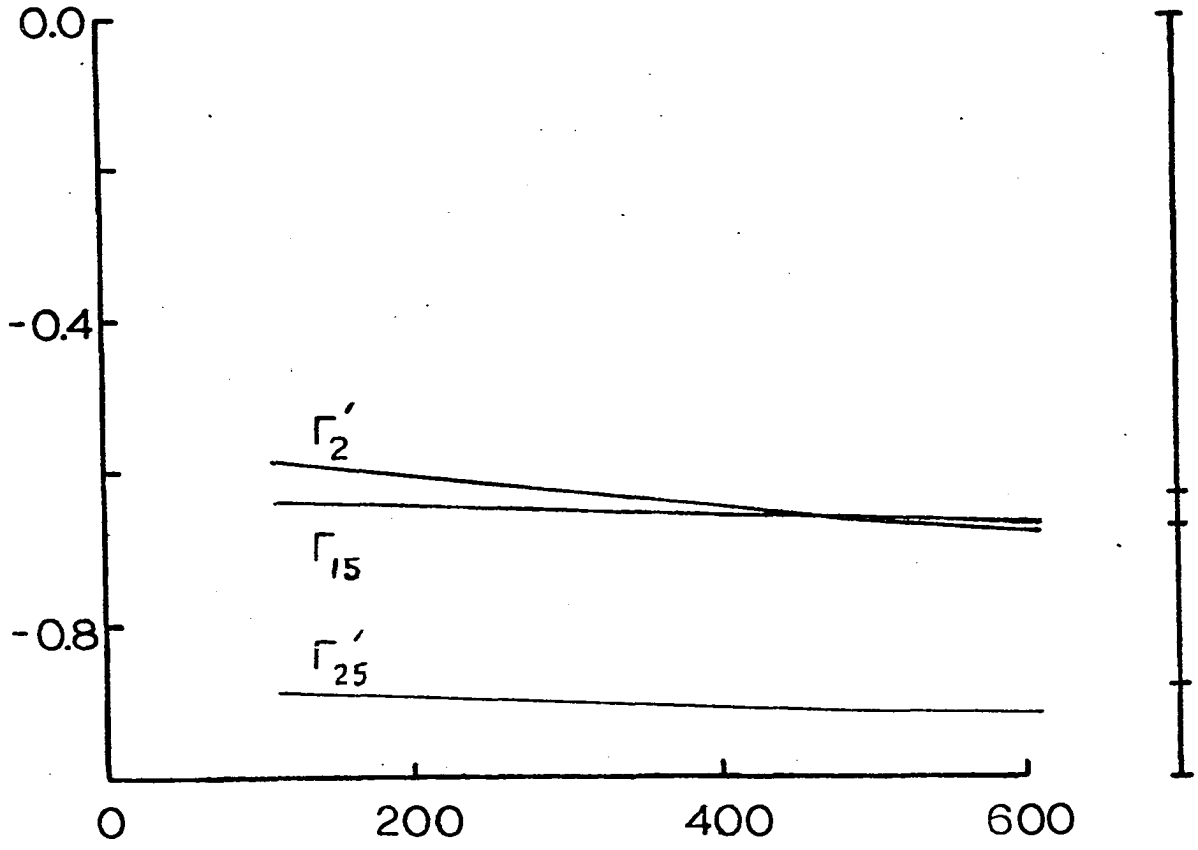

Figure 5. Convergence of the Γ_2^1, Γ_{15} and Γ_{25}^1 energy levels of silicon versus the number of OPW's. The tight binding results are presented on the right for comparison.

CHAPTER VI

Lithium Tight-Binding Calculation Using Gaussians

We stated in chapter II that if the atomic wave functions were expressed in terms of Gaussian-type orbitals (instead of the Slater-type orbitals), the single numerical integration which was present in the Slater-type orbtial calculation could be evaluated analytically. If we started out with atomic functions which had been constructed from Gaussian type orbtials, for example,

$$\phi_{ls}(\vec{r}) = \sum_i a_i e^{-\alpha_i r^2} , \tag{6.1}$$

then no numerical integration would be necessary, as all of the integrals could be evaluated analytically. We decided to perform a tight-binding calculation for the band structure of a lithium crystal and compare our results with the tight-binding calculation of Lafon and Lin.[4] Since lithium is a conductor, it can be expected to be one of the worst cases to test the applicability of the method of tight-binding. Therefore, we can expect that if the Gaussian-type orbital basis set works well for lithium, that it will work as well, or better for other crystals.

Since atomic lithium has electrons in its shells up to n=2, we would expect to need Bloch sums of atomic functions for the 1s, 2s, 2p states of lithium. The 1s and 2s atomic wave functions were obtained from the Gaussian Hartree-Fock orbitals of Huzinaga[14] (nine terms) which are of the form

$$\sum_i w_i \exp(-\alpha_i r^2) . \tag{6.2}$$

The 2p atomic wave functions were obtained by an analytic fit of the numerical Hartree-Fock functions as

$$\phi_{2p\times} = \times \sum_j \beta_j \exp(-\alpha_j r^2) , \tag{6.3}$$

where the α_j are 0.0229434, 0.0764918, 0.444620, 1.15685, 3.15789, 9.35329, and 31.9415 and the associated β_j are 0.00628524, 0.0322162, 0.0632252, -0.0278234, 0.107313, -0.0635848, and 0.118988, respectively. In the analytic fit most of the Gaussian parameters α_j were chosen to be the same as the parameters for the 1s and 2s wave functions in order to simplify the tight-binding computation; however, two new parameters were introduced in order to give the fit more variational freedom in approximating the tail of the wave function. If we represent the Gaussians in the following manner,

$$\begin{aligned} G^s(\alpha,r) &= e^{-\alpha r^2} \\ G^{p_\times}(\alpha,r) &= \times e^{-\alpha r^2} , \end{aligned} \tag{6.4}$$

the potential integral between a wave function centered about the point A and a wave function centered about B (Eq. (2.15)) can be reduced to sums over Gaussian integrals of the form

$$\begin{aligned} &\langle G^s(\alpha_1, \vec{r}-\vec{A}) | V(\vec{r}) | G^s(\alpha_2, \vec{r}-\vec{B}) \rangle \\ &= \sum_\nu V(\vec{K}_\nu) \int \exp(-\alpha_1 r_A^2 - \alpha_2 r_B^2) \cos(\vec{K}_\nu \cdot \vec{r}_C)\, d\tau , \end{aligned} \tag{6.5}$$

where $\vec{r}_C$ is measured from the origin of the Fourier expansion, $\vec{r}_A$ from

the point A, and $\vec{r}_B$ from the point B. From Eq. (14) of Ref. 4 we have that

$$\int \exp(-s_1 r_A^2 - s_2 r_B^2) \cos(\vec{K}_\nu \cdot \vec{r}_C)\, d\tau$$

$$= [\pi/(s_1+s_2)]^{3/2} \exp[-s_1 s_2\, r_{AB}^2/(s_1+s_2)] \cos(\vec{K}_\nu \cdot \vec{r}_{CD}) \exp[-(1/4)K_\nu^2/(s_1+s_2)] , \tag{6.6}$$

where

$$D_i = (\alpha_1 A_i + \alpha_2 B_i)/(\alpha_1+\alpha_2) \quad i = x,y,z$$

$$\vec{r}_C = \vec{r}_D + \vec{r}_{CD} .$$

By replacing s_1 by α_1 and s_2 by α_2 in this equation we have

$$\langle G^s(\alpha_1, \vec{r}-\vec{A}) \mid \cos(\vec{K}_\nu \cdot \vec{r}_C) \mid G_s(\alpha_2, \vec{r}-\vec{B})\rangle$$

$$= [\pi/(\alpha_1+\alpha_2)]^{3/2} \exp[-(\alpha_1\alpha_2\, r_{AB}^2 + (1/4)K_\nu^2)/(\alpha_1+\alpha_2)] \cos(\vec{K}_\nu \cdot \vec{r}_{CD}) . \tag{6.7}$$

The differentiation technique described in Ref. 4 was used to obtain the p-type Gaussian integrals. Expressions for the kinetic-energy and potential-energy integrals involving s- and p-type Gaussians are given in Appendix IV. The overlap integrals may be obtained from the potential-energy integrals by setting $\vec{K}_\nu = 0$.

Using the same Fourier coefficients of the potential as were employed by Lafon and Lin, we calculated the energy band structure of lithium with this scheme of Gaussian orbitals for two different values

of lattice constants, 6.5183 and 6.65 a.u. The calculation of all the necessary integrals and the solution of the secular equations for the two different lattice constants required approximately two minutes each on the Univac 1108 computer. The results which are summarized in Table 7 show excellent agreement with the previous work using Slater-type orbitals. A plot of the Γ point crystal wave function shown in Fig. 6 is very similar to the plot for sodium shown in Fig. 3. Between the neighboring atoms along the [1,0,0] direction, the crystal wave function is essentially flat over more than half of the region. As in the case of sodium the atomic wave functions centered at each site overlap with each other in such a manner that the crystal wave functions exhibit the characteristics expected of free particles and the valence electrons of the crystal are no longer "tightly bound" to the individual atoms. The ability of the method of tight binding to represent a "free particle type" crystal wave function is further born out by the good agreement of the band structure calculated by the method of tight binding with that obtained by the Green's function method, the composite wave method, and a method of modified plane waves.[4]

When $\alpha_1 + \alpha_2$ becomes much greater than $1000/a_o^2$ (a_o being the lattice constant), the convergence of the Fourier summation in Eq. (6.5) becomes rather slow. The converence of this summation is dictated primarily by the factor

$$V(\vec{K}) \exp [-K_\nu^2/4(\alpha_1 + \alpha_2)] .$$

When $\alpha_1 + \alpha_2$ becomes large, the exponential term cannot be expected to make the terms in the series small enough that the infinite fourier

TABLE 7

Comparison of the energies (in rydbergs) of the conduction band of lithium calculated by the tight-binding method using Slater orbitals (Ref. 4) and using Gaussian orbitals, for lattice constant a_o = 6.5183 a.u. and a_o = 6.65 a.u.

Energy (a_o=6.5183)			Energy (a_o=6.65)		
$a_o k_x/2\pi$	Gaussian	Slater	$a_o k_x/2\pi$	Gaussian	Slater
[100]			[100]		
0.0	-0.674	-0.672	0.0000	-0.675	-0.674
0.2	-0.645	-0.643	0.2500	-0.631	-0.629
0.5	-0.496	-0.494	0.5000	-0.502	-0.500
0.8	-0.225	-0.223	0.6250	-0.407	-0.407
0.9	-0.106	-0.106	0.7500	-0.291	-0.290
1.0	-0.039	-0.044	1.0000	-0.059	-0.065
[110]					
0.1	-0.660	-0.657	0.2500	-0.588	-0.587
0.3	-0.548	-0.545	0.3750	-0.487	-0.485
0.5	-0.395	-0.393	0.5000	-0.400	-0.399
[111]					
0.1	-0.652	-0.650	0.1250	-0.642	-0.641
0.2	-0.589	-0.587	0.2500	-0.547	-0.545
0.3	-0.487	-0.485	0.3125	-0.477	-0.478
0.4	-0.348	-0.346	0.3750	-0.393	-0.395
0.5	-0.175	-0.177	0.5000	-0.189	-0.190

expansion can be truncated to several hundred terms in a finite series. The Fourier coefficient ($V(\vec{K}_\nu)$) also dies off very slowly primarily due to the singularity of the crystal potential which varies like $-z/|\vec{r}-\vec{R}_\nu|$ about each nucleus. By using a Ewald-type[16] expansion we have removed these singularities from the Fourier series expansion and calculated their contribution to the potential integral by a direct space integration and have greatly improved the convergence of the Fourier expansion. In this procedure we divide the crystal potential into two parts,

$$V_{crys}(\vec{r}) = V_1(\vec{r}) + [V_{crys}(\vec{r}) - V_1(\vec{r})] \ , \tag{6.8}$$

where $V_1(\vec{r})$ behaves like $-z/|\vec{r}-\vec{R}_\nu|$ about each nucleus. The precise form of $V_1(\vec{r})$ is to some extent arbitrary and will be specified later. Since $[V_{crys}(\vec{r}) - V_1(\vec{r})]$ is a relatively smooth function of $\vec{r}$, it can be expanded in a Fourier series which converges with much fewer terms vis.,

$$\begin{aligned} &\langle G(\alpha_1, \vec{r} - \vec{A}) \mid V(\vec{r}) - V_1(\vec{r}) \mid G(\alpha_2, \vec{r}-B)\rangle \\ &\quad = \sum_\nu a_\nu \langle G(\alpha_1, \vec{r} - \vec{A}) \mid \cos(\vec{K}_\nu \cdot \vec{r}) \mid G(\alpha_2, \vec{r} - \vec{B}) \ . \end{aligned} \tag{6.9}$$

On the other hand $V_1(\vec{r})$ which is responsible for the high frequency Fourier components is now expanded in direct space as a superposition of functions V centered at each site,

$$\begin{aligned} &\langle G(\alpha_1, \vec{r} - \vec{A}) \mid V_1(r) \mid G(\alpha_2, \vec{r} - B) \\ &\quad = \sum_\mu \langle G(\alpha_1, \vec{r} - \vec{A}) \mid V(\vec{r} - \vec{R}_\mu) \mid G(\alpha_2 \vec{r} - \vec{B})\rangle \ . \end{aligned} \tag{6.10}$$

The only restriction on $V(\vec{r})$ is that it reproduce -z/r near the origin. We are free to choose the form of V for the region away from the origin in such a way as to facilitate the calculation. By making $V(\vec{r})$ negligibly small before r becomes as large as the distance to the next-nearest neighbor, one can improve the convergence of the above summation, for the case of large $\alpha_1 + \alpha_2$ to the extent that only one or two terms are needed. A possible choice of $V(\vec{r})$ which would satisfy the above condition is

$$V(\vec{r}) = -(z/r)\ (1+\gamma r^2)\ \exp\ (-\gamma r^2)\ , \tag{6.11}$$

where $\gamma = 2.5$. This choice was used in the present problem because of its simplicity and ease of calculation. Thus for the case of A=B Eq. (6.10) can be well approximated by

$$\begin{aligned} &\langle G(\alpha_1, \vec{r}-\vec{A}) \mid V_1(\vec{r}) \mid G(\alpha_2, \vec{r}-\vec{A}) \\ &\qquad \simeq \langle G(\alpha_1, \vec{r}-\vec{A}) \mid V(r-A) \mid G(\alpha_2, \vec{r}-\vec{A}) \rangle . \end{aligned} \tag{6.12}$$

When A and B refer to two different sites the only nonnegligible integrals of V_1 for $\alpha_1+\alpha_2 > 30$ occur when $\alpha_1 >> \alpha_2$ or $\alpha_2 >> \alpha_1$. The approximations used are

$$\begin{aligned} &\langle G(\alpha_1, \vec{r}-\vec{A}) \mid V_1(\vec{r}) \mid G(\alpha_2, \vec{r}-\vec{B}) \rangle \\ &\qquad \simeq \langle G(\alpha_1, \vec{r}-\vec{A}) \mid V(\vec{r}-\vec{A}) \mid G(\alpha_2, \vec{r}-\vec{B}) \rangle, \text{ for } \alpha_1 >> \alpha_2 \\ &\qquad \simeq \langle G(\alpha_1, \vec{r}-\vec{A}) \mid V(\vec{r}-\vec{B}) \mid G(\alpha_2, \vec{r}-\vec{B}) \rangle, \text{ for } \alpha_2 >> \alpha_1 . \end{aligned} \tag{6.13}$$

Using these three expressions (Eq. (6.12) and Eq. (6.13)) we can easily evaluate the potential-energy integrals involving very short range Gaussians. In this particular calculation we used Eq. (6.12) to evaluate the single-center integrals (A=B) of $V_1(\vec{r})$ whenever $\alpha_1+\alpha_2 > 30$. For such cases the multicenter integrals ($A \neq B$) are entirely negligible with the possible exception of $\alpha_1 > 2$ (or $\alpha_2 > 2$). The multicenter integrals for these high-low combination pairs are handled by Eqs. (6.13). To examine the accuracy of Eq. (6.12) we have computed the contribution to the matrix element of V_1 from the V function centered at a nearest neighbor site of A. This turns out to be less than 10^{-20} of the value given by Eq. (6.12) even for the case of $\alpha_1 + \alpha_2 = 20$. As a further test we evaluated the matrix element of $\langle G^s(31.9415, \vec{r}-\vec{A}) \mid V(r) \mid G^s(0.07663, \vec{r} - B)\rangle$ for $r_{AB} = 5.645$ a.u. using this Ewald-type expansion and obtained a value of -0.04298 for the matrix element. This agrees quite well with the value of -0.04294 which was obtained by carrying the Fourier expansion to convergence.

Rather than confining ourselves to the wave functions of the free atom, we can use each of the Gaussians in Eqs. (6.2) and Eqs. (6.3) to form the Bloch functions, i.e.,

$$B_j(\vec{k},\vec{r}) = [N\Omega_j(\vec{k})]^{-\frac{1}{2}} \sum_{\mu} \exp(i\vec{k}\cdot\vec{R}_\mu)\, G(\alpha_j, \vec{r}-\vec{R}_\mu) \ . \qquad (6.14)$$

The crystal wave function can then be expanded by these single-Gaussian Bloch functions ($B_j(\vec{k},\vec{r})$), and the energy band obtained by solving the secular equation. One could reduce the size of the secular equation by adopting a procedure similar to that of "contraction" as suggested by

Clementi, i.e., we replace the individual Gaussian in Eq. (6.14) with some suitable linear combinations of Gaussians. A convenient way to choose such linear combinations is to divide the Gaussians into several groups according to the magnitudes of their exponent parameters and to take the weighting coefficients from the atomic Hartree-Fock calculation. Thus we form

$$
\begin{aligned}
\chi_{ns,1'}(\vec{r}-\vec{R}_\nu) &= \sum_{i=1}^{3} \omega_i^{ns}\, G^s(\alpha_i, \vec{r}-\vec{R}_\nu), \quad n = 1,2 \\
\chi_{ns,2'}(\vec{r}-\vec{R}_\nu) &= \sum_{i=4}^{6} \omega_i^{ns}\, G^s(\alpha_i, \vec{r}-\vec{R}_\nu) \\
\chi_{ns,3'}(\vec{r}-\vec{R}_\nu) &= \sum_{i=7}^{9} \omega_i^{ns}\, G^s(\alpha_i, \vec{r}-\vec{R}_\nu) \\
\chi_{2p,1'}(\vec{r}-\vec{R}_\nu) &= \sum_{j=1}^{3} \beta_j\, G^p(\alpha_j, \vec{r}-\vec{R}_\nu) \\
\chi_{2p,2'}(\vec{r}-\vec{R}_\nu) &= \sum_{j=4}^{6} \beta_j\, G^p(\alpha_j, \vec{r}-\vec{R}_\nu) \\
\chi_{2p,3'}(\vec{r}-\vec{R}_\nu) &= \beta_7\, G^p(\alpha_7, \vec{r}-\vec{R}_\nu) ,
\end{aligned}
\tag{6.15}
$$

where the α_i are the Gaussian parameters arranged in ascending order, ω_i^{1s} and ω_i^{2s} are their coefficients in the 1s and 2s atomic wave functions as found in Ref. 14 and the α_j and β_j are from Eq. (6.3). The band structure is then calculated using as the basis set the fifteen combined-Gaussian Bloch functions of the form

$$
B'_j(\vec{r},\vec{k}) = [N\Omega'_j(\vec{k})]^{-1/2} \sum_\nu \exp(i\vec{k}\cdot\vec{R}_\nu)\chi'_j(\vec{r}-\vec{R}_\nu), \tag{6.16}
$$

corresponding to 1s, 2s, $2p_x$, $2p_y$, $2p_z$. The results are in all cases

TABLE 8

Comparison of the energies (in rydbergs) of the conduction band of lithium using the basis set composed of 11 Gaussian exponent parameters described in Eqs. (6.15) and using a similar basis set but dropping four of the parameters, for a_o = 6.5183 a.u.

$a_o k/2\pi$	Energy	
	11-parameter set	7-parameter set
[100]		
0.0	- 0.678	- 0.676
0.5	- 0.503	- 0.503
1.0	- 0.039	-0.039

slightly lower than the corresponding ones in Table 7. This can be expected since this is a linear variational procedure and the introduction of additional basis function always tends to suppress the calculated energy levels and bring them closer to the exact eignevalues of the one electron crystal Hamiltonian. The results of a calculation which was performed using this baáis set are presented in Table 8.

Since the wave functions of the indivitual lithium atoms overlap so strongly with each other, it is interesting to speculate as to how well one must reproduce the tail of the atomic wave function which extends beyond the next nearest-neighbor atoms in the tight-binding calculation. In other words, is it possible to drop some of the long-range Gaussians in Eqs. (6.15)? We also observed that near each nucleus the crystal wave function as shown in Fig. 6 does not vary as steeply as the 1s orbital of a free atom, suggesting the possibility of eliminating the very short range components of χ'. Following these ideas we have omitted the Gaussians with α = 921.271, 138.730, 0.028643 and 0.0229434 in Eqs. (6.15) and recalculated the energy band structure. (When this is done $\chi_{1s,3}$ becomes identical to $\chi_{2s,3}$ and is, therefore, removed). The excellent agreement between the two sets of results in Table 8 indicates that the energy band structure is not affected by the removal of the Gaussians of very short and very long range, provided a linear variational method is used to readjust the mixing of the combined-Gaussian Bloch functions.

Another interesting calculation would be to solve the secular equation using the single-Gaussian Bloch functions which were defined

Figure 6. Crystal wavefunction and Bloch sums at the Γ point of lithium along the [100] line of the crystal. The solid curve is the crystal wavefunction, the long dashes are for the basis set composed of 11 Gaussian exponent parameters (Eqs. (6.15)). The short dashes are for the basis set composed of 7 exponent parameters.

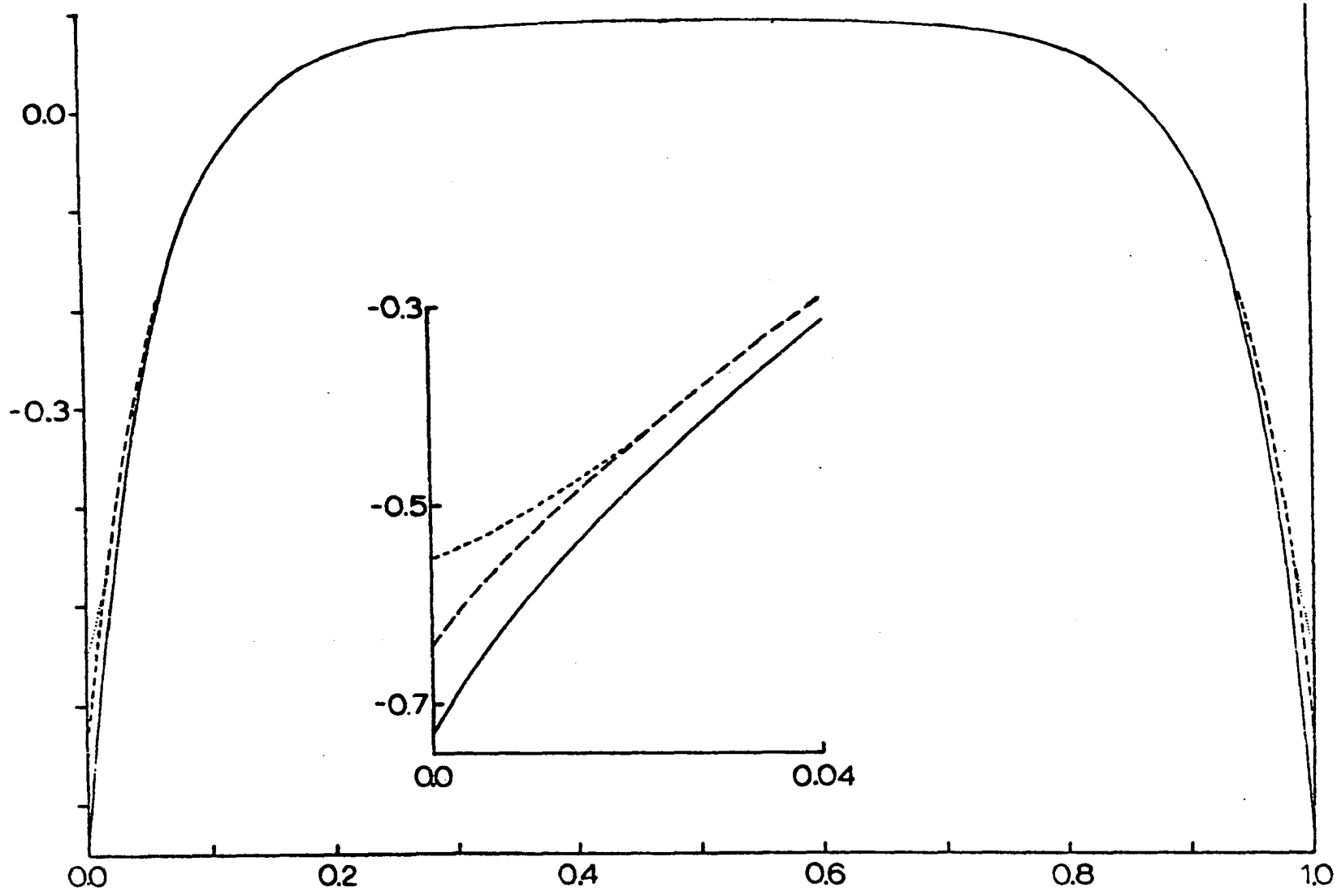

in Eq. (6.14) and see how much the increased variational freedom lowers the energy levels. This was done for a few selected points in the Brillouine zone for $a_o = 6.65$ and the results are presented in Table 9, along with a comparison with the Greenes function results which were obtained by Ham,[17] and APW results which were obtained using an identical potential by Rudge.[18] The agreement between the two methods is to within .002 Ry. indicating that tight binding can be expected to give results which are equally as good as any other technique for band structure calculation for almost any type of crystaline structure. One type of crystal for which the method of tight binding is particularly well suited is the alkali-halides. Very little first principles work has been done on this type of crystal due to the fact that the plane wave type methods have not been able to obtain adequate representations for the crystal wave function. We, therefore, decided to perform a calculation of the band structure of lithium fluoride.

TABLE 9

Comparison of Energies of the Band Edge

(a_o = 6.65)

	GTAO	CONTR-G	Expanded-Gauss	APW[a]	Greenes function[b]
H_{15}	- 0.059	- 0.059	- 0.061	- 0.062	- 0.061
N'_1	- 0.400	- 0.401	- 0.411	- 0.411	- 0.411
P_4	- 0.189	- 0.190	- 0.191	- 0.193	- 0.191

[a] See Ref. 18

[b] See Ref. 17

CHAPTER VII

Lithium Fluoride by the Method of Tight Binding

The lithium fluoride lattice is similar to the silicon lattice in that it can be thought of as being constructed from two interpenetrating sublattices of face-centered cubic (fcc) structure which we designate as sublattice 1 and 2. However for the case of lithium fluoride, sublattice 1 is composed entirely of fluorine atoms while sublattice 2 is composed entirely of lithium atoms. Each lattice site of the second sublattice is separated from the corresponding member of the first by a nonprimitive translation $\vec{T}$ directed along the body diagonal of the face-centered cube of the first sublattice and of magnitude $\sqrt{3}\, a_o/2$ where a_o is the lattice constant of the sublattice. Since there is inversion symmetry about the fluorine atoms (as well as the lithium atoms), we placed the origin of our coordinate system on one of the fluoride atoms with axes parallel to the edges of the face-centered cubes. The Wigner-Seitz cell situated about the origin has a volume $\Omega = (1/4)a_o^3$ and contains one fluorine atom and one lithium atom. All of the atoms in the crystal can be mapped out by a translation of the form $\vec{R}_\nu + \Delta_i \vec{T}$ where $\vec{R}_\nu$ is any symmetry translation corresponding to a face centered cubic crystal, the i in Δ_i refers to which sublattices we are interested in, and $\Delta_1 = 0$ and $\Delta_2 = +1$. Since the crystal potential is invariant under inversion about our origin (on a fluorine atom), it can be represented by the Fourier series

$$V_{crys}(\vec{r}) = \sum_{\nu} V_{crys}(\vec{K}_{\nu}) \cos (\vec{K}_{\nu}\cdot\vec{r}) \ . \tag{7.1}$$

The crystal potential can also be expressed as a superposition of functions centered about the atmoic aites of the crystal (as was done for silicon). However, for the case of lithium fluroide the functions are different for the two different sublattices. If we define $V_1(r)$ to be the contribution to the crystal potential due to a fluorine atom in sublattice one and $V_2(r)$ to be the contribution due to a lithium atom in sublattice two, we can express the crystal potential as,

$$V_{crys}(\vec{r}) = \sum_{\nu} \{V_1[\vec{r}-\vec{R}_{\nu}] + V_2[\vec{r}-(\vec{R}_{\nu}+\vec{T})]\}. \tag{7.2}$$

Taking $V_1(\vec{r})$ and $V_2(\vec{r})$ to be spherically symmetric, the Fourier coefficients of the potential are given by

$$\begin{aligned} V_{crys}(\vec{K}_{\nu}) &= (N\Omega)^{-1} \int V_{crys}(\vec{r}) \cos (\vec{K}_{\nu}\cdot\vec{r}) \, d\tau \\ &= \Omega^{-1}\{ \int V_1(r) \cos (\vec{K}_{\nu}\cdot\vec{r}) d\tau + \cos(\vec{K}_{\nu}\cdot\vec{T}) \int V_2(r)\cos(\vec{K}_{\nu}\cdot r) d\tau \}. \end{aligned} \tag{7.3}$$

Our choice of the model for the potential is similar to the overlapping atomic potential model (OAP)[9] which was used for silicon. We again introduce the free-atom charge density ρ_1 for the fluorine atom and ρ_2 for the lithium atom. These functions are obtained from the radial part of the Hartree-Foch Roothan calculation by Clementi[10] for the

$(1s)^2\ (2s)^2\ (2p)^2$ state of fluorine and the $(1s)^2\ (2s)$ state of lithium by the relations

$$\begin{aligned} 4\pi\ \rho_1(r) &= 2[R^F_{1s}(r)]^2 + 2[R^F_{2s}(r)]^2 + 5[R^F_{2p}(r)]^2 \\ 4\pi\ \rho_2(r) &= 2[R^{Li}_{1s}(r)]^2 + [R^{Li}_{2s}(r)]^2 . \end{aligned} \tag{7.4}$$

We could then form an initial approximation to the crystal charge density $\rho_{crys}(\vec{r})$ by forming

$$\rho_{crys}(\vec{r}) = \sum_\nu \{\rho_1[\vec{r}-\vec{R}_\nu] + \rho_2[\vec{r}-(\vec{R}_\nu+\vec{T})]\} . \tag{7.5}$$

We then decompose $V_{crys}(\vec{r})$ into two parts; the part due to the coulomb interaction with the nucleus and with the other electrons $V^{coul}_{crys}(\vec{r})$ and the exchange contribution $V^{exch}_{crys}(\vec{r})$.

$$V_{crys}(\vec{r}) = V^{coul}_{crys}(\vec{r}) + V^{exch}_{crys}(\vec{r}) \tag{7.6}$$

The Fourier coefficients can also be split up into.

$$V_{crys}(\vec{K}_\nu) = V^{coul}_{crys}(\vec{K}_\nu) + V^{exch}_{crys}(\vec{K}_\nu) \tag{7.7}$$

The Fourier coefficient for the coulomb contribution becomes

$$\begin{aligned} V^{coul}_{crys}(\vec{K}_\nu) = -\frac{4\pi}{K_\nu^2\Omega}\{z_F - \frac{4\pi}{K_\nu}\int_0^\infty r\,\rho_1(r)\sin(K_\nu r)\,dr \\ + \cos(\vec{K}_\nu\cdot\vec{T})[z_{L_i} - \frac{4\pi}{K_\nu}\int_0^\infty r\,\rho_2(r)\sin(K_\nu r)\,dr]\} . \end{aligned} \tag{7.8}$$

where z_F is the atomic number for fluorine and z_{Li} is the atomic number for lithium. The necessary integrals for the coulomb crystal potential can be evaluated directly in terms of the Slater-type orbitals from the Hartree-Fock Roothan calculation by Clementi. A more accurate way to handle exchange is to apply the Slater exchange approximation to the crystal charge density (instead of the atomic charge density which was done for silicon). This means that

$$V_{crys}^{exch}(\vec{r}) = -(3/2)\,[3\,\rho_{crys}(\vec{r})/\pi]^{1/3} . \tag{7.9}$$

Following a technique suggested by Lafon,[19] V_{crys}^{exch} is then curve fit by a three dimensional curve fit program using spherical harmonics centered about each of the lattice sites. In other words

$$V_{crys}^{exch}(\vec{r}) = \sum_{\nu} [f_1(\vec{r} - \vec{R}_\nu) + f_2(\vec{r} - \{\vec{R}_\nu + \vec{T}\})] , \tag{7.10}$$

where f_1 is a function centered about the fluorine atom and f_2 is a function centered about the lithium atom. We chose f_1 and f_2 to have the form of

$$f_1(r) = e^{-\beta r} \sum_{i=0}^{4} a_i r^i \tag{7.11}$$

and

$$f_2(r) = e^{-\beta' r} \sum_{i=0}^{4} a'_i r^i .$$

The values of β and a_i and β' and a'_i which were obtained by our curve fit can be found in Tables 10 and 11.

TABLE 10

Coefficients for $f_1(r)$

$\beta = 3.75012$

i	a_i
0	- 11.0179
1	+ 43.3233
2	-109.103
3	+ 74.7205
4	+ 33.3935

TABLE 11

Coefficients for $f_2(r)$

$\beta' = 2.00753$

i	a'_i
0	- 3.41696
1	- 0.01889
2	- 0.38340
3	+ 1.31608
4	- 0.745599

We can then evaluate $V_{crys}^{exch}(\vec{K}_\nu)$ as:

$$V_{crys}^{exch}(\vec{K}_\nu) = \frac{4\pi}{K_\nu \Omega}\{\int_0^\infty r\, f_1(r)\, \sin(K_\nu r)\, dr + \cos(\vec{K}_\nu \cdot \vec{T}) \int_0^\infty r\, f_2(r)\, \sin(K_\nu r)\, dr\}. \tag{7.12}$$

The Fourier components of the crystal potential are then obtained as a sum of the coulomb contribution plus the exchange contribution. A few of them are given in Table 12.

We used the analytic Gaussian-type orbital functions generated by Huzinaga[14] for the 1s, 2s, $2p_x$, $2p_y$, $2p_z$ free atom states of fluorine to construct Bloch sums of fluorine wave functions about each of the sites in sublattice one. The five atomic functions used to form Bloch sums of lithium wave functions centered about each of the sites in sublattice two are the same as those described in the previous chapter. The Bloch sums then have the form:

$$b^{F}_{n\ell m}(\vec{k},\vec{r}) = \frac{1}{\sqrt{N\Omega}} \sum_\nu e^{i\vec{k}\cdot\vec{R}_\nu} \phi^{F}_{n\ell m}(\vec{r} - \vec{R}_\nu)$$

$$b^{L_i}_{n\ell m}(\vec{k},\vec{r}) = \frac{1}{\sqrt{N\Omega}} \sum_\nu e^{i\vec{k}\cdot\{\vec{R}_\nu+\vec{T}\}} \phi^{L_i}_{n\ell m}(\vec{r}-\{\vec{R}_\nu+\vec{T}\}) \tag{7.13}$$

where $\phi^{F}_{n\ell m}$ is the free atomic wave function for the $n\ell m$ state of fluorine and $\phi^{L_i}_{n\ell m}$ is the free atomic wave function for the n, ℓ, m state of lithium.

The 10 x 10 secular equation is then formed from the matrix elements of the overlap and Hamiltonian operators and is solved for

TABLE 12

Fourier coefficients for the crystal potential of lithium fluoride.

$2\pi/a_o(k_x,k_y,k_z)$	$V(K_\nu)$
0, 0, 0	- 1.0712256
1, 1, 1	- 0.1144801
2, 0, 0	- 0.2658392
2, 2, 0	- 0.1683456
3, 1, 1	- 0.0528263
2, 2, 2	- 0.1233327
4, 0, 0	- 0.0974406
3, 3, 1	- 0.0360021
4, 2, 0	- 0.0806272
4, 2, 2	- 0.0688152
3, 3, 3	- 0.0273551

various values of $\vec{k}$. The results are presented in Fig. 7. The direct band gap as determined by the difference between the Γ_{15} and Γ_1 energy levels is 15.1 e.v. This agrees quite well with the value of 13.6 e.v. which is obtained by experiment.[20]

One may question the use of a superposition of free atom potentials as the starting potential in the tight-binding calculation instead of a superposition of lithium and fluorine ionic potentials. This point is currently under investigation as well as the investigation of the effect of including the Bloch sums of the d states in the variational calculation. The primary purpose of this calculation was to show that the method of tight binding is a versitile technique and is quite applicable to the alkali halide crystals.

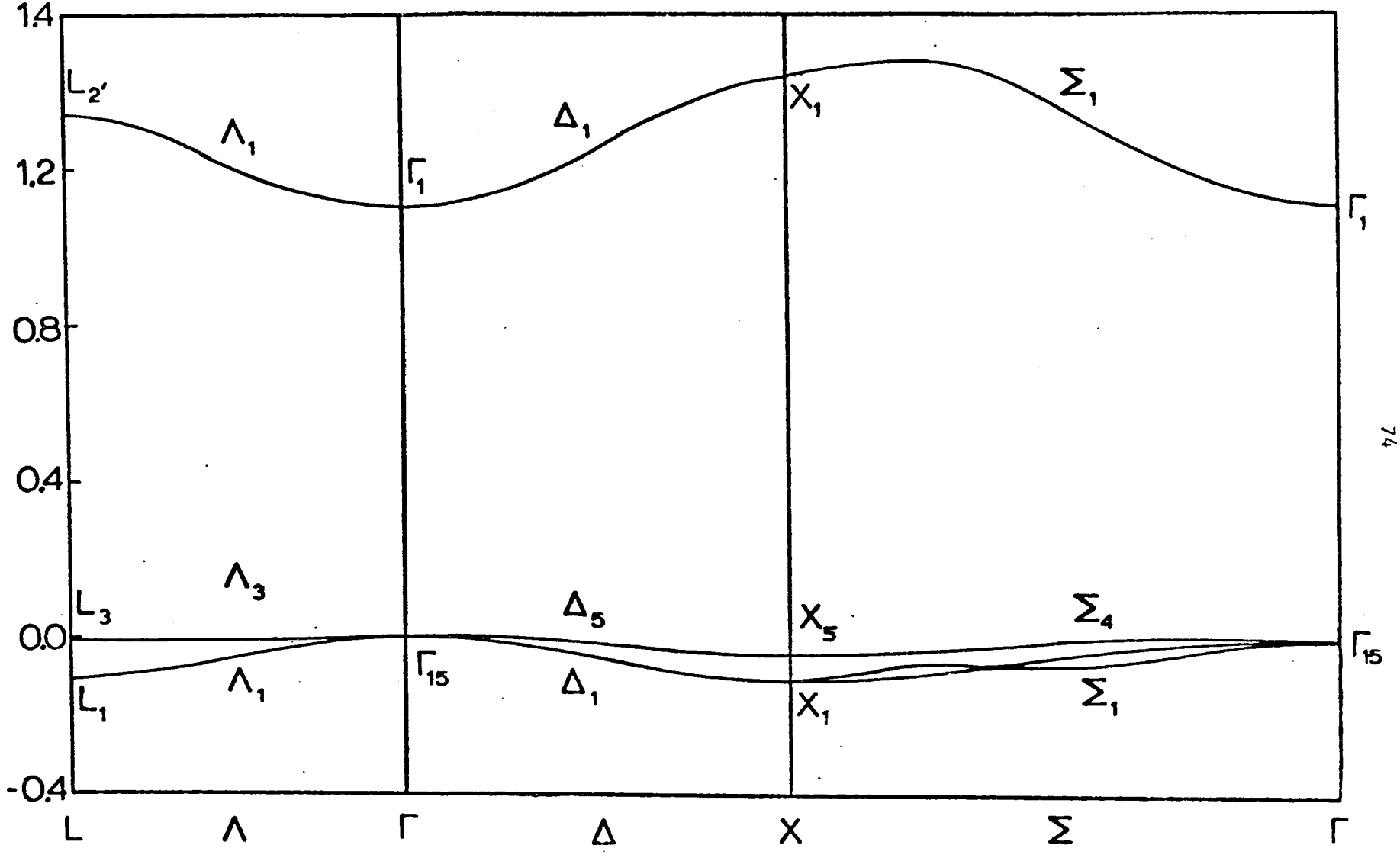

Figure 7. Energy band structure of a lithium fluoride crystal.

CHAPTER VIII

The LCAO Method as Applied to the Electronic States of Impurities

The versatility of the method of tight binding or LCAO method becomes even more apparent when it is applied to the calculation of the electronic states of impurities in crystaline solids. Since the basis set consists of linear combinations of atomic orbitals centered about each of the lattice sites in the crystal, the term in the summation which corresponds to the contribution from a particular atom in the perfect crystal can be suitably altered and one has the basis function for an impurity at the location of the atom.

Several calculations have been made on the electronic states of impurities using linear combinations of atomic orbitals.[21] The difficulty in evaluating the multicenter integrals, however, has necessitated many approximations which have limited the applicability of the technique. Now that we have mastered the calculation of the multicenter integrals, a more accurate calculation of the impurity states can be made, using a basis set of linear combinations of atomic orbitals.

The impurity problem is somewhat more difficult than a tight-binding band structure calculation. This is due to the fact that the introduction of the impurity destroys the translational symmetry of the crystal. The only symmetry which remains is the rotational symmetry about the impurity. The effect of this reduction in symmetry is that although we can say that our crystal wave function can be written as a

sum of atomic wave functions centered about the different lattice sites,

$$\psi(\vec{r}) = \sum_{R_\nu} a_\nu \, \phi_{n\ell m}(\vec{r} - \vec{R}_\nu) \, , \tag{8.1}$$

we can no longer invoke the Bloch theorem to tell us that $a_\nu = e^{i\vec{k}\cdot\vec{R}_\nu}$. This means that the different values of a_ν must be determined by solving the secular equation. This can make the secular equation for the impurity calculation somewhat larger than the band structure secular equation.

In order to test the applicability of this technique to the electronic states of impurities, we have performed a calculation of the ground state energy of a color center impurity in a lithium fluoride crystal. The color center impurity for an alkali halide crystal consists of an electron trapped in a halide vacancy. For this initial calculation we will neglect the distortion of the crystal lattice due to the removal of the halide ion and will assume that any polarization of the neighboring electrons can be taken into account by carrying the variational calculation to self-consistency. Our approximation for the initial Hamiltonian will be the Hamiltonian of the perfect crystal minus the Hamiltonian due to a fluorine atom. The removal of this fluorine atom will automatically leave an extra electron to be trapped in the vacancy. When we center our coordinate system about the location of the color center, our one electron Hamiltonian, under these approximations, has the form of

$$H = -\tfrac{1}{2}\nabla^2 + V^{coul}_{crys}(\vec{r}) - V^{coul}_{F\text{-}atom}(\vec{r}) + V_{exch}(\vec{r}), \tag{8.2}$$

where $V^{coul}_{crys}(\vec{r})$ was defined in the lithium fluoride band structure formulation. The coulomb potential for the fluoride atom $V^{coul}_{F\text{-}atom}(\vec{r})$ is written in terms of the electron charge density ρ_F and the nuclear charge z_F as

$$V^{coul}_{F\text{-}atom}(\vec{r}) = -\frac{z_F}{r} + \frac{4\pi}{r}\int_o^r \rho_F(r')\, r'^2\, dr' + 4\pi\int_r^\infty \rho_F(r')r'\, dr'. \tag{8.3}$$

If we use the Slater approximation for exchange, we can say that

$$V_{exch}(\vec{r}) = -[3/2]\,[3\,\{\rho_{crys}(\vec{r}) - \rho_F(r)\}/\pi],^{1/3} \tag{8.4}$$

where $\rho_{crys}(\vec{r})$ was defined in Eq. (7.5). Alternatively we could define a

$$V'_{exch}(\vec{r}) = V_{exch}(\vec{r}) - V^{exch}_{crys}(\vec{r}), \tag{8.5}$$

where $V^{exch}_{crys}(\vec{r})$ is defined in Eq. (7.9). Then the Hamiltonian could be written as

$$H = H_1 - H_2$$

where

$$H_1 = -\tfrac{1}{2}\nabla^2 + V^{coul}_{crys}(\vec{r}) + V^{exch}_{crys}(\vec{r})$$

and

$$H_2 = V^{coul}_{F\text{-}atom}(\vec{r}) - V'_{exch}(\vec{r}) \tag{8.6}$$

The first term in the Hamiltonian(H_1)is the Hamiltonian of the perfect crystal and can be expanded in terms of a Fourier series as was done in

the band structure calculation. The term $V'_{exch}(\vec{r})$ is plotted in three dimensions and is curve fitted using spherical harmonics centered about the impurity site. The results of this curve fit are presented in Table 13. If Clementi's Slater-type orbitals[10] are used to construct the charge density, $\rho_F = \rho_1$ from Eq. (7.4) and $V^{coul}_{F\text{-atom}}(\vec{r})$ can be expressed as a summation over Slater-type orbitals,

$$V^{coul}_{F\text{-atom}}(\vec{r}) = \sum_L a_L r^{m_i} e^{-\rho_L r} \tag{8.7}$$

where the value of a_L and m_L are determined by evaluating Eq. (8.3).

We will use linear combinations of the atomic orbitals of the neighboring atoms as our basis function in this variational calculation. In other words, we can approximate the wave function of the trapped electron as

$$\psi_T = \sum_\nu a_\nu \phi_{n\ell m}(\vec{r} - \vec{R}_\nu) \tag{8.8}$$

The full rotational symmetry of the O_n groups about the fluorine atom which occurred in the perfect crystal is maintained when the fluorine atom is removed. We, therefore, would expect the basis function of the trapped electron to transform according to some representation of the octahedral group. We can expect the ground state of the trapped electron to transform according to the identity representation so we set up our basis function to transform according to this representation.

TABLE 13

Analytic form of correction to the exchange potential for the color center in lithium fluoride.

$$V'_{exch}(\vec{r}) = \sum_{i=1}^{4} q_i \, r^{m_i} \, e^{-\gamma_i r}$$

i	q_i	m_i	γ_i
1	- 2.75526	0	+ 25.9016
2	- 8.24072	0	+ 8.56059
3	- 8.81361	1	+ 2.24929
4	+ 0.466705	1	+ 1.36362

Since the electron is trapped at the vacancy site, we know that it cannot extend too far away from this site. We should then be able to represent the wave function of the ground state using symmetrized combinations of the atomic wave functions of the atoms which are near the vacancy site.

In this work we included in our variational calculation, linear combinations of the atomic wave functions of the six nearest neighbor lithium atoms plus the twelve atomic wave functions of the next nearest neighbor fluorine atoms. The symmetrized wave functions from the first layer (six nearest neighbors) have the form

$$\Phi_{1,1s} = (\Omega_{1,1s})^{-\frac{1}{2}}[\phi^{Li}_{1s}(\vec{r}_{1,1}) + \phi^{Li}_{1s}(\vec{r}_{1,2}) + \phi^{Li}_{1s}(\vec{r}_{1,3}) + \phi^{Li}_{1s}(\vec{r}_{1,4}) + \phi^{Li}_{1s}(\vec{r}_{1,5}) + \phi^{Li}_{1s}(\vec{r}_{1,6})] ,$$

$$\Phi_{1,2s} = (\Omega_{1,2s})^{-\frac{1}{2}}[\phi^{Li}_{2s}(\vec{r}_{1,1}) + \phi^{Li}_{2s}(\vec{r}_{1,2}) + \phi^{Li}_{2s}(\vec{r}_{1,3}) + \phi^{Li}_{2s}(\vec{r}_{1,4}) + \phi^{Li}_{2s}(\vec{r}_{1,5}) + \phi^{Li}_{2s}(\vec{r}_{1,6})],$$

$$\Phi_{1,2p} = (\Omega_{1,2p})^{-\frac{1}{2}}[\phi^{Li}_{2p_x}(\vec{r}_{1,1}) - \phi^{Li}_{2p_x}(\vec{r}_{1,2}) + \phi^{Li}_{2p_z}(\vec{r}_{1,3}) - \phi^{Li}_{2p_z}(\vec{r}_{1,4}) + \phi^{Li}_{2p_y}(\vec{r}_{1,5}) - \phi^{Li}_{2p_y}(\vec{r}_{1,6})] ,$$

where

$$\vec{r}_{1,1} = \vec{r} - \frac{a_o}{2}(1, 0, 0)$$

$$\vec{r}_{1,2} = \vec{r} - \frac{a_o}{2}(-1, 0, 0)$$

$$\begin{aligned}
\vec{r}_{1,3} &= \vec{r} - \frac{a_o}{2}(0, 0, 1) \\
\vec{r}_{1,4} &= \vec{r} - \frac{a_o}{2}(0, 0, -1) \\
\vec{r}_{1,5} &= \vec{r} - \frac{a_o}{2}(0, 1, 0) \\
\vec{r}_{1,6} &= \vec{r} - \frac{a_o}{2}(0, -1, 0) \ .
\end{aligned} \tag{8.9}$$

The three wave functions from the second layer have the form

$$\begin{aligned}
\Phi_{2,1s} = (\Omega_{2,1s})^{-\frac{1}{2}}[&\phi^F_{2,1s}(\vec{r}_{2,1}) + \phi^F_{2,1s}(\vec{r}_{2,2}) + \phi^F_{2,1s}(\vec{r}_{2,3}) + \phi^F_{2,1s}(\vec{r}_{2,4}) \\
&+ \phi^F_{2,1s}(\vec{r}_{2,5}) + \phi^F_{2,1s}(\vec{r}_{2,6}) + \phi^F_{2.1s}(\vec{r}_{2,7}) + \phi^F_{2,1s}(\vec{r}_{2,8}) \\
&+ \phi^F_{2,1s}(\vec{r}_{2,9}) + \phi^F_{2,1s}(\vec{r}_{2,10}) + \phi^F_{2,1s}(\vec{r}_{2,11}) + \phi^F_{2,1s}(\vec{r}_{2,12})] \ ,
\end{aligned}$$

$$\begin{aligned}
\Phi^F_{2,2s} = (\Omega_{2,2s})^{-\frac{1}{2}}[&\phi^F_{2,2s}(\vec{r}_{2,1}) + \phi^F_{2,2s}(\vec{r}_{2,2}) + \phi^F_{2,2s}(\vec{r}_{2,3}) + \phi^F_{2,2s}(\vec{r}_{2,4}) \\
&+ \phi^F_{2,2s}(\vec{r}_{2,5}) + \phi^F_{2,2s}(\vec{r}_{2,6}) + \phi^F_{2,2s}(\vec{r}_{2,7}) + \phi^F_{2,2s}(\vec{r}_{2,8}) \\
&+ \phi^F_{2,2s}(\vec{r}_{2,9}) + \phi^F_{2,2s}(\vec{r}_{2,10}), + \phi^F_{2,2s}(\vec{r}_{2,11}) + \phi^F_{2,2s}(\vec{r}_{2,12})] \ ,
\end{aligned}$$

$$\begin{aligned}
\Phi^F_{2,2p} = (\Omega_{2,2p})^{-\frac{1}{2}}[&\phi^F_{2,2p_x}(\vec{r}_{2,1}) + \phi^F_{2,2p_y}(\vec{r}_{2,1}) + \phi^F_{2,2p_x}(\vec{r}_{2,2}) - \phi^F_{2,2p_y}(\vec{r}_{2,2}) \\
&- \phi^F_{2,2p_x}(\vec{r}_{2,3}) + \phi^F_{2,2p_y}(\vec{r}_{2,3}) - \phi^F_{2,2p_x}(\vec{r}_{2,4}) - \phi^F_{2,2p_y}(\vec{r}_{2,4}) \\
&+ \phi^F_{2,2p_z}(\vec{r}_{2,5}) + \phi^F_{2,2p_x}(\vec{r}_{2,5}) - \phi^F_{2,2p_z}(\vec{r}_{2,6}) - \phi^F_{2,2p_x}(\vec{r}_{2,6}) \\
&+ \phi^F_{2,2p_z}(\vec{r}_{2,7}) - \phi^F_{2,2p_x}(\vec{r}_{2,7}) - \phi^F_{2,2p_z}(\vec{r}_{2,8}) + \phi^F_{2,2p_x}(\vec{r}_{2,8})
\end{aligned}$$

$$+ \phi^F_{2,2p_y}(\vec{r}_{2,9}) + \phi^F_{2,2p_z}(\vec{r}_{2,9}) - \phi^F_{2,2p_y}(\vec{r}_{2,10}) + \phi^F_{2,2p_z}(\vec{r}_{2,10})$$

$$- \phi^F_{2,2p_y}(\vec{r}_{2,9}) - \phi^F_{2,2p_z}(\vec{r}_{2,11}) + \phi^F_{2,2p_y}(\vec{r}_{2,12}) - \phi^F_{2,2p_z}(\vec{r}_{2,13})],$$

where

$$\begin{aligned}
&\vec{r}_{2,1} = \vec{r} - \frac{a_o}{2}(1, 1, 0) \quad , \quad \vec{r}_{2,2} = \vec{r} - \frac{a_o}{2}(1, -1, 0) \\
&\vec{r}_{2,3} = \vec{r} - \frac{a_o}{2}(-1, 1, 0) \quad , \quad \vec{r}_{2,4} = \vec{r} - \frac{a_o}{2}(-1, -1, 0) \\
&\vec{r}_{2,5} = \vec{r} - \frac{a_o}{2}(1, 0, 1) \quad , \quad \vec{r}_{2,6} = \vec{r} - \frac{a_o}{2}(-1, 0, -1) \\
&\vec{r}_{2,7} = \vec{r} - \frac{a_o}{2}(-1, 0, 1) \quad , \quad \vec{r}_{2,8} = \vec{r} - \frac{a_o}{2}(1, 0, -1) \\
&\vec{r}_{2,9} = \vec{r} - \frac{a_o}{2}(0, 1, 1) \quad , \quad \vec{r}_{2,10} = \vec{r} - \frac{a_o}{2}(0, -1, 1) \\
&\vec{r}_{2,11} = \vec{r} - \frac{a_o}{2}(0, -1, -1), \quad \vec{r}_{2,12} = \vec{r} - \frac{a_o}{2}(0, 1, -1) \ .
\end{aligned} \tag{8.10}$$

Now that we have set up the basis functions, we must solve for the matrix elements of the overlap and Hamiltonian operators in order to solve our secular equation.

$$| H_{ij} - \lambda S_{ij} | = 0 \ ,$$

where

$$H_{ij} = \langle \phi_i | H | \phi_j \rangle$$

and

$$S_{ij} = \langle \phi_i | \phi_i \rangle \tag{8.11}$$

and i and j correspond to some combination of the lattice layer and the atomic wave function (for example, $\phi_{1,2s}$). These matrix elements can be

reduced down to sums of integrals of the following form (for the 1s type Gaussians).

$$\int e^{-\alpha_1 r_A^2} e^{-\alpha_2 r_B^2} d\tau \tag{8.12}$$

$$\int e^{-\alpha_1 r_A^2} H_1 e^{-\alpha_2 r_B^2} d\tau \tag{8.13}$$

and

$$\int e^{-\alpha_1 r_A^2} H_2 e^{-\alpha_2 r_B^2} d\tau \tag{8.14}$$

The first two integrals (Eqs. (8.12) and (8.13)) have been evaluated in the tight-binding band structure calculation so we will only concern ourselves with the evaluation of the third integral.

$$H_2 = V_{F\text{-atom}}^{coul} - V'_{exch}(\vec{r}) \tag{8.15}$$

From the curve fit of $V'_{exch}(\vec{r})$ and the analytic form of $V_{F\text{-atom}}^{coul}$, we see that H_2 can be expressed as a summation of Slater-type orbitals;

$$H_2 = \sum_i a_i r^{m_i} e^{-\beta_i r} . \tag{8.16}$$

Then

$$\int e^{-\alpha_1 r_A^2} H_2 e^{-\alpha_2 r_B^2} d\tau = \sum_i a_i \int e^{-\alpha_1 r_A^2} r_C^{m_i} e^{-\beta_i r_C} e^{-\alpha_2 r_B^2} d\tau . \tag{8.17}$$

Suppose we consider the case where $m_i = 0$. (The rest of the cases can be obtained by differentiating Eq. (8.17) with respect to β_i). Then we must evaluate the integral

$$I = \int e^{-\alpha_1 r_A^2} e^{-\beta_i r_C} e^{-\alpha_2 r_B^2} d\tau , \qquad (8.18)$$

where

$$\vec{r}_A = \vec{r} - \vec{A}$$

$$\vec{r}_B = \vec{r} - \vec{B}$$

$$\vec{r}_C = \vec{r} - \vec{C}$$

and $\vec{C}$ is the location of the impurity site. Using the property of Gaussians which was used to evaluate the multicenter integrals in the band structure calculation we see that

$$e^{-\alpha_1 r_A^2} e^{-\alpha_2 r_B^2} = e^{-\left(\frac{\alpha_1 \alpha_2}{\alpha_1+\alpha_2} r_{AB}^2\right)} e^{-(\alpha_1+\alpha_2) r_D^2} , \qquad (8.19)$$

where $\vec{r}_D = \vec{r} - \vec{D}$

$$D_i = \frac{\alpha_1 A_i + \alpha_2 B_i}{\alpha_1 + \alpha_2} \qquad , \qquad i = x,y,z$$

and

$$\vec{r}_{AB} = \vec{B} - \vec{A}$$

Then

$$I = e^{-\left(\frac{\alpha_1 \alpha_2}{\alpha_1+\alpha_2} r_{AB}^2\right)} \int e^{-(\alpha_1+\alpha_2) r_D^2} e^{-\beta_i r_C} d\tau$$

$$= e^{-\left(\frac{\alpha_1 \alpha_2}{\alpha_1+\alpha_2} r_{AB}^2\right)} e^{-(\{\alpha_1+\alpha_2\} r_{CD}^2)} \int \exp\{-(\alpha_1+\alpha_2)(r_C^2 - 2\vec{r}_{CD}\cdot\vec{r}_C)$$

$$e^{-\beta_i r_C} d\tau .$$

Let

$$C = \frac{\pi}{(\alpha_1+\alpha_2)r_{CD}} \; e^{-\left(\frac{\alpha_1\alpha_2}{\alpha_1+\alpha_2} r_{AB}^2\right)} \; e^{-\left(\{\alpha_1+\alpha_2\}r_{CD}^2\right)}$$

$$a = 2(\alpha_1 + \alpha_2)\, r_{CD} \qquad b = \alpha_1 + \alpha_2$$

$$I = -C \int_0^\infty r_C \, e^{-br_C^2} \left(e^{-(\beta_1+a) r_C} - e^{-(\beta_i-a)r_C}\right) dr_C \; . \tag{8.20}$$

This integral can be expressed in terms of the error function since

$$\int_0^\infty e^{-(br^2+gr)} \, dr = \frac{1}{2} \frac{\sqrt{\pi}}{\sqrt{b}} \; e^{\frac{g^2}{4b}} \; \text{erfc} \left(\frac{g}{2\sqrt{b}}\right) .$$

By differentiating this integral with respect to g and letting $q = \frac{g}{2\sqrt{b}}$ and $Y = \frac{\sqrt{\pi}}{2} e^{q^2}$ erfc (q) we have that:

$$\int_0^\infty r \, e^{-(br^2+gr)} \, dr = \frac{1}{b} \left[\tfrac{1}{2} - qY\right] . \tag{8.21}$$

Let

$$g_1 = \beta_i + a \; , \qquad g_2 = \beta_i - a \; ,$$

$$q_1 = \frac{g_1}{2\sqrt{b}} \; , \qquad q_2 = \frac{g_2}{2\sqrt{b}} \; ,$$

$$Y_1 = \frac{\sqrt{\pi}}{2} e^{q_1^2} \; \text{erfc}(q_1) \; , \quad Y_2 = \frac{\sqrt{\pi}}{2} e^{q_2^2} \; \text{erfc} \; (q_2) \; ,$$

and Eq. (8.20) becomes

$$I = C \, \frac{1}{b} \left[\quad q_1 Y_1 - q_2 Y_2 \right] .$$

The integrals involving Gaussians of p type symmetry can be obtained in a manner similar to the differentiation technique which was used to obtain the p symmetry integrals in the band structure formulation.

Now that we have the necessary integrals formulated, we can evaluate the matrix elements and solve the 6 x 6 secular equation for the energy level of the ground state of the color center. When this was done we obtained a value of -0.58115 a.u.

This work has demonstrated that the calculation of the electronic states of impurities using linear combinations of atomic orbitals is computationally feasable. The technique can now be extended to the calculation of the excited states of the color center electron and direct comparison can be made with the experimentally determined transition energy between the ground state and the excited state. Further refinements such as the inclusion of the effects due to distortion of the lattice and polarization of the neighboring electrons can be incorporated by an extension of this scheme.

CHAPTER IX

Conclusions

The method of tight binding has been shown to be a very useful technique in calculating the electronic states of crystaline solids. It has proven to be a much more flexible method for band structure calculations in that it is not limited as to the choice of potential and that it does not require the solution of a large secular equation. The fact that the multicenter integrals which make up the matrix elements in the secular equation are independent of $\vec{k}$ means that there is very little work involved in obtaining the energies for many values of $\vec{k}$ in the Brillouin zone over obtaining the energy for one value of k. Another nice feature of tight binding is that the crystal wave functions are expressed in terms of the wave functions of the constituent atoms. It is, therefore, possible to make direct correlation between the properties of the crystals and those of the free atoms on both quantitative and qualitative level. The method of tight binding has been shown to give energy band structure for several crystals which compare favorably with the results obtained using other methods of calculation, and has been shown to be more flexible than other technqiues by the fact that it gives good values for the energy band structure of lithium fluoride, a crystal for which the calculation of the energy band has proved difficult using any other technique. We can, therefore, conclude that for a general crystal that the method of tight binding can be used to obtain accurate values of the energy bands.

The application of the method of tight binding to impurities, although only in the preliminary stages, has shown that there are no computational difficulties associated with using this technique. The logical extension of the impurity calculation will be to calculate the energy level of the excited state of a color center electron in lithium fluoride and include the effects due to distortion of the crystal lattice and polarization of the neighboring electrons on both the ground state and excited state energy levels.

List of References

1. SLATER, J. C., Quantum Theory of Molecules and Solids, vol. 2, (McGraw-Hill Book Company, New York, 1965).

2. SLATER, J. C., The Electronic Structure of Solids, in Handbuck der Physik, 3rd ed., vol. 19, Springer-Verlag OHG, Berlin, 1956.

3. CALAWAY, J., Energy Band Theory (Academic Press Inc., New York, 1964).

4. LAFON, E. E. and LIN, C. C., Phys. Rev. 152, 579 (1966).

5. CHANEY, R. C., TUNG, T. K., LIN, C. C. and LAFON, E. E., J. Chem Phys. 52, 361 (1970).

6. PROKOFJEW, W., Z. Physik 58, 255 (1929). Discontinuities were found at the boundaries between some of the regions of the potential as expressed in polynomial form in Table I of this reference. These discontinuities can be removed by changing the coefficient -0.0264 in the second region to -0.00264 and the coefficient -1.508 in the fourth region to 1.508. These changes were adopted in our calculations.

7. SCHLOSSER, H. C., and MARCUS, P. M., Phys. Rev. 131, 2529 (1963); SCHLOSSER, H. C. Ph. D. Thesis, Carnegie Institute of Technology, 1960 (unpublished).

8. FOCK, V. and PETRASHEN, M., Physik. Z. Sowjetunion 6, 368 (1934).

9. WOODRUFF, T. O., Solid State Phys. 4, 367 (1957).

10. CLEMENTI, E., IBM Res. Develop. 9, 2 (1965) and the supplement to this paper.

11. BASSANI, F. and YOSHIMINE, M., Phys. Rev. 130, 20 (1963).

12. LAFON, E. E., private communication.

13. STUKEL, D. J. and EUWEMA, R. N., Phys. Rev., B1, 1635 (1970).

14. HUZINAGA, S., J. Chem. Phys. 42, 1293 (1965), Tables XI and XIII.

15. FOCK, V. and PETRASHEN, M. J., Physik Z. Sowjetunion 8, 547 (1935).

16. EWALD, P. P., Ann. Physik 64, 253 (1921); Nachr. Akad. Wiss. Goettingen, Math. Physik. Kl. II. 55 (1938).

17. HAM, F. S., Phys. Rev. 128, 82 (1962).

18. Rudge, W. E., private communication.

19. LAFON, E., Massachusetts Institute of Technology, Solid-State and Molecular Theory Group Quarterly Progress Report No. 69, p. 66, 1968 (unpublished).

20. ROESSLER, D. M. and WALKER, W. C., J. Phys. Chem. Solids 28, 1507 (1967).

21. See, WOOD, R. F. and KORRINGA, J. Phys. Rev. 123, 1138 (1961), and the references listed therein.

Appendix I

The form of the multicenter integrals for the Slater type orbitals of 3s ($r^2 e^{-\alpha r}$), $3p_x$($rxe^{-\alpha r}$), $3d_{xy}$ ($xye^{-\alpha r}$), $3d_{x^2}$($x^2e^{-\alpha r}$) can be obtained by an appropriate differentiation of the 1s, 2s and 2p integrals reported by Lafon and Lin. The differentiation technique which is used in this work was also described in their paper. The potential integrals can be written in the form of

$$\langle\psi^s(A)|\cos(\vec{K}_\nu\cdot\vec{r}_c)|\phi^s(B) = \pi \sum_i B_i \int_0^1 \gamma_i(u)(fg)^{-\ell/2} \{\sum_{n=o}^{6} u_{i,n}(fg)^{n/2}\}$$

$$\exp\{-(fg)^{\frac{1}{2}}\}\{1+\xi_i\}\cos[\vec{K}_\nu\cdot(\vec{r}_{CB} - u\vec{r}_{AB})]$$

$$+ (1-\xi_i)\sin[\vec{K}_\nu\cdot(\vec{r}_{CB} - u\vec{r}_{AB})]\}\, du$$

where

$$f = u(1-u)\, r_{AB}^2$$

$$g = \alpha_1^2/u + \alpha_2^2/(1-u) + K_\nu^2 , \qquad \text{(AI.1)}$$

ℓ is a function of i only, $\vec{r}_{AB}$ is a vector from lattice site A to lattice site B, C is the coordinate system for the Fourier expansion, and $\vec{r}_{CB}$ is a vector from C to lattice site B. The superscript s in Ψ and ϕ stands for unnormalized Slater-type orbitals. It was found that for the potential integrals that there were only ten different types of polynomials of the form of $\sum_{n=o}^{6} u_{i,n}(fg)^{n/2}$ i.e., ten different

sets of $u_{i,n}$. In order to simplify the tabulation of the potential integrals we express these ten different types of polynomials in Table AI-1 and only refer to the polynomial type in the tabulation of the potential integrals which is contained in Table AI-2.

The overlap integrals $\langle\psi^S(A)|\phi^S(B)\rangle$ can be obtained from the potential integrals of Eq. (AI-1) by setting $\vec{K}_\nu = [0,0,0]$.

The kinetic energy integrals can be obtained by the same method of differentiation and have a form similar to the potential integrals,

$$\langle\psi^S(A)|-\tfrac{1}{2}\nabla^2|\phi^S(B)\rangle = \pi \sum_i w_i \int_0^1 n_i(u) \{\sum_{n=o}^{6} \rho_{i,n}$$

$$(fG)^{-\frac{1}{2}(\ell-n)}\} \exp\{-(fG)^{\frac{1}{2}}\}\, du\ ,$$

where

$$G = \alpha_2^2/(1-u) + \alpha_1^2/u \qquad \text{(AI.2)}$$

Table AI-3 lists all of the coefficients appearing in this equation.

TABLE AI-1

Different forms of the polynomial $\sum_{n=o}^{6} \mu_{i,n}(fg)^{n/2}$

Polynomial type	$\mu_{i,0}$	$\mu_{i,1}$	$\mu_{i,2}$	$\mu_{i,3}$	$\mu_{i,4}$	$\mu_{i,5}$	$\mu_{i,6}$
I	3	3	1	0	0	0	0
II	12	12	5	1	0	0	0
III	15	15	6	1	0	0	0
IV	60	60	27	7	1	0	0
V	90	90	39	9	1	0	0
VI	105	105	45	10	1	0	0
VII	630	630	285	75	12	1	0
VIII	840	840	375	95	14	1	0
IX	945	945	420	105	15	1	0
X	10395	10395	4725	1260	210	21	1

TABLE AI-2

Coefficients for $\langle \psi^s(A) | \cos(\vec{K}_\nu \cdot \vec{r}_A) | \phi^s(B) \rangle$

ψ^s	ϕ^s	i	ℓ	B_i	γ_i	Polynomial Type	ξ_i
3s	1s	1	7	$-3\alpha_1\alpha_2\overline{AB}^3$	f^2/u	III	+1
		2	9	$+\alpha_1^3\alpha_2\overline{AB}^3$	f^3/u^2	VI	+1
3s	2s	1	7	$-\alpha_1\overline{AB}^3$	f^2/u	IV	+1
		2	9	$-2\alpha_1\alpha_2^2\overline{AB}^5$	f^2	VI	+1
		3	9	$+\alpha_1\overline{AB}^3K_\nu^2$	f^3/u	VI	+1
		4	11	$+\alpha_1^3\alpha_2^2\overline{AB}^5$	f^3/u	IX	+1
3s	3s	1	9	$-3\alpha_1\alpha_2\overline{AB}^5$	f^2	VII	+1
		2	11	$+3\alpha_1\alpha_2\overline{AB}^5K_\nu^2$	f^3	IX	+1
		3	13	$+\alpha_1^3\alpha_2^3\overline{AB}^7$	f^3	X	+1
$3p_x$	1s	1	5	$-\alpha_2\overline{AB}\ \overline{AB}_x$	f^2/u	I	+1
		2	7	$+\alpha_1^2\alpha_2\overline{AB}\ \overline{AB}_x$	f^3/u^2	III	+1
		3	7	$+\alpha_2(\vec{K}_\nu)_x\overline{AB}^3$	f^2	III	-1
		4	9	$-\alpha_1^2\alpha_2(\vec{K}_\nu)_x\overline{AB}^3$	f^3/u	VI	-1
$3p_x$	2s	1	5	$-\overline{AB}\ \overline{AB}_x$	f^2/u	II	+1
		2	7	$+\overline{AB}\ \overline{AB}_xK_\nu^2$	f^3/u	III	+1

TABLE AI-2 - Continued

ψ^s	ϕ^s	i	ℓ	B_i	γ_i	Polynomial Type	ξ_i
		3	7	$+(\vec{K}_\nu)_\times \overline{AB}^3$	f^2	V	-1
		4	9	$-K_\nu^2 \overline{AB}^3 (\vec{K}_\nu)_\times$	f^3	VI	-1
		5	9	$+\alpha_1^2 \alpha_2^2 \overline{AB}^3 \overline{AB}_\times$	f^3/u	VI	+1
		6	11	$-\alpha_1^2 \alpha_2^2 (\vec{K}_\nu)_\times \overline{AB}^5$	f^3	IX	-1
$3p_\times$	3s	1	7	$-\alpha_2 \overline{AB}^3 \overline{AB}_\times$	f^2	IV	+1
		2	9	$+\alpha_2 \overline{AB}^3 \overline{AB}_\times K_\nu^2$	f^3	VI	+1
		3	9	$-2\alpha_1^2 \alpha_2 \overline{AB}^3 \overline{AB}_\times$	f^3/u	VI	+1
		4	9	$+\alpha_2 \overline{AB}^3 (\vec{K}_\nu)_\times$	$f^3/(1-u)$	VII	-1
		5	11	$-\alpha_2 K_\nu^2 \overline{AB}^3 (\vec{K}_\nu)_\times$	$f^4/(1-u)$	IX	-1
		6	11	$+\alpha_1^2 \alpha_2^3 \overline{AB}^5 (\overline{AB}_\times)$	f^3	IX	+1
		7	11	$+2\alpha_1^2 \alpha_2 (\vec{K}_\nu)_\times \overline{AB}^5$	f^3	IX	-1
		8	13	$-\alpha_1^2 \alpha_2^3 (\vec{K}_\nu)_\times \overline{AB}^5$	$f^4/(1-u)$	X	-1
$2p_\times$	3s	1	7	$-3\alpha_1 \alpha_2 \overline{AB}^3 \overline{AB}_\times$	f^2	III	+1
		2	9	$+3\alpha_1 \alpha_2 \overline{AB}^3 (\vec{K}_\nu)_\times$	$f^3/(1-u)$	VI	-1
		3	9	$+\alpha_1 \alpha_2^3 \overline{AB}^3 \overline{AB}_\times$	$f^3/(1-u)$	VI	+1
		4	11	$-\alpha_1 \alpha_2^3 (\vec{K}_\nu)_\times \overline{AB}^3$	$f^4/(1-u)^2$	IX	-1

TABLE AI-2 - Continued

ψ^s	ϕ^s	i	ℓ	B_i	γ_i	Polynomial Type	ξ_i
$3p_x$	$2p_x$	1	5	$+\alpha_2 \overline{AB}\ \overline{AB}^2_x$	f^2	I	+1
		2	7	$-\alpha_2 \overline{AB}^3$	f^2	III	+1
		3	7	$-\alpha_1^2\alpha_2 \overline{AB}\ \overline{AB}^2_x$	f^3/u	III	+1
		4	7	$-\alpha_2 (\vec{K}_\nu)_x \overline{AB}^3 \overline{AB}_x$	$f^2(2u-1)$	III	-1
		5	9	$+\alpha_1^2\alpha_2 \overline{AB}^3$	f^3/u	VI	+1
		6	9	$+\alpha_2 (\vec{K}_\nu)^2_x \overline{AB}^3$	f^3	VI	+1
		7	9	$+\alpha_1^2\alpha_2 (\vec{K}_\nu)_x \overline{AB}^3 \overline{AB}_x$	$(2u-1)f^3/u$	VI	-1
		8	11	$-\alpha_1^2\alpha_2 (\vec{K}_\nu)^2_x \overline{AB}^3$	f^4/u	IX	+1
$3p_x$	$3p_x$	1	5	$+\ \overline{AB}\ \overline{AB}^2_x$	f^2	II	+1
		2	7	$-\ \overline{AB}\ \overline{AB}^2_x K^2_\nu$	f^3	III	+1
		3	7	$-\ \overline{AB}^3$	f^2	V	+1
		4	7	$-(\vec{K}_\nu)_x \overline{AB}^3 \overline{AB}_x$	$f^2(2u-1)$	V	-1
		5	9	$+\ \overline{AB}^3 K^2_\nu$	f^3	VI	+1
		6	9	$-\alpha_1^2\alpha_2^2 \overline{AB}^3 \overline{AB}^2_x$	f^3	VI	+1
		7	9	$+(\vec{K}_\nu)_x K^2_\nu \overline{AB}^3 \overline{AB}_x$	$f^3(2u-1)$	VI	-1
		8	9	$+(\vec{K}_\nu)^2_x \overline{AB}^3$	f^3	VIII	+1

TABLE AI-2 - Continued

ψ^s	ϕ^s	i	η	B_i	γ_i	Polynomial Type	ξ_i
		9	11	$+\alpha_1^2\alpha_2^2\overline{AB}^5$	f^3	IX	+1
		10	11	$-(\vec{K}_\nu)_x^2 K_\nu^2 \overline{AB}^3$	f^4	IX	+1
		11	11	$+\alpha_1^2\alpha_2^2(\vec{K}_\nu)_x\overline{AB}^5\overline{AB}_x$	$f^3(2u-1)$	IX	-1
		12	13	$-\alpha_1^2\alpha_2^2(\vec{K}_\nu)_x^2\overline{AB}^5$	f^4	X	+1
$3p_x$	$2p_y$	1	5	$+\alpha_2\overline{AB}\ \overline{AB}_x\overline{AB}_y$	f^2	I	+1
		2	7	$-\alpha_1^2\alpha_2\overline{AB}\ \overline{AB}_x\overline{AB}_y$	f^3/u	III	+1
		3	7	$-\alpha_2\overline{AB}^3$	$\{[(\vec{K}_\nu)_x\overline{AB}_y + (\vec{K}_\nu)_y\overline{AB}_x]u - (\vec{K}_\nu)_y\overline{AB}_x\}f^2$	III	-1
		4	9	$+\alpha_1^2\alpha_2\overline{AB}^3$	$\{[(\vec{K}_\nu)_x\overline{AB}_y + (\vec{K}_\nu)_y\overline{AB}_x]u - (\vec{K}_\nu)_y\overline{AB}_x\}f^3/u$	VI	-1
		5	9	$+\alpha_2\overline{AB}^3(\vec{K}_\nu)_x(\vec{K}_\nu)_y$	f^3	VI	+1
		6	11	$-\alpha_1^2\alpha_2\overline{AB}^3(\vec{K}_\nu)_x(\vec{K}_\nu)_y$	f^4/u	IX	+1
$3p_x$	$3p_y$	1	5	$+\ \overline{AB}\ \overline{AB}_x\overline{AB}_y$	f^2	II	+1
		2	7	$-\ \overline{AB}\ \overline{AB}_x\overline{AB}_y K_\nu^2$	f^3	III	+1
		3	7	$-\ \overline{AB}^3$	$\{[(\vec{K}_\nu)_x\overline{AB}_y + (\vec{K}_\nu)_y\overline{AB}_x]u - (\vec{K}_\nu)_y\overline{AB}_x\}f^2$	V	-1

TABLE AI-2 - Continued

ψ^s	ϕ^s	i	ℓ	B_i	γ_i	Polynomial Type	ξ_i
		4	9	$-\alpha_1^2\alpha_2^2\overline{AB}^3\overline{AB}_x\overline{AB}_y$	f^3	VI	+1
		5	9	$+\overline{AB}^3K_\nu^2$	$\{[(K_\nu)_x\overline{AB}_y+(\vec{K}_\nu)_y\overline{AB}_x]u-(\vec{K}_\nu)_y\overline{AB}_x\}f^3$	VI	-1
		6	9	$+\overline{AB}^3(\vec{K}_\nu)_x(\vec{K}_\nu)_y$	f^3	VIII	+1
		7	11	$+\alpha_1^2\alpha_2^2\overline{AB}^5$	$\{[(\vec{K}_\nu)_x\overline{AB}_y+(\vec{K}_\nu)_y\overline{AB}_x]u-(\vec{K}_\nu)_y\overline{AB}_x\}f^3$	IX	-1
		8	11	$-\overline{AB}^3(\vec{K}_\nu)_x(\vec{K}_\nu)_yK_\nu^2$	f^4	IX	+1
		9	13	$-\alpha_1^2\alpha_2^2\overline{AB}^5(\vec{K}_\nu)_x(\vec{K}_\nu)_y$	f^4	X	+1
$3d_{x^2}$	1s	1	5	$+\alpha_1\alpha_2\overline{AB}_x^2/\overline{AB}$	f^3/u^2	I	+1
		2	7	$+\alpha_1\alpha_2\overline{AB}^3$	f^2/u	III	+1
		3	7	$-\alpha_1\alpha_2\overline{AB}$	f^3/u^2	III	+1
		4	7	$-2\alpha_1\alpha_2\overline{AB}\,\overline{AB}_x(K_\nu)_x$	f^3/u	III	-1
		5	9	$-\alpha_1\alpha_2\overline{AB}^3(K_\nu)_x^2$	f^3	VI	+1
$3d_{x^2}$	2s	1	5	$-\alpha_1\overline{AB}_x^2/\overline{AB}$	f^3/u^2	I	+1
		2	7	$+2\alpha_1\overline{AB}\,\overline{AB}_x(K_\nu)_x$	f^3/u	III	-1

TABLE AI-2 - Continued

ψ^s	ϕ^s	i	ℓ	B_i	γ_i	Polynomial Type	ξ_i
		3	7	$+\alpha_1 \overline{AB}$	f^3/u^2	III	+1
		4	7	$+\alpha_1 \alpha^2 \overline{AB}\ \overline{AB}^2_\times$	f^3/u	III	+1
		5	7	$-\alpha_1 \overline{AB}^3$	f^2/u	III	+1
		6	9	$-2\alpha_1 \alpha^2 \overline{AB}^3 \overline{AB}_\times (K_\nu)_\times$	f^3	VI	-1
		7	9	$+\alpha_1 \overline{AB}^3 (K_\nu)^2_\times$	f^3	VI	+1
		8	9	$-\alpha_1 \alpha^2 \overline{AB}^3$	f^3/u	VI	+1
		9	9	$+\alpha_1 \alpha^2 \overline{AB}^5$	f^2	VI	+1
		10	11	$-\alpha_1 \alpha^2 \overline{AB}^3 (K_\nu)^2_\times$	$f^4/(1-u)$	IX	+1
$3d_{x^2}$	3s	1	7	$-3\alpha_1 \alpha_2 \overline{AB}\ \overline{AB}^2_\times$	f^3/u	III	+1
		2	9	$+6\alpha_1 \alpha_2 \overline{AB}^3 \overline{AB}_\times (K_\nu)_\times$	f^3	VI	-1
		3	9	$+3\alpha_1 \alpha_2 \overline{AB}^3$	f^3/u	VI	+1
		4	9	$+\alpha_1 \alpha_2 {}^3\overline{AB}^3 \overline{AB}^2_\times$	f^3	VI	+1
		5	9	$-3\alpha_1 \alpha_2 \overline{AB}^5$	f^2	VI	+1
		6	11	$-2\alpha_1 \alpha_2 {}^3\overline{AB}^3 \overline{AB}_\times (K_\nu)_\times$	$f^4/(1-u)$	IX	-1
		7	11	$+3\alpha_1 \alpha_2 \overline{AB}^3 (K_\nu)^2_\times$	$f^4/(1-u)$	IX	+1
		8	11	$-\alpha_1 \alpha_2 {}^3\overline{AB}^5$	f^3	IX	+1
		9	11	$+\alpha_1 \alpha_2 {}^3\overline{AB}^5$	$f^3/(1-u)$	IX	+1
		10	13	$-\alpha_1 \alpha_2 {}^3\overline{AB}^3 (K_\nu)^2_\times$	$f^5/(1-u)^2$	X	+1

TABLE AI-2 - Continued

ψ^s	ϕ^s	i	ℓ	B_i	γ_i	Polynomial Type	ξ_i
$3d_{x^2}$	$2p_x$	1	5	$-\alpha_1\alpha_2\overline{AB}_x^3/\overline{AB}$	f^3/u	I	+1
		2	7	$+2\alpha_1\alpha_2\overline{AB}\ \overline{AB}_x^2(K_\nu)_x$	f^3	III	-1
		3	7	$+3\alpha_1\alpha_2\overline{AB}\ \overline{AB}_x$	f^3/u	III	+1
		4	7	$-\alpha_1\alpha_2\overline{AB}_x^2(K_\nu)_x/\overline{AB}$	f^4/u^2	III	-1
		5	7	$-\alpha_1\alpha_2\overline{AB}^3\overline{AB}_x$	f^2	III	+1
		6	9	$-2\alpha_1\alpha_2\overline{AB}^3(K_\nu)_x$	f^3	VI	-1
		7	9	$-2\alpha_1\alpha_2\overline{AB}\ \overline{AB}_x(K_\nu)_x^2$	f^4/u	VI	+1
		8	9	$+\alpha_1\alpha_2\overline{AB}\ \overline{AB}_x(K_\nu)_x^2$	$f^4/(1-u)$	VI	+1
		9	9	$+\alpha_1\alpha_2\overline{AB}(K_\nu)_x$	f^4/u^2	VI	-1
		10	9	$-\alpha_1\alpha_2\overline{AB}^3(K_\nu)_x$	f^3/u	VI	-1
		11	11	$+\alpha_1\alpha_2\overline{AB}^3(K_\nu)_x^3$	f^4	IX	-1
$3d_{x2}$	$3p_x$	1	5	$+\alpha_1\overline{AB}_x^3/\overline{AB}$	f^3/u	I	+1
		2	7	$-2\alpha_1\overline{AB}\ \overline{AB}_x^2(K_\nu)_x$	f^3	III	-1
		3	7	$-3\alpha_1\overline{AB}\ \overline{AB}_x$	f^3/u	III	+1
		4	7	$-\alpha_1\alpha_2^2\overline{AB}\ \overline{AB}_x^3$	f^3	III	+1
		5	7	$+\alpha_1\overline{AB}_x^2(K_\nu)_x/\overline{AB}$	f^4/u^2	III	-1
		6	7	$+\alpha_1\overline{AB}^3\overline{AB}_x$	f^2	III	+1

TABLE AI-2 - Continued

ψ^s	ϕ^s	i	ℓ	B_i	γ_i	Polynomial Type	ξ_i
		7	9	$+2\alpha_1 \overline{AB}^3 (K_\nu)_\times$	f^3	VI	-1
		8	9	$+2\alpha_1\alpha_2^2 \overline{AB}\ \overline{AB}^2_\times (K_\nu)_\times$	$f^4/(1-u)$	VI	-1
		9	9	$+2\alpha_1 \overline{AB}\ \overline{AB}_\times (K_\nu)^2_\times$	f^4/u	VI	+1
		10	9	$-\alpha_1 \overline{AB}\ \overline{AB}_\times (K_\nu)^2_\times$	$f^4/(1-u)$	VI	+1
		11	9	$+3\alpha_1\alpha_2^2 \overline{AB}^3 \overline{AB}_\times$	f^3	VI	+1
		12	9	$-\alpha_1 \overline{AB} (K_\nu)_\times$	f^4/u^2	VI	-1
		13	9	$-\alpha_1\alpha_2^2 \overline{AB}\ \overline{AB}^2_\times (K_\nu)_\times$	f^4/u	VI	-1
		14	9	$-\alpha_1\alpha_2^2 \overline{AB}^3 \overline{AB}_\times$	$f^3/(1-u)$	VI	+1
		15	9	$+\alpha_1 \overline{AB}^3 (K_\nu)_\times$	f^3/u	VI	-1
		16	11	$-2\alpha_1\alpha_2^2 \overline{AB}^3 (K_\nu)_\times$	$f^4/(1-u)$	IX	-1
		17	11	$-2\alpha_1\alpha_2^2 \overline{AB}^3 \overline{AB}_\times (K_\nu)^2_\times$	f^4	IX	+1
		18	11	$+\alpha_1\alpha_2^2 \overline{AB}\ \overline{AB}_\times (K_\nu)^2_\times$	$f^5/(1-u)^2$	IX	+1
		19	11	$-\alpha_1 \overline{AB}^3 (K_\nu)^3_\times$	f^4	IX	-1
		20	11	$+\alpha_1\alpha_2^2 \overline{AB}^3 (K_\nu)_\times$	f^4/u	IX	-1
		21	11	$-\alpha_1\alpha_2^2 \overline{AB}^5 (K_\nu)_\times$	f^3	IX	-1
		22	13	$+\alpha_1\alpha_2^2 \overline{AB}^3 (K_\nu)^3_\times$	$f^5/(1-u)$	X	-1

TABLE AI-2 - Continued

ψ^s	ϕ^s	i	ℓ	B_i	γ_i	Polynomial Type	ξ_i
$3d_{x^2}$	$2p_y$	1	5	$-\alpha_1\alpha_2\overline{AB^2_x AB}_y/\overline{AB}$	f^3/u	I	+1
		2	7	$+2\alpha_1\alpha_2\overline{AB}\ \overline{AB}_x\overline{AB}_y(K_\nu)_x$	f^3	III	-1
		3	7	$+\alpha_1\alpha_2\overline{AB}\ \overline{AB}_y$	f^3/u	III	+1
		4	7	$-\alpha_1\alpha_2\overline{AB^2_x}(K_\nu)_y/\overline{AB}$	f^4/u^2	III	-1
		5	7	$-\alpha_1\alpha_2\overline{AB^3 AB}_y$	f^2	III	+1
		6	9	$-2\alpha_1\alpha_2\overline{AB}\ \overline{AB}_x(K_\nu)_x(K_\nu)_y$	f^4/u	VI	+1
		7	9	$+\alpha_1\alpha_2\overline{AB}\ \overline{AB}_y(K_\nu)^2_x$	$f^4/(1-u)$	VI	+1
		8	9	$+\alpha_1\alpha_2\overline{AB}(K_\nu)_y$	f^4/u^2	VI	-1
		9	9	$-\alpha_1\alpha_2\overline{AB^3}(K_\nu)_y$	f^3/u	VI	-1
		10	11	$+\alpha_1\alpha_2\overline{AB^3}(K_\nu)^2_x(K_\nu)_y$	f^4	IX	-1
$3d_{x^2}$	$3p_y$	1	5	$+\alpha_1\overline{AB^2_x AB}_y/\overline{AB}$	f^3/u	I	+1
		2	7	$-2\alpha_1\overline{AB}\ \overline{AB}_x\overline{AB}_y(K_\nu)_x$	f^3	III	-1
		3	7	$-\alpha_1\overline{AB}\ \overline{AB}_y$	f^3/u	III	+1
		4	7	$-\alpha_1\alpha^2_2\overline{AB}\ \overline{AB^2_x AB}_y$	f^3	III	+1
		5	7	$+\alpha_1\overline{AB^2_x}(K_\nu)_y/\overline{AB}$	f^4/u^2	III	-1
		6	7	$+\alpha_1\overline{AB^3 AB}_y$	f^2	III	+1

TABLE AI-2 - Continued

ψ^s	ϕ^s	i	ℓ	B_i	γ_i	Polynomial Type	ξ_i
		7	9	$+2\alpha_1\alpha_2^2\overline{AB}\ \overline{AB}_x\overline{AB}_y(K_\nu)_x$	$f^4/(1-u)$	VI	-1
		8	9	$+2\alpha_1\overline{AB}\ \overline{AB}_x(K_\nu)_x(K_\nu)_y$	f^4/u	VI	+1
		9	9	$-\alpha_1\overline{AB}\ \overline{AB}_y(K_\nu)_x^2$	$f^4/(1-u)$	VI	+1
		10	9	$+\alpha_1\alpha_2^2\overline{AB}^3\overline{AB}_y$	f^3	VI	+1
		11	9	$-\alpha_1\overline{AB}(K_\nu)_y$	f^4/u^2	VI	-1
		12	9	$-\alpha_1\alpha_2^2\overline{AB}\ \overline{AB}_x^2(K_\nu)_y$	f^4/u	VI	-1
		13	9	$-\alpha_1\alpha_2^2\overline{AB}^3\overline{AB}_y$	$f^3/(1-u)$	VI	+1
		14	9	$+\alpha_1\overline{AB}^3(K_\nu)_y$	f^3/u	VI	-1
		15	11	$-2\alpha_1\alpha_2^2\overline{AB}^3\overline{AB}_x(K_\nu)_x(K_\nu)_y$	f^4	IX	+1
		16	11	$+\alpha_1\alpha_2^2\overline{AB}\ \overline{AB}_y(K_\nu)_x^2$	$f^5/(1-u)^2$	IX	+1
		17	11	$-\alpha_1\overline{AB}^3(K_\nu)_x^2(K_\nu)_y$	f^4	IX	-1
		18	11	$+\alpha_1\alpha_2^2\overline{AB}^3(K_\nu)_y$	f^4/u	IX	-1
		19	11	$-\alpha_1\alpha_2^2\overline{AB}^5(K_\nu)_y$	f^3	IX	-1
		20	13	$+\alpha_1\alpha_2^2\overline{AB}^3(K_\nu)_x^2(K_\nu)_y$	$f^5/(1-u)$	X	-1
$3d_{x^2}$	$3d_{yz}$	1	5	$+\alpha_1\alpha_2\overline{AB}_x^2\overline{AB}_y\overline{AB}_z/\overline{AB}$	f^3	I	+1
		2	7	$-2\alpha_1\alpha_2\overline{AB}_x\overline{AB}_y\overline{AB}_z(K_\nu)_x/\overline{AB}$	$f^4/(1-u)$	III	-1
		3	7	$-\alpha_1\alpha_2\overline{AB}\ \overline{AB}_y\overline{AB}_z$	f^3	III	+1

TABLE AI-2 - Continued

ψ^s	ϕ^s	i	ℓ	B_i	γ_i	Polynomial Type	ξ_i
		4	7	$+\alpha_1\alpha_2\overline{AB}^2_x\overline{AB}_z(K_\nu)_y/\overline{AB}$	f^4/u	III	-1
		5	7	$+\alpha_1\alpha_2\overline{AB}^2_x\overline{AB}_y(K_\nu)_z/\overline{AB}$	f^4/u	III	-1
		6	7	$+\alpha_1\alpha_2\overline{AB}\ \overline{AB}_y\overline{AB}_z$	$f^3/(1-u)$	III	+1
		7	9	$+2\alpha_1\alpha_2\overline{AB}\ \overline{AB}_x\overline{AB}_z(K_\nu)_x(K_\nu)_y$	f^4	VI	+1
		8	9	$+2\alpha_1\alpha_2\overline{AB}\ \overline{AB}_x\overline{AB}_y(K_\nu)_x(K_\nu)_z$	f^4	VI	+1
		9	9	$-\alpha_1\alpha_2\overline{AB}_y\overline{AB}_z(K_\nu)^2_x/\overline{AB}$	$f^5/(1-u)^2$	VI	+1
		10	9	$-\alpha_1\alpha_2\overline{AB}\ \overline{AB}_z(K_\nu)_y$	f^4/u	VI	-1
		11	9	$-\alpha_1\alpha_2\overline{AB}\ \overline{AB}_y(K_\nu)_z$	f^4/u	VI	-1
		12	9	$-\alpha_1\alpha_2\overline{AB}^2_x(K_\nu)_y(K_\nu)_z/\overline{AB}$	f^5/u^2	VI	+1
		13	9	$+\alpha_1\alpha_2\overline{AB}^3\overline{AB}_z(K_\nu)_y$	f^3	VI	-1
		14	9	$+\alpha_1\alpha_2\overline{AB}^3\overline{AB}_y(K_\nu)_z$	f^3	VI	-1
		15	11	$+2\alpha_1\alpha_2\overline{AB}\ \overline{AB}_x(K_\nu)_x(K_\nu)_y(K_\nu)_z$	f^5/u	IX	-1
		16	11	$-\alpha_1\alpha_2\overline{AB}\ \overline{AB}_z(K_\nu)^2_x(K_\nu)_y$	$f^5/(1-u)$	IX	-1
		17	11	$-\alpha_1\alpha_2\overline{AB}\ \overline{AB}_y(K_\nu)^2_x(K_\nu)_z$	$f^5/(1-u)$	IX	-1
		18	11	$+\alpha_1\alpha_2\overline{AB}(K_\nu)_y(K_\nu)_z$	f^5/u^2	IX	+1
		19	11	$-\alpha_1\alpha_2\overline{AB}^3(K_\nu)_y(K_\nu)_z$	f^4/u	IX	+1
		20	13	$+\alpha_1\alpha_2\overline{AB}^3(K_\nu)^2_x(K_\nu)_y(K_\nu)_z$	f^3	X	+1

TABLE AI-2 - Continued

ψ^s	ϕ^s	i	ℓ	B_i	γ_i	Polynomial Type	ξ_i
$3d_{x^2}$	$3d_{xy}$	1	5	$+\alpha_1\alpha_2\overline{AB}_x^3\overline{AB}_y/\overline{AB}$	f^3	I	+1
		2	7	$-2\alpha_1\alpha_2\overline{AB}_x^2\overline{AB}_y(K_\nu)_x/\overline{AB}$	$f^4/(1-u)$	III	-1
		3	7	$-3\alpha_1\alpha_2\overline{AB}\ \overline{AB}_x\overline{AB}_y$	f^3	III	+1
		4	7	$+\alpha_1\alpha_2\overline{AB}_x^3(K_\nu)_y/\overline{AB}$	f^4/u	III	-1
		5	7	$+\alpha_1\alpha_2\overline{AB}_x^2\overline{AB}_y(K_\nu)_x/\overline{AB}$	f^4/u	III	-1
		6	7	$+\alpha_1\alpha_2\overline{AB}\ \overline{AB}_x\overline{AB}_y$	$f^3/(1-u)$	III	+1
		7	9	$+2\alpha_1\alpha_2\overline{AB}\ \overline{AB}_y(K_\nu)_x$	$f^4/(1-u)$	VI	-1
		8	9	$+2\alpha_1\alpha_2\overline{AB}\ \overline{AB}_x^2(K_\nu)_x(K_\nu)_y$	f^4	VI	+1
		9	9	$+2\alpha_1\alpha_2\overline{AB}\ \overline{AB}_x\overline{AB}_y(K_\nu)_x^2$	f^4	VI	+1
		10	9	$-\alpha_1\alpha_2\overline{AB}_x\overline{AB}_y(K_\nu)_x^2/\overline{AB}$	$f^5/(1-u)^2$	VI	+1
		11	9	$-3\alpha_1\alpha_2\overline{AB}\ \overline{AB}_x(K_\nu)_y$	f^4/u	VI	-1
		12	9	$-\alpha_1\alpha_2\overline{AB}\ \overline{AB}_y(K_\nu)_x$	f^4/u	VI	-1
		13	9	$-\alpha_1\alpha_2\overline{AB}_x^2(K_\nu)_x(K_\nu)_y/\overline{AB}$	f^5/u^2	VI	+1
		14	9	$+\alpha_1\alpha_2\overline{AB}^3\overline{AB}_x(K_\nu)_y$	f^3	VI	-1
		15	9	$+\alpha_1\alpha_2\overline{AB}^3\overline{AB}_y(K_\nu)_x$	f^3	VI	-1
		16	11	$-2\alpha_1\alpha_2\overline{AB}^3(K_\nu)_x(K_\nu)_y$	f^4	IX	+1
		17	11	$+2\alpha_1\alpha_2\overline{AB}\ \overline{AB}_x(K_\nu)_x^2(K_\nu)_y$	f^5/u	IX	-1

TABLE AI-2 - Continued

ψ^s	ϕ^s	i	ℓ	B_i	γ_i	Polynomial Type	ξ_i
		18	11	$-\alpha_1\alpha_2\overline{AB}\ \overline{AB}_x(K_\nu)_x^2(K_\nu)_y$	$f^5/(1-u)$	IX	-1
		19	11	$-\alpha_1\alpha_2\overline{AB}\ \overline{AB}_y(K_\nu)_{x5}$	$f^5/(1-u)$	IX	-1
		20	11	$+\alpha_1\alpha_2\overline{AB}\ (K_\nu)_x(K_\nu)_y$	f^5/u^2	IX	+1
		21	11	$-\alpha_1\alpha_2\overline{AB}^3(K_\nu)_x(K_\nu)_y$	f^4/u	IX	+1
		22	13	$+\alpha_1\alpha_2\overline{AB}^3(K_\nu)_x^3(K_\nu)_y$	f^5	X	+1
$3d_{x^2}$	$3d_{y^2}$	1	5	$+\alpha_1\alpha_2\overline{AB}_x^2\overline{AB}_y^2/\overline{AB}$	f^3	I	+1
		2	7	$-2\alpha_1\alpha_2\overline{AB}_x\overline{AB}_y^2(K_\nu)_x/\overline{AB}$	$f^4/(1-u)$	III	-1
		3	7	$-\alpha_1\alpha_2\overline{AB}\ \overline{AB}_y^2$	f^3	III	+1
		4	7	$-\alpha_1\alpha_2\overline{AB}\ \overline{AB}_x^2$	f^3	III	+1
		5	7	$+2\alpha_1\alpha_2\overline{AB}_x^2\overline{AB}_y(K_\nu)_y/\overline{AB}$	f^4/u	III	-1
		6	7	$+\alpha_1\alpha_2\overline{AB}\ \overline{AB}_y^2$	$f^3/(1-u)$	III	+1
		7	7	$+\alpha_1\alpha_2\overline{AB}\ \overline{AB}_x^2$	f^3/u	III	+1
		8	9	$+2\alpha_1\alpha_2\overline{AB}\ \overline{AB}_x(K_\nu)_x$	$f^4/(1-u)$	VI	-1
		9	9	$+4\alpha_1\alpha_2\overline{AB}\ \overline{AB}_x\overline{AB}_y(K_\nu)_x(K_\nu)_y$	f^4	VI	+1
		10	9	$-\alpha_1\alpha_2\overline{AB}_y^2(K_\nu)_x^2/\overline{AB}$	$f^5/(1-u)^2$	VI	+1
		11	9	$+\alpha_1\alpha_2\overline{AB}^3$	f^3	VI	+1
		12	9	$-2\alpha_1\alpha_2\overline{AB}\ \overline{AB}_y(K_\nu)_y$	f^4/u	VI	-1

TABLE AI-2 - Continued

ψ^s	ϕ^s	i	ℓ	B_i	γ_i	Polynomial Type	ξ_i
		13	9	$-\alpha_1\alpha_2\overline{AB}^2_x(K_\nu)^2_y/\overline{AB}$	f^5/u^2	VI	+1
		14	9	$-\alpha_1\alpha_2\overline{AB}^3$	$f^3/(1-u)$	VI	+1
		15	9	$+2\alpha_1\alpha_2\overline{AB}^3\overline{AB}_y(K_\nu)_y$	f^3	VI	-1
		16	9	$-2\alpha_1\alpha_2\overline{AB}^3\overline{AB}_x(K_\nu)_x$	f^3	VI	-1
		17	9	$-\alpha_1\alpha_2\overline{AB}^3$	f^3/u	VI	+1
		18	9	$+\alpha_1\alpha_2\overline{AB}^5$	f^2	VI	+1
		19	11	$+2\alpha_1\alpha_2\overline{AB}\ \overline{AB}_x(K_\nu)_x(K_\nu)^2_y$	f^5/u	IX	-1
		20	11	$+\alpha_1\alpha_2\overline{AB}\ (K_\nu)^2_x$	$f^5/(1-u)^2$	IX	+1
		21	11	$-2\alpha_1\alpha_2\overline{AB}\ \overline{AB}_y(K_\nu)^2_x(K_\nu)_y$	$f^5/(1-u)$	IX	-1
		22	11	$+\alpha_1\alpha_2\overline{AB}(K_\nu)^2_y$	f^5/u^2	IX	+1
		23	11	$-\alpha_1\alpha_2\overline{AB}^3(K_\nu)^2_y$	f^4/u	IX	+1
		24	11	$-\alpha_1\alpha_2\overline{AB}^3(K_\nu)^2_x$	$f^4/(1-u)$	IX	+1
		25	13	$+\alpha_1\alpha_2\overline{AB}^3(K_\nu)^2_x(K_\nu)^2_y$	f^5	X	+1
$3d_{x^2}$	$3d_{x^2}$	1	5	$+\alpha_1\alpha_2\overline{AB}^4_x/\overline{AB}$	f^3	I	+1
		2	7	$-2\alpha_1\alpha_2\overline{AB}^3_x(K_\nu)_x/\overline{AB}$	$f^4/(1-u)$	III	-1
		3	7	$-6\alpha_1\alpha_2\overline{AB}\ \overline{AB}^2_x$	f^3	III	+1
		4	7	$+2\alpha_1\alpha_2\overline{AB}^3_x(K_\nu)_x/\overline{AB}$	f^4/u	III	-1

TABLE AI-2 - Continued

ψ^s	ϕ^s	i	ℓ	B_i	γ_i	Polynomial Type	ξ_i
		5	7	$+\alpha_1\alpha_2\overline{AB}\ \overline{AB}_x^2$	$f^3/(1-u)$	III	+1
		6	7	$+\alpha_1\alpha_2\overline{AB}\ \overline{AB}_x^2$	f^3/u	III	+1
		7	9	$+6\alpha_1\alpha_2\overline{AB}\ \overline{AB}_x(K_\nu)_x$	$f^4/(1-u)$	VI	-1
		8	9	$+4\alpha_1\alpha_2\overline{AB}\ \overline{AB}_x^2(K_\nu)_x^2$	f^4	VI	+1
		9	9	$-\alpha_1\alpha_2\overline{AB}_x^2(K_\nu)_x^2/\overline{AB}$	$f^5/(1-u)^2$	VI	+1
		10	9	$+3\alpha_1\alpha_2\overline{AB}^3$	f^3	VI	+1
		11	9	$-6\alpha_1\alpha_2\overline{AB}\ \overline{AB}_x(K_\nu)_x$	f^4/u	VI	-1
		12	9	$-\alpha_1\alpha_2\overline{AB}_x^2(K_\nu)_x^2/\overline{AB}$	f^5/u^2	VI	+1
		13	9	$-\alpha_1\alpha_2\overline{AB}^3$	$f^3/(1-u)$	VI	+1
		14	9	$-\alpha_1\alpha_2\overline{AB}^3$	f^3/u	VI	+1
		15	9	$+\alpha_1\alpha_2\overline{AB}^5$	f^2	VI	+1
		16	11	$-4\alpha_1\alpha_2\overline{AB}^3(K_\nu)_x^2$	f^4	IX	+1
		17	11	$+2\alpha_1\alpha_2\overline{AB}\ \overline{AB}_x(K_\nu)_x^3$	f^5/u	IX	-1
		18	11	$+\alpha_1\alpha_2\overline{AB}\ (K_\nu)_x^2$	$f^5/(1-u)^2$	IX	+1
		19	11	$-2\alpha_1\alpha_2\overline{AB}\ \overline{AB}_x(K_\nu)_x^3$	$f^5/(1-u)$	IX	-1
		20	11	$+\alpha_1\alpha_2\overline{AB}\ (K_\nu)_x^2$	f^5/u^2	IX	+1
		21	11	$-\alpha_1\alpha_2\overline{AB}^3(K_\nu)_x^2$	$f^4/(1-u)$	IX	+1

TABLE AI-2 - Continued

ψ^s	ϕ^s	i	ℓ	B_i	γ_i	Polynomial Type	ξ_i
		22	11	$-\alpha_1\alpha_2\overline{AB}^3(K_\nu)^2_\times$	f^4/u	IX	+1
		23	13	$+\alpha_1\alpha_2\overline{AB}^3(K_\nu)^4_\times$	f^5	X	+1
$3d_{xy}$	1s	1	5	$+\alpha_1\alpha_2\overline{AB}_x\overline{AB}_y/\overline{AB}$	f^3/u^2	I	+1
		2	7	$-\alpha_1\alpha_2\overline{AB}\ \overline{AB}_y(K_\nu)_\times$	f^3/u	III	-1
		3	7	$-\alpha_1\alpha_2\overline{AB}\ \overline{AB}_x(K_\nu)_y$	f^3/u	III	-1
		4	9	$-\alpha_1\alpha_2\overline{AB}^3(K_\nu)_\times(K_\nu)_y$	f^3	VI	+1
$3d_{xy}$	2s	1	5	$-\alpha_1\overline{AB}_x\overline{AB}_y/\overline{AB}$	f^3/u^2	I	+1
		2	7	$+\alpha_1\overline{AB}\ \overline{AB}_y(K_\nu)_\times$	f^3/u	III	-1
		3	7	$+\alpha_1\alpha_2^2\overline{AB}\ \overline{AB}_x\overline{AB}_y$	f^3/u	III	+1
		4	7	$+\alpha_1\overline{AB}\ \overline{AB}_x(K_\nu)_y$	f^3/u	III	-1
		5	9	$-\alpha_1\alpha_2^2\overline{AB}^3\overline{AB}_y(K_\nu)_\times$	f^3	VI	-1
		6	9	$+\alpha_1\overline{AB}^3(K_\nu)_\times(K_\nu)_y$	f^3	VI	+1
		7	9	$-\alpha_1\alpha_2^2\overline{AB}^3\overline{AB}_x(K_\nu)_y$	f^3	VI	-1
		8	11	$-\alpha_1\alpha_2^2\overline{AB}^3(K_\nu)_\times(K_\nu)_y$	$f^4/(1-u)$	IX	+1
$3d_{xy}$	3s	1	7	$-3\alpha_1\alpha_2\overline{AB}\ \overline{AB}_x\overline{AB}_y$	f^3/u	III	+1
		2	9	$+3\alpha_1\alpha_2\overline{AB}^3\overline{AB}_y(K_\nu)_\times$	f^3	VI	-1
		3	9	$+\alpha_1\alpha_2^3\overline{AB}^3\overline{AB}_x\overline{AB}_y$	f^3	VI	+1

TABLE AI-2 - Continued

ψ^s	ϕ^s	i	ℓ	B_i	γ_i	Polynomial Type	ξ_i
		4	9	$+3\alpha_1\alpha_2\overline{AB}^3\overline{AB}_x(K_\nu)_y$	f^3	VI	-1
		5	11	$-\alpha_1\alpha_2^3\overline{AB}^3\overline{AB}_y(K_\nu)_x$	$f^4/(1-u)$	IX	-1
		6	11	$+3\alpha_1\alpha_2\overline{AB}^3(K_\nu)_x(K_\nu)_y$	$f^4/(1-u)$	IX	+1
		7	11	$-\alpha_1\alpha_2^3\overline{AB}^3\overline{AB}_x(K_\nu)_y$	$f^4/(1-u)$	IX	-1
		8	13	$-\alpha_1\alpha_2^3\overline{AB}^3(K_\nu)_x(K_\nu)_y$	$f^5/(1-u)^2$	X	+1
$3d_{xy}$	$2p_x$	1	5	$-\alpha_1\alpha_2\overline{AB}_x^2\overline{AB}_y/\overline{AB}$	f^3/u	I	+1
		2	7	$+\alpha_1\alpha_2\overline{AB}\ \overline{AB}_y$	f^3/u	III	+1
		3	7	$+\alpha_1\alpha_2\overline{AB}\ \overline{AB}_x\overline{AB}_y(K_\nu)_x$	f^3	III	-1
		4	7	$-\alpha_1\alpha_2\overline{AB}_x\overline{AB}_y(K_\nu)_x/\overline{AB}$	f^4/u^2	III	-1
		5	7	$+\alpha_1\alpha_2\overline{AB}\ \overline{AB}_x^2(K_\nu)_y$	f^3	III	-1
		6	9	$-\alpha_1\alpha_2\overline{AB}\ \overline{AB}_y(K_\nu)_x^2$	f^4/u	VI	+1
		7	9	$-\alpha_1\alpha_2\overline{AB}^3(K_\nu)_y$	f^3	VI	-1
		8	9	$+\alpha_1\alpha_2\overline{AB}\ \overline{AB}_x(K_\nu)_x(K_\nu)_y$	$f^4/(1-u)$	VI	+1
		9	9	$-\alpha_1\alpha_2\overline{AB}\ \overline{AB}_x(K_\nu)_x(K_\nu)_y$	f^4/u	VI	+1
		10	11	$+\alpha_1\alpha_2\overline{AB}^3(K_\nu)_x^2(K_\nu)_y$	f^4	IX	-1
$3d_{xy}$	$3p_x$	1	5	$+\alpha_1\overline{AB}_x^2\overline{AB}_y/\overline{AB}$	f^3/u	I	+1
		2	7	$-\alpha_1\overline{AB}\ \overline{AB}_y$	f^3/u	III	+1

TABLE AI-2 - Continued

ψ^s	ϕ^s	i	ℓ	B_i	γ_i	Polynomial Type	ξ_i
		3	7	$-\alpha_1 \overline{AB}\ \overline{AB}_x \overline{AB}_y (K_\nu)_x$	f^3	III	-1
		4	7	$+\alpha_1 \overline{AB}_x \overline{AB}_y (K_\nu)_x / \overline{AB}$	f^4/u^2	III	-1
		5	7	$-\alpha_1 \alpha_2^2 \overline{AB}\ \overline{AB}_x^2 \overline{AB}_y$	f^3	III	+1
		6	7	$-\alpha_1 \overline{AB}\ \overline{AB}_x^2 (K_\nu)_y$	f^3	III	-1
		7	9	$+\alpha_1 \overline{AB}\ \overline{AB}_y (K_\nu)_x^2$	f^4/u	VI	+1
		8	9	$+\alpha_1 \alpha_2^2 \overline{AB}^3 \overline{AB}_y$	f^3	VI	+1
		9	9	$+\alpha_1 \overline{AB}^3 (K_\nu)_y$	f^3	VI	-1
		10	9	$+\alpha_1 \alpha_2^2 \overline{AB}\ \overline{AB}_x \overline{AB}_y (K_\nu)_x$	$f^4/(1-u)$	VI	-1
		11	9	$-\alpha_1 \overline{AB}\ \overline{AB}_x (K_\nu)_x (K_\nu)_y$	$f^4/(1-u)$	VI	+1
		12	9	$-\alpha_1 \alpha_2^2 \overline{AB}\ \overline{AB}_x \overline{AB}_y (K_\nu)_x$	f^4/u	VI	-1
		13	9	$+\alpha_1 \overline{AB}\ \overline{AB}_x (K_\nu)_x (K_\nu)_y$	f^4/u	VI	+1
		14	9	$+\alpha_1 \alpha_2^2 \overline{AB}\ \overline{AB}_x^2 (K_\nu)_y$	$f^4/(1-u)$	VI	-1
		15	11	$-\alpha_1 \alpha_2^2 \overline{AB}^3 \overline{AB}_y (K_\nu)_x^2$	f^4	IX	+1
		16	11	$-\alpha_1 \overline{AB}^3 (K_\nu)_x^2 (K_\nu)_y$	f^4	IX	-1
		17	11	$-\alpha_1 \alpha_2^2 \overline{AB}^3 (K_\nu)_y$	$f^4/(1-u)$	IX	-1
		18	11	$+\alpha_1 \alpha_2^2 \overline{AB}\ \overline{AB}_x (K_\nu)_x (K_\nu)_y$	$f^5/(1-u)^2$	IX	+1
		19	11	$-\alpha_1 \alpha_2^2 \overline{AB}^3 \overline{AB}_x (K_\nu)_x (K_\nu)_y$	f^4	IX	+1

TABLE AI-2 - Continued

ψ^s	ϕ^s	i	ℓ	B_i	γ_i	Polynomial Type	ξ_i
		20	13	$+\alpha_1\alpha_2^2\overline{AB}^3(K_\nu)_x^2(K_\nu)_y$	$f^5/(1-u)$	X	-1
$3d_{xy}$	$2p_z$	1	5	$-\alpha_1\alpha_2\overline{AB}_x\overline{AB}_y\overline{AB}_z/\overline{AB}$	f^3/u	I	+1
		2	7	$+\alpha_1\alpha_2\overline{AB}\ \overline{AB}_y\overline{AB}_z(K_\nu)_x$	f^3	III	-1
		3	7	$-\alpha_1\alpha_2\overline{AB}_x\overline{AB}_y(K_\nu)_z/\overline{AB}$	f^4/u^2	III	-1
		4	7	$+\alpha_1\alpha_2\overline{AB}\ \overline{AB}_x\overline{AB}_z(K_\nu)_y$	f^3	III	-1
		5	9	$-\alpha_1\alpha_2\overline{AB}\ \overline{AB}_y(K_\nu)_x(K_\nu)_z$	f^4/u	VI	+1
		6	9	$+\alpha_1\alpha_2\overline{AB}\ \overline{AB}_z(K_\nu)_x(K_\nu)_y$	$f^4/(1-u)$	VI	+1
		7	9	$-\alpha_1\alpha_2\overline{AB}\ \overline{AB}_x(K_\nu)_y(K_\nu)_z$	f^4/u	VI	1
		8	11	$+\alpha_1\alpha_2\overline{AB}^3(K_\nu)_x(K_\nu)_y(K_\nu)_z$	f^4	IX	-1
$3d_{xy}$	$3p_z$	1	5	$+\alpha_1\overline{AB}_x\overline{AB}_y\overline{AB}_z/\overline{AB}$	f^3/u	I	+1
		2	7	$-\alpha_1\overline{AB}\ \overline{AB}_y\overline{AB}_z(K_\nu)_x$	f^3	III	-1
		3	7	$+\alpha_1\overline{AB}_x\overline{AB}_y(K_\nu)_z/\overline{AB}$	f^4/u^2	III	-1
		4	7	$-\alpha_1\alpha_2^2\overline{AB}\ \overline{AB}_x\overline{AB}_y\overline{AB}_z$	f^3	III	+1
		5	7	$-\alpha_1\overline{AB}\ \overline{AB}_x\overline{AB}_z(K_\nu)_y$	f^3	III	-1
		6	9	$+\alpha_1\overline{AB}\ \overline{AB}_y(K_\nu)_x(K_\nu)_z$	f^4/u	VI	+1
		7	9	$+\alpha_1\alpha_2^2\overline{AB}\ \overline{AB}_y\ \overline{AB}_z(K_\nu)_x$	$f^4/(1-u)$	VI	-1
		8	9	$-\alpha_1\overline{AB}\ \overline{AB}_z(K_\nu)_x(K_\nu)_y$	$f^4/(1-u)$	VI	+1

TABLE AI-2 - Continued

ψ^s	ϕ^s	i	ℓ	B_i	γ_i	Polynomial Type	ξ_i
		9	9	$-\alpha_1\alpha_2^2\overline{AB}\ \overline{AB}_x\overline{AB}_y(K_\nu)_z$	f^4/u	VI	-1
		10	9	$+\alpha_1\overline{AB}\ \overline{AB}_x(K_\nu)_y(K_\nu)_z$	f^4/u	VI	+1
		11	9	$+\alpha_1\alpha_2^2\overline{AB}\ \overline{AB}_x\overline{AB}_z(K_\nu)_y$	$f^4/(1-u)$	VI	-1
		12	11	$-\alpha_1\alpha_2^2\overline{AB}^3\overline{AB}_y(K_\nu)_x(K_\nu)_z$	f^4	IX	+1
		13	11	$-\alpha_1\overline{AB}^3(K_\nu)_x(K_\nu)_y(K_\nu)_z$	f^4	IX	-1
		14	11	$+\alpha_1\alpha_2^2\overline{AB}\ \overline{AB}_z(K_\nu)_x(K_\nu)_y$	$f^5/(1-u)^2$	IX	+1
		15	11	$-\alpha_1\alpha_2^2\overline{AB}^3\overline{AB}_x(K_\nu)_y(K_\nu)_z$	f^4	IX	+1
		16	13	$+\alpha_1\alpha_2^2\overline{AB}^3(K_\nu)_x(K_\nu)_y(K_\nu)_z$	$f^5/(1-u)$	X	-1
$3d_{xy}$	$3d_{xz}$	1	5	$+\alpha_1\alpha_2\overline{AB}^2_x\overline{AB}_y\overline{AB}_z/\overline{AB}$	f^3	I	+1
		2	7	$-\alpha_1\alpha_2\overline{AB}_x\overline{AB}_y\overline{AB}_z(K_\nu)_x/\overline{AB}$	$f^4/(1-u)$	III	-1
		3	7	$+\alpha_1\alpha_2\overline{AB}^2_x\overline{AB}_y(K_\nu)_z/\overline{AB}$	f^4/u	III	-1
		4	7	$-\alpha_1\alpha_2\overline{AB}\ \overline{AB}_y\ \overline{AB}_z$	f^3	III	+1
		5	7	$+\alpha_1\alpha_2\overline{AB}_x\overline{AB}_y\ \overline{AB}_z(K_\nu)_x/\overline{AB}$	f^4/u	III	-1
		6	7	$-\alpha_1\alpha_2\overline{AB}^2_x\overline{AB}_z(K_\nu)_y/\overline{AB}$	$f^4/(1-u)$	III	-1
		7	9	$+\alpha_1\alpha_2\overline{AB}\ \overline{AB}_x\overline{AB}_y(K_\nu)_x(K_\nu)_z$	f^4	VI	+1
		8	9	$+\alpha_1\alpha_2\overline{AB}\ \overline{AB}_y\ \overline{AB}_z(K_\nu)^2_x$	f^4	VI	+1
		9	9	$-\alpha_1\alpha_2\overline{AB}_x\overline{AB}_z(K_\nu)_x(K_\nu)_y/\overline{AB}$	$f^5/(1-u)^2$	VI	+1
		10	9	$-\alpha_1\alpha_2\overline{AB}\ \overline{AB}_y(K_\nu)_z$	f^4/u	VI	-1

TABLE AI-2 - Continued

ψ^s	ϕ^s	i	ℓ	B_i	γ_i	Polynomial Type	ξ_i
		11	9	$-\alpha_1\alpha_2\overline{AB}_\times\overline{AB}_y(K_\nu)_\times(K_\nu)_z/\overline{AB}$	f^5/u^2	VI	+1
		12	9	$+\alpha_1\alpha_2\overline{AB}\ \overline{AB}^2_\times(K_\nu)_y(K_\nu)_z$	f^4	VI	+1
		13	9	$+\alpha_1\alpha_2\overline{AB}\ \overline{AB}_z(K_\nu)_y$	$f^4/(1-u)$	VI	-1
		14	9	$+\alpha_1\alpha_2\overline{AB}\ \overline{AB}_\times\overline{AB}_z(K_\nu)_\times(K_\nu)_y$	f^4	VI	+1
		15	11	$+\alpha_1\alpha_2\overline{AB}\ \overline{AB}_y(K_\nu)^2_\times(K_\nu)_z$	f^5/u	IX	-1
		16	11	$-\alpha_1\alpha_2\overline{AB}\ \overline{AB}_\times(K_\nu)_\times(K_\nu)_y(K_\nu)_z$	$f^5/(1-u)$	IX	-1
		17	11	$-\alpha_1\alpha_2\overline{AB}\ \overline{AB}_z(K_\nu)^2_\times(K_\nu)_y$	$f^5/(1-u)$	IX	-1
		18	11	$-\alpha_1\alpha_2\overline{AB}^3(K_\nu)_y(K_\nu)_z$	f^4	IX	+1
		19	11	$+\alpha_1\alpha_2\overline{AB}\ \overline{AB}_\times(K_\nu)_\times(K_\nu)_y(K_\nu)_z$	f^5/u	IX	-1
		20	13	$+\alpha_1\alpha_2\overline{AB}^3(K_\nu)^2_\times(K_\nu)_y(K_\nu)_z$	f^5	X	+1
$3d_{xy}$	$3d_{xy}$	1	5	$+\alpha_1\alpha_2\overline{AB}^2_\times\overline{AB}^2_y/\overline{AB}$	f^3	I	+1
		2	7	$-\alpha_1\alpha_2\overline{AB}\ \overline{AB}^2_y$	f^3	III	+1
		3	7	$-\alpha_1\alpha_2\overline{AB}_\times\overline{AB}^2_y(K_\nu)_\times/\overline{AB}$	$f^4/(1-u)$	III	-1
		4	7	$+\alpha_1\alpha_2\overline{AB}_\times\overline{AB}^2_y(K_\nu)_\times/\overline{AB}$	f^4/u	III	-1
		5	7	$-\alpha_1\alpha_2\overline{AB}\ \overline{AB}^2_\times$	f^3	III	+1
		6	7	$+\alpha_1\alpha_2\overline{AB}^2_\times\overline{AB}_y(K_\nu)_y/\overline{AB}$	f^4/u	III	-1
		7	7	$-\alpha_1\alpha_2\overline{AB}^2_\times\overline{AB}_y(K_\nu)_y/\overline{AB}$	$f^4/(1-u)$	III	-1

TABLE AI-2 - Continued

ψ^s	ϕ^s	i	ℓ	B_i	γ_i	Polynomial Type	ξ_i
		8	9	$+\alpha_1\alpha_2\overline{AB}\ \overline{AB}_y^2(K_\nu)_x^2$	f^4	VI	+1
		9	9	$+\alpha_1\alpha_2\overline{AB}^3$	f^3	VI	+1
		10	9	$-\alpha_1\alpha_2\overline{AB}\ \overline{AB}_y(K_\nu)_y$	f^4/u	VI	-1
		11	9	$+\alpha_1\alpha_2\overline{AB}\ \overline{AB}_y(K_\nu)_y$	$f^4/(1-u)$	VI	-1
		12	9	$+\alpha_1\alpha_2\overline{AB}\ \overline{AB}_x(K_\nu)_x$	$f^4/(1-u)$	VI	-1
		13	9	$+2\alpha_1\alpha_2\overline{AB}\ \overline{AB}_x\overline{AB}_y(K_\nu)_x(K_\nu)_y$	f^4	VI	+1
		14	9	$-\alpha_1\alpha_2\overline{AB}_x\overline{AB}_y(K_\nu)_x(K_\nu)_y/\overline{AB}$	$f^5/(1-u)^2$	VI	+1
		15	9	$-\alpha_1\alpha_2\overline{AB}\ \overline{AB}_x(K_\nu)_x$	f^4/u	VI	-1
		16	9	$-\alpha_1\alpha_2\overline{AB}_x\overline{AB}_y(K_\nu)_x(K_\nu)_y/\overline{AB}$	f^5/u^2	VI	+1
		17	9	$+\alpha_1\alpha_2\overline{AB}\ \overline{AB}_x^2(K_\nu)_y^2$	f^4	VI	+1
		18	11	$-\alpha_1\alpha_2\overline{AB}^3(K_\nu)_x^2$	f^4	IX	+1
		19	11	$+\alpha_1\alpha_2\overline{AB}\ \overline{AB}_y(K_\nu)_x^2(K_\nu)_y$	f^5/u	IX	-1
		20	11	$-\alpha_1\alpha_2\overline{AB}\ \overline{AB}_y(K_\nu)_x^2(K_\nu)_y$	$f^5/(1-u)$	IX	-1
		21	11	$-\alpha_1\alpha_2\overline{AB}^3(K_\nu)_y^2$	f^4	IX	+1
		22	11	$-\alpha_1\alpha_2\overline{AB}\ \overline{AB}_x(K_\nu)_x(K_\nu)_y^2$	$f^5/(1-u)$	IX	-1
		23	11	$+\alpha_1\alpha_2\overline{AB}\ \overline{AB}_x(K_\nu)_x(K_\nu)_y^2$	f^5/u	IX	-1
		24	13	$+\alpha_1\alpha_2\overline{AB}^3(K_\nu)_x^2(K_\nu)_y^2$	f^5	X	+1

TABLE AI-3

Coefficients for $\langle \psi^s(A) | -\frac{1}{2}\nabla^2 | \phi^s(B) \rangle$

ψ^s	ϕ^s	i	ℓ	w_i	$n_i(u)$	$\rho_{i,0}$	$\rho_{i,1}$	$\rho_{i,2}$	$\rho_{i,3}$	$\rho_{i,4}$	$\rho_{i,5}$	$\rho_{i,6}$
3s	1s	1	5	$-3\alpha_1\alpha_2\overline{AB}$	f^2/u	9	9	2	-1	0	0	0
		2	7	$+\alpha_1^3\alpha_2\overline{AB}$	f^3/u^2	45	45	15	0	-1	0	0
3s	2s	1	5	$+3\alpha_1\overline{AB}$	f^2/u	9	9	2	-1	0	0	0
		2	7	$-3\alpha_1\alpha_2^2\overline{AB}^3$	f^2	45	45	15	0	-1	0	0
		3	7	$-\alpha_1^3\overline{AB}$	f^3/u^2	45	45	15	0	-1	0	0
		4	9	$+\alpha_1^3\alpha_2^2\overline{AB}^3$	f^3/u	315	315	120	15	-3	-1	0
3s	3s	1	7	$-3\alpha_1\alpha_2\overline{AB}^3$	f^2	180	180	75	15	0	-1	0
		2	11	$+\alpha_1^3\alpha_2^3\overline{AB}^5$	f^3	2835	2835	1155	210	0	7	-1
$3p_x$	1s	1	3	$-\alpha_2\overline{AR}_x/\overline{AB}$	f^2/u	5	5	-1	0	0	0	0

TABLE AI-3 - Continued

ψ^s	ϕ^s	i	ℓ	w_i	$n_i(u)$	$\rho_{i,0}$	$\rho_{i,1}$	$\rho_{i,2}$	$\rho_{i,3}$	$\rho_{i,4}$	$\rho_{i,5}$	$\rho_{i,6}$
		2	5	$+\alpha_1^2\alpha_2\overline{AB}_x/\overline{AB}$	f^3/u^2	15	15	4	-1	0	0	0
$3p_x$	2s	1	3	$+\overline{AB}_x/\overline{AB}$	f^2/u	5	5	-1	0	0	0	0
		2	5	$-\alpha_2^2\overline{AB}_x\overline{AB}$	f^2	15	15	4	-1	0	0	0
		3	5	$-\alpha_1^2\overline{AB}_x/\overline{AB}$	f^3/u^2	15	15	4	-1	0	0	0
		4	7	$+\alpha_1^2\alpha_2^2\overline{AB}_x\overline{AB}$	f^3/u	75	75	27	2	-1	0	0
$3p_x$	3s	1	5	$-\alpha_2\overline{AB}_x\overline{AB}$	f^2	30	30	15	5	-1	0	0
		2	7	$-2\alpha_1^2\alpha_2\overline{AB}_x\overline{AB}$	f^3/u	75	75	27	2	-1	0	0
		3	9	$+\alpha_1^2\alpha_2^3\overline{AB}_x\overline{AB^3}$	f^3	525	525	210	35	-1	-1	0
$2p_x$	3s	1	5	$-3\alpha_1\alpha_2\overline{AB}_x\overline{AB}$	f^2	15	15	4	-1	0	0	0
		2	7	$+\alpha_1\alpha_2^3\overline{AB}_x\overline{AB}$	$f^3/(1-u)$	75	75	27	2	-1	0	0

TABLE AI-3 - Continued

ψ^s	ϕ^s	i	ℓ	w_i	$n_i(u)$	$\rho_{i,0}$	$\rho_{i,1}$	$\rho_{i,2}$	$\rho_{i,3}$	$\rho_{i,4}$	$\rho_{i,5}$	$\rho_{i,6}$
$3p_x$	$2p_x$	1	3	$+\alpha_2 \overline{AB}_x^2/\overline{AB}$	f^2	7	7	-1	0	0	0	0
		2	5	$-\alpha_2 \overline{AB}$	f^2	15	15	4	-1	0	0	0
		3	5	$-\alpha_1^2\alpha_2 \overline{AB}_x^2/\overline{AB}$	f^3/u	21	21	6	-1	0	0	0
		4	7	$+\alpha_1^2\alpha_2 \overline{AB}$	f^3/u	75	75	27	2	-1	0	0
$3p_x$	$3p_x$	1	3	$+\overline{AB}_x^2/\overline{AB}$	f^2	14	14	7	-1	0	0	0
		2	5	$-\overline{AB}$	f^2	60	60	23	3	-1	0	0
		3	7	$-\alpha_1^2\alpha_2^2\overline{AB}_x^2\overline{AB}$	f^3	105	105	39	4	-1	0	0
		4	9	$+\alpha_1^2\alpha_2^2\overline{AB}^3$	f^3	525	525	210	35	-1	-1	0
$3p_x$	$2p_y$	1	3	$+\alpha_2 \overline{AB}_x\overline{AB}_y/\overline{AB}$	f^2	7	7	-1	0	0	0	0
		2	5	$-\alpha_1^2\alpha_2 \overline{AB}_x\overline{AB}_y/\overline{AB}$	f^3/u	21	21	6	-1	0	0	0

TABLE AI-3 - Continued

ψ^s	ϕ^s	i	ℓ	w_i	$n_i(u)$	$\rho_{i,0}$	$\rho_{i,1}$	$\rho_{i,2}$	$\rho_{i,3}$	$\rho_{i,4}$	$\rho_{i,5}$	$\rho_{i,6}$
$3p_x$	$3p_y$	1	3	$+\overline{AB}_x\overline{AB}_y/\overline{AB}$	f^2	14	14	7	-1	0	0	0
		2	7	$-\alpha_1^2\alpha_2^2\overline{AB}_x\overline{AB}_y\overline{AB}$	f^3	105	105	39	4	-1	0	0
$3d_x^2$	1s	1	3	$+\alpha_1\alpha_2\overline{AB}_x^2/\overline{AB}^3$	f^3/u^2	7	7	-1	0	0	0	0
		2	5	$+\alpha_1\alpha_2\overline{AB}$	f^2/u	9	9	2	-1	0	0	0
		3	5	$-\alpha_1\alpha_2/\overline{AB}$	f^3/u^2	15	15	4	-1	0	0	0
$3d_x^2$	2s	1	3	$-\alpha_1\overline{AB}_x^2/\overline{AB}^3$	f^3/u^2	7	7	-1	0	0	0	0
		2	5	$-\alpha_1\overline{AB}$	f^2/u	9	9	2	-1	0	0	0
		3	5	$+\alpha_1/\overline{AB}$	f^3/u^2	15	15	4	-1	0	0	0
		4	5	$+\alpha_1\alpha_2^2\overline{AB}_x^2/\overline{AB}$	f^3/u	21	21	6	-1	0	0	0
		5	7	$+\alpha_1\alpha_2^2\overline{AB}^3$	f^2	45	45	15	0	-1	0	0
		6	7	$-\alpha_1\alpha_2^2\overline{AB}$	f^3/u	75	75	27	2	-1	0	0

TABLE AI-3 - Continued

ψ^s	ϕ^s	i	ℓ	w_i	$n_i(u)$	$\rho_{i,0}$	$\rho_{i,1}$	$\rho_{i,2}$	$\rho_{i,3}$	$\rho_{i,4}$	$\rho_{i,5}$	$\rho_{i,6}$
$3d_x^2$	3s	1	5	$-3\alpha_1\alpha_2\overline{AB}_x^2/\overline{AB}$	f^3/u	21	21	6	-1	0	0	0
		2	7	$-3\alpha_1\alpha_2\overline{AB}^3$	f^2	45	45	15	0	-1	0	0
		3	7	$+3\alpha_1\alpha_2\overline{AB}$	f^3/u	75	75	27	2	-1	0	0
		4	7	$+\alpha_1\alpha_2^3\overline{AB}\ \overline{AB}_x^2$	f^3	105	105	39	4	-1	0	0
		5	9	$+\alpha_1\alpha_2^3\overline{AB}^3$	$f^3/(1-u)$	315	315	120	15	-3	-1	0
		6	9	$-\alpha_1\alpha_2^3\overline{AB}^3$	f^3	525	525	210	35	-1	-1	0
$3d_x^2$	$2p_x$	1	3	$-\alpha_1\alpha_2\overline{AB}_x^3/\overline{AB}^3$	f^3/u	9	9	-1	0	0	0	0
		2	5	$-\alpha_1\alpha_2\overline{AB}\ \overline{AB}_x$	f^2	15	15	4	-1	0	0	0
		3	5	$+3\alpha_1\alpha_2\overline{AB}_x/\overline{AB}$	f^3/u	21	21	6	-1	0	0	0
$3d_x^2$	$3p_x$	1	3	$+\alpha_1\overline{AB}_x^3/\overline{AB}^3$	f^3/u	9	9	-1	0	0	0	0
		2	5	$+\alpha_1\overline{AB}\ \overline{AB}_x$	f^2	15	15	4	-1	0	0	0
		3	5	$-3\alpha_1\overline{AB}_x/\overline{AB}$	f^3/u	21	21	6	-1	0	0	0
		4	5	$-\alpha_1\alpha_2^2\overline{AB}_x^3/\overline{AB}$	f^3	27	27	8	-1	0	0	0

TABLE AI-3 - Continued

ψ^s	ϕ^s	i	ℓ	w_i	$n_i(u)$	$\rho_{i,0}$	$\rho_{i,1}$	$\rho_{i,2}$	$\rho_{i,3}$	$\rho_{i,4}$	$\rho_{i,5}$	$\rho_{i,6}$
		5	7	$-\alpha_1\alpha_2^2\overline{AB}\,\overline{AB}_x$	$f^3/(1-u)$	75	75	27	2	-1	0	0
		6	7	$+3\alpha_1\alpha_2^2\overline{AB}\,\overline{AB}_x$	f^3	105	105	39	4	-1	0	0
$3d_x^2$	$2p_y$	1	3	$-\alpha_1\alpha_2\overline{AB}_x^2\overline{AB}_y/\overline{AB}^3$	f^3/u	9	9	-1	0	0	0	0
		2	5	$-\alpha_1\alpha_2\overline{AB}\,\overline{AB}_y$	f^2	15	15	4	-1	0	0	0
		3	5	$+\alpha_1\alpha_2\overline{AB}_y/\overline{AB}$	f^3/u	21	21	6	-1	0	0	0
$3d_x^2$	$3p_y$	1	3	$+\alpha_1\overline{AB}_x^2\overline{AB}_y/\overline{AB}^3$	f^3/u	9	9	-1	0	0	0	0
		2	5	$+\alpha_1\overline{AB}\,\overline{AB}_y$	f^2	15	15	4	-1	0	0	0
		3	5	$-\alpha_1\overline{AB}_y/\overline{AB}$	f^3/u	21	21	6	-1	0	0	0
		4	5	$-\alpha_1\alpha_2^2\overline{AB}_x^2\overline{AB}_y/\overline{AB}$	f^3	27	27	8	-1	0	0	0
		5	7	$-\alpha_1\alpha_2^2\overline{AB}\,\overline{AB}_y$	$f^3/(1-u)$	75	75	27	2	-1	0	0
		6	7	$+\alpha_1\alpha_2^2\overline{AB}\,\overline{AB}_y$	f^3	105	105	39	4	-1	0	0

TABLE AI-3 - Continued

ψ^S	ϕ^S	i	ℓ	w_i	$n_i(u)$	$\rho_{i,0}$	$\rho_{i,1}$	$\rho_{i,2}$	$\rho_{i,3}$	$\rho_{i,4}$	$\rho_{i,5}$	$\rho_{i,6}$
$3d_x^2$	$3d_{yz}$	1	3	$+\alpha_1\alpha_2\overline{AB}_x^2\overline{AB}_y\overline{AB}_z/\overline{AB}^3$	f^3	11	11	-1	0	0	0	0
		2	5	$+\alpha_1\alpha_2\overline{AB}_y\overline{AB}_z/\overline{AB}$	$f^3/(1-u)$	21	21	6	-1	0	0	0
		3	5	$-\alpha_1\alpha_2\overline{AB}_y\overline{AB}_z/\overline{AB}$	f^3	27	27	8	-1	0	0	0
$3d_x^2$	$3d_{xy}$	1	3	$+\alpha_1\alpha_2\overline{AB}_x^3\overline{AB}_y/\overline{AB}^3$	f^3	11	11	-1	0	0	0	0
		2	5	$+\alpha_1\alpha_2\overline{AB}_x\overline{AB}_y/\overline{AB}$	$f^3/(1-u)$	21	21	6	-1	0	0	0
		3	5	$-3\alpha_1\alpha_2\overline{AB}_x\overline{AB}_y/\overline{AB}$	f^3	27	27	8	-1	0	0	0
$3d_x^2$	$3d_y^2$	1	3	$+\alpha_1\alpha_2\overline{AB}_x^2\overline{AB}_y^2/\overline{AB}^3$	f^3	11	11	-1	0	0	0	0
		2	5	$+\alpha_1\alpha_2\overline{AB}_y^2/\overline{AB}$	$f^3/(1-u)$	21	21	6	-1	0	0	0
		3	5	$+\alpha_1\alpha_2\overline{AB}_x^2/\overline{AB}$	f^3/u	21	21	6	-1	0	0	0
		4	5	$-\alpha_1\alpha_2\overline{AB}_y^2/\overline{AB}$	f^3	27	27	8	-1	0	0	0
		5	5	$-\alpha_1\alpha_2\overline{AB}_x^2/\overline{AB}$	f^3	27	27	8	-1	0	0	0
		6	7	$+\alpha_1\alpha_2\overline{AB}^3$	f^2	45	45	15	0	-1	0	0
		7	7	$-\alpha_1\alpha_2\overline{AB}$	$f^3/(1-u)$	75	75	27	2	-1	0	0

TABLE AI-3 - Continued

ψ^s	ϕ^s	i	ℓ	w_i	$n_i(u)$	$\rho_{i,0}$	$\rho_{i,1}$	$\rho_{i,2}$	$\rho_{i,3}$	$\rho_{i,4}$	$\rho_{i,5}$	$\rho_{i,6}$
		8	7	$-\alpha_1\alpha_2\overline{AB}$	f^3/u	75	75	27	2	-1	0	0
		9	7	$+\alpha_1\alpha_2\overline{AB}$	f^3	105	105	39	4	-1	0	0
$3d_x^2$	$3d_x^2$	1	3	$+\alpha_1\alpha_2\overline{AB}_x^4/\overline{AB}^3$	f^3	11	11	-1	0	0	0	0
		2	5	$+\alpha_1\alpha_2\overline{AB}_x^2/\overline{AB}$	$f^3/(1-u)$	21	21	6	-1	0	0	0
		3	5	$+\alpha_1\alpha_2\overline{AB}_x^2/\overline{AB}$	f^3/u	21	21	6	-1	0	0	0
		4	5	$-6\alpha_1\alpha_2\overline{AB}_x^2/\overline{AB}$	f^3	27	27	8	-1	0	0	0
		5	7	$+\alpha_1\alpha_2\overline{AB}^3$	f^2	45	45	15	0	-1	0	0
		6	7	$-\alpha_1\alpha_2\overline{AB}$	$f^3/(1-u)$	75	75	27	2	-1	0	0
		7	7	$-\alpha_1\alpha_2\overline{AB}$	f^3/u	75	75	27	2	-1	0	0
		8	7	$+3\alpha_1\alpha_2\overline{AB}$	f^3	105	105	39	4	-1	0	0
$3d_{xy}$	1s	1	3	$+\alpha_1\alpha_2\overline{AB}_x\overline{AB}_y/\overline{AB}^3$	f^3/u^2	7	7	-1	0	0	0	0
$3d_{xy}$	2s	1	3	$-\alpha_1\overline{AB}_x\overline{AB}_y/\overline{AB}^3$	f^3/u^2	7	7	-1	0	0	0	0
		2	5	$+\alpha_1\alpha_2^2\overline{AB}_x\overline{AB}_y/\overline{AB}$	f^3/u	21	21	6	-1	0	0	0

TABLE AI-3 - Continued

ψ^s	ϕ^s	i	ℓ	w_i	$n_i(u)$	$\rho_{i,0}$	$\rho_{i,1}$	$\rho_{i,2}$	$\rho_{i,3}$	$\rho_{i,4}$	$\rho_{i,5}$	$\rho_{i,6}$
$3d_{xy}$	$3s$	1	5	$-3\alpha_1\alpha_2\overline{AB}_x\overline{AB}_y/\overline{AB}$	f^3/u	21	21	6	-1	0	0	0
		2	7	$+\alpha_1\alpha_2^3\overline{AB}\ \overline{AB}_x\overline{AB}_y$	f^3	105	105	39	4	-1	0	0
$3d_{xy}$	$2p_x$	1	3	$-\alpha_1\alpha_2\overline{AB}_x^2\overline{AB}_y/\overline{AB}^3$	f^3/u	9	9	-1	0	0	0	0
		2	5	$+\alpha_1\alpha_2\overline{AB}_y/\overline{AB}$	f^3/u	21	21	6	-1	0	0	0
$3d_{xy}$	$3p_x$	1	3	$+\alpha_1\overline{AB}_x^2\overline{AB}_y/\overline{AB}^3$	f^3/u	9	9	-1	0	0	0	0
		2	5	$-\alpha_1\overline{AB}_y/\overline{AB}$	f^3/u	21	21	6	-1	0	0	0
		3	5	$-\alpha_1\alpha_2^2\overline{AB}_x^2\overline{AB}_y/\overline{AB}$	f^3	27	27	8	-1	0	0	0
		4	7	$+\alpha_1\alpha_2^2\overline{AB}\ \overline{AB}_y$	f^3	105	105	39	4	-1	0	0
$3d_{xy}$	$2p_z$	1	3	$-\alpha_1\alpha_2\overline{AB}_x\overline{AB}_y\overline{AB}_z/\overline{AB}^3$	f^3/u	9	9	-1	0	0	0	0
$3d_{xy}$	$3p_z$	1	3	$+\alpha_1\overline{AB}_x\overline{AB}_y\overline{AB}_z/\overline{AB}^3$	f^3/u	9	9	-1	0	0	0	0
		2	5	$-\alpha_1\alpha_2^2\overline{AB}_x\overline{AB}_y\overline{AB}_z/\overline{AB}$	f^3	27	27	8	-1	0	0	0

TABLE AI-3 - Continued

ψ^s	ϕ^s	i	ℓ	w_i	$n_i(u)$	$\rho_{i,0}$	$\rho_{i,1}$	$\rho_{i,2}$	$\rho_{i,3}$	$\rho_{i,4}$	$\rho_{i,5}$	$\rho_{i,6}$
$3d_{xy}$	$3d_{xz}$	1	3	$+\alpha_1\alpha_2\overline{AB}_x^2\overline{AB}_y\overline{AB}_z/\overline{AB}^3$	f^3	11	11	-1	0	0	0	0
		2	5	$-\alpha_1\alpha_2\overline{AB}_y\overline{AB}_z/\overline{AB}$	f^3	27	27	8	-1	0	0	0
$3d_{xy}$	$3d_{xy}$	1	3	$+\alpha_1\alpha_2\overline{AB}_x^2\overline{AB}_y^2/\overline{AB}^3$	f^3	11	11	-1	0	0	0	0
		2	5	$-\alpha_1\alpha_2\overline{AB}_y^2/\overline{AB}$	f^3	27	27	8	-1	0	0	0
		3	5	$-\alpha_1\alpha_2\overline{AB}_x^2/\overline{AB}$	f^3	27	27	8	-1	0	0	0
		4	7	$+\alpha_1\alpha_2\overline{AB}$	f^3	105	105	39	4	-1	0	0

Appendix II

Method of obtaining an analytic form for coulomb and exchange potential of silicon.

From Eq. (4.5) we have that

$$V_{crys}(\vec{K}_\nu) = -\frac{8\pi}{K_\nu^2\Omega}\cos(\vec{K}_\nu\cdot\vec{t}_1)\{z - K_\nu^{-1}\int_o^\infty 4\pi r\rho(r)\sin(K_\nu r)\,dr + K_\nu\int_o^\infty \frac{3}{2}r[3\rho(r)/\pi]^{1/3}\sin(K_\nu r)\,dr\}. \quad \text{(A2-1)}$$

If we define

$$Q(r) = 4\pi r\,\rho(r)$$

and

$$E(r) = \frac{3}{2}r[3\rho(r)/\pi]^{1/3}$$

Then $V_{crys}(\vec{K}_\nu)$ can be expressed as

$$V_{crys}(\vec{K}_\nu) = -\frac{8\pi}{K_\nu^2\Omega}\cos(\vec{K}_\nu\cdot\vec{t}_1)\{z - K_\nu^{-1}\int_o^\infty Q(\vec{r})\sin(K_\nu r)\,dr + K_\nu\int_o^\infty E(r)\sin(K_\nu r)\,dr\ . \quad \text{(A2-2)}$$

We then curve fit Q(r) and E(r) using a combination of a polynomial in r and an exponential. The curve fit expressions were:

$$Q(r) = \sum_{i=1}^{3}\delta_i r^{K_i}\exp(-n_i r) + \sum_{j=1}^{4} a_j(r)\,r^{(j-1)}$$

and

$$E(r) = \sum_{i=1}^{2} \delta'_i \, r^{K'_i} \exp(-n'_i r) + \sum_{j=1}^{4} a'_j(r) \, r^{(j-1)}$$

The values of δ_i, K_i and n_i are contained in Table A2-1. The value of $a_j(r)$ depends on what the value of r is, and is tabulated for the different regions of r in Table A2-2. The values of δ'_i, K'_i and n'_i are contained in Table A2-3 and the values of $a'_j(r)$ for the different regions of r are contained in Table A2-4.

TABLE A2-1

i	δ_i	R_i	N_i
1	$+ 1.096164 \times 10^{-11}$	20.54610	+ 3.358661
2	$+ 2.503153 \times 10^{-28}$	+ 55.43703	+ 7.666828
3	$+ 5.804757 \times 10^{-5}$	+ 5.766948	+ 1.488461

TABLE A2-2

from	to	$a_1(r)$	$a_2(r)$	$a_3(r)$	$a_4(r)$
r=0.00	r=0.03	0.0	$+2.184522 \times 10^{+4}$	$-5.580415 \times 10^{+5}$	$+5.008750 \times 10^{+6}$
0.03	0.06	$+8.380707 \times 10^{+1}$	$+1.342638 \times 10^{+4}$	$-2.637692 \times 10^{+5}$	$+1.449976 \times 10^{+6}$
0.06	0.10	$+3.328367 \times 10^{+2}$	$+9.490420 \times 10^{+2}$	$-5.287181 \times 10^{+4}$	$+2.480925 \times 10^{+5}$
0.10	0.19	$+6.014007 \times 10^{+2}$	$-7.339429 \times 10^{+3}$	$+3.307254 \times 10^{+4}$	$-5.104946 \times 10^{+4}$
0.19	0.26	$+3.726285 \times 10^{+2}$	$-3.785215 \times 10^{+3}$	$+1.460434 \times 10^{+4}$	$-1.895182 \times 10^{+4}$
0.26	0.36	$+7.810396 \times 10^{+1}$	$-3.634535 \times 10^{+2}$	$+1.302745 \times 10^{+3}$	$-1.652660 \times 10^{+3}$
0.36	0.55	+7.227253	$+4.196663 \times 10^{+2}$	$-1.078697 \times 10^{+3}$	$+7.493997 \times 10^{+2}$
0.55	0.76	$+1.130473 \times 10^{+2}$	$-2.471195 \times 10^{+2}$	$+1.595399 \times 10^{+2}$	$-2.065374 \times 10^{+1}$
0.76	1.00	$+1.337298 \times 10^{+2}$	$-3.412449 \times 10^{+2}$	$+3.005113 \times 10^{+2}$	$-9.031780 \times 10^{+1}$
1.00	1.30	$+7.318620 \times 10^{+1}$	$-1.610204 \times 10^{+2}$	$+1.212160 \times 10^{+2}$	$-3.070131 \times 10^{+1}$
1.30	1.60	$+2.089290 \times 10^{+1}$	$-3.782623 \times 10^{+1}$	$+2.430651 \times 10^{+1}$	-5.249389
1.60	2.10	$+1.452035 \times 10^{-1}$	+2.178235	-1.090230	$+1.330528 \times 10^{-1}$
2.10	2.70	$+1.950165 \times 10^{-1}$	+2.064504	-1.215946	$+1.819896 \times 10^{-1}$
2.70	3.70	+4.347943	-2.599668	$+5.344188 \times 10^{-1}$	-3.747822×10^{-2}
3.70	4.50	+3.708273	-2.125240	$+4.184184 \times 10^{-1}$	-2.815516×10^{-2}

TABLE A2-2 - Continued

from	to	$a_1(r)$	$a_2(r)$	$a_3(r)$	$a_4(r)$
4.50	5.30	+2.210481	-1.118426	$+1.925391 \times 10^{-1}$	-1.124218×10^{-2}
5.30	6.00	+1.248844	-5.672467×10^{-1}	$+8.715551 \times 10^{-2}$	-4.521103×10^{-3}
6.00	6.70	$+6.819038 \times 10^{-1}$	-2.818470×10^{-1}	$+3.923877 \times 10^{-2}$	-1.838023×10^{-3}
6.70	7.40	$+3.603265 \times 10^{-1}$	-1.370177×10^{-1}	$+1.748807 \times 10^{-2}$	-7.487612×10^{-4}
7.40	8.10	$+1.853165 \times 10^{-1}$	-6.569126×10^{-2}	$+7.795212 \times 10^{-3}$	-3.095580×10^{-4}
8.10	8.70	$+8.757885 \times 10^{-2}$	-2.924858×10^{-2}	$+3.264715 \times 10^{-3}$	-1.217705×10^{-4}
8.70	9.40	$+3.348683 \times 10^{-2}$	-1.055227×10^{-2}	$+1.110237 \times 10^{-3}$	-3.899716×10^{-5}
9.40	10.00	$+9.236438 \times 10^{-3}$	-2.744353×10^{-3}	$+2.721366 \times 10^{-4}$	-9.005472×10^{-6}
10.00	11.50	$+8.263697 \times 10^{-4}$	-2.217874×10^{-4}	$+1.984950 \times 10^{-5}$	-5.923494×10^{-7}
11.50	13.50	$+1.694967 \times 10^{-5}$	-3.937459×10^{-6}	$+3.048176 \times 10^{-7}$	-7.863266×10^{-9}
13.50	∞	0.0	0.0	0.0	0.0

TABLE A2-3

i	δ'_i	K'_i	N'_i
1	$+ 3.091138 \times 10^{-2}$	+ 2.471882	$+ 4.900283 \times 10^{-1}$
2	$+ 5.187311 \times 10^{-23}$	$+ 3.694527 \times 10^{+1}$	+ 3.858810

TABLE A2-4

from	to	$a_1(r)$	$a_2(r)$	$a_3(r)$	$a_4(r)$
r=0.00	r=0.05	$+3.120298 \times 10^{-5}$	$+1.779470 \times 10^{+1}$	$-1.604933 \times 10^{+2}$	$+5.884123 \times 10^{+2}$
0.05	0.13	$+4.525809 \times 10^{-2}$	$+1.540715 \times 10^{+1}$	$-1.163809 \times 10^{+2}$	$+3.004062 \times 10^{+2}$
0.13	0.20	$+5.875951 \times 10^{-1}$	+3.343420	$-2.584254 \times 10^{+1}$	$+7.091928 \times 10^{+1}$
0.20	0.33	+1.187546	-7.230805	$+3.487086 \times 10^{+1}$	$-4.334803 \times 10^{+1}$
0.33	0.81	$+3.192869 \times 10^{-1}$	+6.983263	$-1.009635 \times 10^{+1}$	+4.338062
0.81	1.20	+1.218634	+1.325962	-3.061943	+1.381236
1.20	1.60	+4.620999	-8.025926	+5.473333	-1.206242
1.60	2.50	$+3.969857 \times 10^{-1}$	+1.401235	-4.518377×10^{-1}	$+3.952299 \times 10^{-2}$
2.50	3.90	$+1.390803 \times 10^{-1}$	$+9.128637 \times 10^{-1}$	-3.178244×10^{-1}	$+2.978814 \times 10^{-2}$
3.90	6.50	+1.693090	-3.124634×10^{-1}	$+6.767802 \times 10^{-3}$	$+9.229329 \times 10^{-4}$
6.50	12.00	+2.126803	-5.366310×10^{-1}	$+4.528990 \times 10^{-2}$	-1.278149×10^{-3}
12.00	∞	0.0	0.0	0.0	0.0

Appendix III

Simplification of OPW matrix elements

From Eq. (5.3) we see that the overlap matrix can be written as

$$
\begin{aligned}
S_{i,j} = (N\Omega)^{-1} & \int \exp\{-i(\vec{k}+\vec{K}_{h_i})\cdot\vec{r}\} \exp\{i(\vec{k}+\vec{K}_{h_j})\cdot\vec{r}\}\, d\tau \\
& - (N\Omega)^{-\frac{1}{2}} \sum_{\alpha,\Delta} \beta(h_i,\alpha,\Delta)^* \int b^*_{\alpha,\Delta}(\vec{k},\vec{r}) \exp\{i(\vec{k}+\vec{K}_{h_j})\cdot\vec{r}\} d\tau \\
& - (N\Omega)^{-\frac{1}{2}} \sum_{\alpha',\Delta'} \beta(h_j,\alpha',\Delta') \int \exp\{-i(\vec{k}+\vec{K}_{h_i})\cdot\vec{r}\}\, b_{\alpha',\Delta'}(\vec{k},\vec{r})\, d\tau \\
& + \sum_{\alpha,\Delta} \sum_{\alpha',\Delta'} \beta(h_i,\alpha,\Delta)^* \beta(h_j,\alpha',\Delta') \int b^*_{\alpha,\Delta}(\vec{k},\vec{r})\, b_{\alpha',\Delta'}(\vec{k},\vec{r})\, d\tau .
\end{aligned}
\tag{A3.1}
$$

From the equations which determine $\beta(h_i,\alpha,\Delta)$ (Eq. (5.2)) we have that

$$
\int \psi^*_{h_i}(\vec{k},\vec{r})\, b_{\alpha',\Delta'}(\vec{k},\vec{r})\, d\tau = 0 \tag{A3.2}
$$

or

$$
\begin{aligned}
& - (N\Omega)^{-\frac{1}{2}} \int \exp\{-i(\vec{k}+\vec{K}_{h_i})\cdot\vec{r}\}\, b_{\alpha',\Delta'}(\vec{k},\vec{r})\, d\tau \\
& + \sum_{\alpha,\Delta} \beta(h_i,\alpha,\Delta)^* \int b^*_{\alpha,\Delta}(\vec{k},\vec{r})\, b_{\alpha',\Delta'}(\vec{k},\vec{r})\, d\tau = 0.
\end{aligned}
\tag{A3.3}
$$

Summing this equation over α' and Δ' and multiplying it by $\beta(h_j,\alpha',\Delta')$ does not change it. We therefore have

$$-(N\Omega)^{-\frac{1}{2}} \sum_{\alpha',\Delta'} \beta(h_j,\alpha',\Delta') \int \exp\{-i(\vec{k}+\vec{K}_{h_i})\cdot\vec{r}\}\, b_{\alpha',\Delta'}(\vec{k},\vec{r})\, d\tau$$

$$+ \sum_{\alpha,\Delta} \sum_{\alpha',\Delta'} \beta(h_i,\alpha,\Delta)^* \beta(h_j,\alpha',\Delta') \int b^*_{\alpha,\Delta}(\vec{k},\vec{r})\, b_{\alpha',\Delta'}(\vec{k},\vec{r})\, d\tau = 0 . \qquad \text{(A3.4)}$$

The last two terms in Eq. (A3.1), therefore cancel and we have

$$S_{i,j} = (N\Omega)^{-1} \int \exp\{-i(\vec{k}+\vec{K}_{h_i})\cdot r\} \exp\{i(\vec{k}+\vec{K}_{h_j})\cdot\vec{r}\}\, d\tau$$

$$- (N\Omega)^{-\frac{1}{2}} \sum_{\alpha,\Delta} \beta(h_i,\alpha,\Delta)^* \int b^*_{\alpha,\Delta}(\vec{k},\vec{r}) \exp\{i(\vec{k}+\vec{K}_{h_j})\cdot\vec{r}\}\, d\tau . \qquad \text{(A3.5)}$$

The first term in Eq. (A3.5)

$$(N\Omega)^{-1}\int \exp\{-i(\vec{k}+\vec{K}_{h_i})\cdot\vec{r}\}\exp\{i(\vec{k}+\vec{K}_{h_j})\cdot\vec{r}\}d\tau = (N\Omega)^{-1}\int \exp\{i(\vec{K}_{h_j}-\vec{K}_{h_i})\cdot\vec{r}\}d\tau =$$

$$= \delta_{\vec{K}_{h_i},\,\vec{K}_{h_j}} ,$$

where

$$\delta_{\vec{K}_{h_o},\,\vec{K}_{h_j}} = 1 \quad \text{if} \quad \vec{K}_{h_i} = \vec{K}_{h_j}$$

$$= 0 \quad \text{if} \quad \vec{K}_{h_i} \neq \vec{K}_{h_j} .$$

The second term in Eq. (A3.5) can be simplified after substituting for $b^*_{\alpha,\Delta}(\vec{k},\vec{r})$ from Eq. (4.7).

$$(N\Omega)^{-\frac{1}{2}}\sum_{\alpha,\Delta}\beta(h_i,\alpha,\Delta)^*\int b^*_{\alpha,\Delta}(\vec{k},\vec{r})\exp\{i(\vec{k}+\vec{K}_{h_j})\cdot\vec{r}\}\,d\tau$$

$$= I^*(\alpha,\Delta)\,N^{-1}[\Omega\Omega^{\Delta}_{\alpha}(\vec{k})]^{-\frac{1}{2}}\sum_{\alpha,\Delta}\beta(h_i,\alpha,\Delta)^*\Big(\sum_{\nu}e^{-i\vec{k}\cdot\{\vec{R}_\nu+\vec{t}_1\}}\int\phi_\alpha(\vec{r}-\vec{R}_\nu-\vec{t}_1)\exp\{i(\vec{k}+\vec{K}_{h_j})\cdot\vec{r}\}\,d\tau + \Delta\sum_{\nu}e^{-i\vec{k}\cdot\{\vec{R}_\nu+\vec{t}_2\}}\int\phi_\alpha(\vec{r}-\vec{R}_\nu-\vec{t}_2)\exp\{i(\vec{k}+\vec{K}_{h_j})\cdot\vec{r}\}\,d\tau\Big)\,. \tag{A3.6}$$

Make a change of variables in these two integrals. In the first integral let $\vec{r}' = \vec{r}-\vec{R}_\nu-\vec{t}_1$. In the second integral let $\vec{r}'' = \vec{r}-\vec{R}_\nu-\vec{t}_2$. We then have

$$(N\Omega)^{-\frac{1}{2}}\sum_{\alpha,\Delta}\beta(h_i,\alpha,\Delta)^*\int b^*_{\alpha,\Delta}(\vec{k},\vec{r})\exp\{i(\vec{k}+\vec{K}_{h_j})\cdot\vec{r}\}\,d\tau$$

$$= I^*(\alpha,\Delta)\,N^{-1}[\Omega\Omega^{\Delta}_{\alpha}(\vec{k})]^{-\frac{1}{2}}\sum_{\alpha,\Delta}\beta(h_i,\alpha,\Delta)^*\Big(\sum_{\nu}\exp\{i\,\vec{K}_{h_j}\cdot(\vec{R}_\nu+\vec{t}_1)\}\int\phi_\alpha(\vec{r}')\exp\{i(\vec{k}+\vec{K}_{h_j})\cdot\vec{r}'\}\,d\tau' + \Delta\sum_{\nu}\exp\{i\vec{K}_{h_j}\cdot(\vec{R}_\nu+\vec{t}_2)\}\int\phi_\alpha(\vec{r}'')\exp\{i(\vec{k}+\vec{K}_{h_j})\cdot\vec{r}''\}\,d\tau''\Big) \tag{A3.7}$$

$$= I^*(\alpha,\Delta)N^{-1}[\Omega\Omega^{\Delta}_{\alpha}(\vec{k})]^{-\frac{1}{2}}\sum_{\alpha,\Delta}\beta(h_i,\alpha,\Delta)^*\Big(\Big[\sum_{\nu}\{\exp(i\vec{K}_{h_j}\cdot\vec{t}_1) + \Delta\exp(i\vec{K}_{h_j}\cdot\vec{t}_2)\}\Big]\int\phi_\alpha(\vec{r})\exp\{i(\vec{k}+\vec{K}_{h_j})\cdot\vec{r}\}\,d\tau\Big).$$

Since $\vec{K}_{h_j}\cdot\vec{R}_\nu = 2m\pi$

where m is an integer.

Upon summing over ν we get the final expression for the overlap matrix element.

$$S_{i,j} = \delta_{\vec{K}_{h_i}, \vec{K}_{h_j}} - I^*(\alpha,\Delta)\,[\Omega\Omega_\alpha^\Delta(\vec{k})]^{-\frac{1}{2}} \sum_{\alpha,\Delta} \beta(h_i,\alpha,\Delta)^* \tag{A3.8}$$
$$[\exp(i\vec{K}_{h_j}\cdot\vec{t}_1) + \Delta \exp(i\vec{K}_{h_j}\cdot\vec{t}_2)] \int \phi_\alpha(\vec{r}) \exp\{i(\vec{k}+\vec{K}_{h_j})\cdot\vec{r}\}d\tau \ .$$

Now lets look at the Hamiltonian matrix. From Eq. (5.4) the Hamiltonian has the form

$$H_{i,j} = (N\Omega)^{-1} \int \exp\{-i(\vec{k}+\vec{K}_{h_i})\cdot\vec{r}\} \not{H} \exp\{i(\vec{k}+\vec{K}_{h_j})\cdot\vec{r}\}\, d\tau$$
$$- (N\Omega)^{-\frac{1}{2}} \sum_{\alpha,\Delta} \beta(h_i,\alpha,\Delta)^* \int b^*_{\alpha,\Delta}(\vec{k},\vec{r}) \not{H} \exp\{i(\vec{k}+\vec{K}_{h_j})\cdot\vec{r}\}\, d\tau \tag{A3.9}$$
$$- (N\Omega)^{-\frac{1}{2}} \sum_{\alpha',\Delta'} \beta(h_j,\alpha',\Delta') \int \exp\{-i(\vec{k}+\vec{K}_{h_i})\cdot\vec{r}\} \not{H} b_{\alpha',\Delta'}(\vec{k},\vec{r})\, d\tau$$
$$+ \sum_{\alpha,\Delta} \sum_{\alpha',\Delta'} \beta(h_i,\alpha,\Delta)^* \beta(h_j,\alpha',\Delta') \int b^*_{\alpha,\Delta}(\vec{k},\vec{r}) \not{H} b_{\alpha',\Delta'}(\vec{k},\vec{r})\, d\tau \ .$$

Since the Hamiltonian is a hermitian operator we can say that

$$\int b^*_{\alpha,\Delta}(\vec{k},\vec{r}) \not{H} \exp\{i(\vec{k}+\vec{K}_{h_j})\cdot\vec{r}\}\, d\tau = \int \exp\{-i(\vec{k}+\vec{K}_{h_j})\cdot\vec{r}\} \not{H} b_{\alpha,\Delta}(\vec{k},\vec{r})\, d\tau . \tag{A3.10}$$

Substituting for $b_{\alpha,\Delta}(\vec{k},\vec{r})$ we have

$$\int \exp\{-i(\vec{k}+\vec{K}_{h_j})\cdot\vec{r}\}\,\mathcal{H}(\vec{r})\; b_{\alpha,\Delta}(\vec{k},\vec{r})\,d\tau = I(\alpha,\Delta)[N\Omega_\alpha^\Delta(\vec{k})]^{-\frac{1}{2}}$$

$$[\Sigma_\nu e^{i\vec{k}\cdot(\vec{R}_\nu+\vec{t}_1)} \int \exp\{-i(\vec{k}+\vec{K}_{h_j})\cdot\vec{r}\}\,\mathcal{H}(\vec{r})\;\phi_\alpha(\vec{r}-\vec{R}_\nu-\vec{t}_1)\,d\tau \qquad \text{(A3.11)}$$

$$+\Delta\,\Sigma_\nu e^{i\vec{k}\cdot(\vec{R}_\nu+\vec{t}_2)} \int \exp\{-i(\vec{k}+\vec{K}_{h_j})\cdot\vec{r}\}\,\mathcal{H}(\vec{r})\phi_\alpha(\vec{r}-\vec{R}_\nu-\vec{t}_2)\,d\tau] \,.$$

Substituting $\vec{r}'=\vec{r}-\vec{R}_\nu$ into both of the integrals and remembering that the periodicity of the crystal lattice requires that

$$\mathcal{H}(\vec{r}' + \vec{R}_\nu) = \mathcal{H}(\vec{r}')$$

and that

$$\vec{K}_{h_j}\cdot\vec{R}_\nu = 2m\pi \,.$$

Eq. (A3.11) becomes

$$\int \exp\{-i(\vec{k}+\vec{K}_{h_j})\cdot\vec{r}\}\,\mathcal{H}(\vec{r})\; b_{\alpha,\Delta}(\vec{k},\vec{r})\,d\tau = I(\alpha,\Delta)[N\Omega_\alpha^\Delta(\vec{k})]^{-\frac{1}{2}}$$

$$[\Sigma_\nu\, e^{i\vec{k}\cdot\vec{t}_1} \int \exp\{-i(\vec{k}+\vec{K}_{h_j})\cdot\vec{r}'\}\,\mathcal{H}(r')\;\phi_\alpha(\vec{r}'-\vec{t}_1)\,d\tau'. \qquad \text{(A3.12)}$$

$$+\Delta\,\Sigma_\nu e^{i\vec{k}\cdot\vec{t}_2} \int \exp\{-i(\vec{k}+\vec{K}_{h_j})\cdot\vec{r}'\}\,\mathcal{H}(r')\;\phi_\alpha(\vec{r}'-\vec{t}_2)\,d\tau'\} \,.$$

After summing over ν in Eq. (A3.11) and using Eq. (A3.12) to simplify the Hamiltonian matrix element we have

$$H_{ij} = (N\Omega)^{-1} \int \exp\{-i(\vec{k}+\vec{K}_{h_i})\cdot\vec{r}\} \not{\mathcal{H}} \exp\{i(\vec{k}+\vec{K}_{h_j})\cdot\vec{r}\} d\tau$$

$$- I(\alpha,\Delta)^* [\Omega\Omega_\alpha^\Delta(\vec{k})]^{-\frac{1}{2}} \sum_{\alpha,\Delta} \beta(h_i,\alpha,\Delta)^* \int \exp\{-i(\vec{k}+\vec{K}_{h_j})\cdot\vec{r}\} \not{\mathcal{H}}$$

$$[e^{i\vec{k}\cdot\vec{t}_1} \phi_\alpha(\vec{r}-\vec{t}_1) + \Delta\, e^{i\vec{k}\cdot\vec{t}_2} \phi_\alpha(\vec{r}-\vec{t}_2)]\, d\tau \qquad \text{(A3.13)}$$

$$- I(\alpha',\Delta') [\Omega\Omega_{\alpha'}^{\Delta'}(\vec{k})]^{-\frac{1}{2}} \sum_{\alpha',\Delta'} \beta(h_j,\alpha',\Delta') \int \exp\{-i(\vec{k}+\vec{K}_{h_i})\cdot\vec{r}\} \not{\mathcal{H}}$$

$$[e^{i\vec{k}\cdot\vec{t}_1} \phi_{\alpha'}(\vec{r}-\vec{t}_1) + \Delta\, e^{i\vec{k}\cdot\vec{t}_2} \phi_{\alpha'}(\vec{r}-\vec{t}_2)]\, d\tau$$

$$+ \sum_{\alpha,\Delta} \sum_{\alpha',\Delta'} \beta(h_i,\alpha,\Delta)^* \beta(h_j,\alpha',\Delta') \int b^*_{\alpha,\Delta}(\vec{k},\vec{r}) \not{\mathcal{H}} b_{\alpha',\Delta'}(\vec{k},\vec{r})\, d\tau \,.$$

Appendix IV

The integrals of kinetic and potential energies are as follows:

$$\langle G^{s}(\alpha_1, \underset{\sim}{r}-\underset{\sim}{A}) | -\tfrac{1}{2}\nabla^2 | G^{s}(\alpha_2, \underset{\sim}{r}-\underset{\sim}{B}) \rangle = \lambda\Delta\zeta(3-2\lambda\overline{AB}^2) ,$$

$$\langle G^{px}(\alpha_1, \underset{\sim}{r}-\underset{\sim}{A}) | -\tfrac{1}{2}\nabla^2 | G^{s}(\alpha_2, \underset{\sim}{r}-\underset{\sim}{B}) \rangle = \lambda^2\Delta\zeta\overline{AB}_x(5-2\lambda\overline{AB}^2)/\alpha_1 ,$$

$$\langle G^{px}(\alpha_1, \underset{\sim}{r}-\underset{\sim}{A}) | -\tfrac{1}{2}\nabla^2 | G^{px}(\alpha_2, \underset{\sim}{r}-\underset{\sim}{B}) \rangle = \lambda^2\Delta\zeta(\tfrac{5}{2}-7\lambda\overline{AB}_x^2-\lambda\overline{AB}^2+2\lambda^2\overline{AB}^2\overline{AB}_x^2)/\alpha_1\alpha_2 ,$$

$$\langle G^{px}(\alpha_1, \underset{\sim}{r}-\underset{\sim}{A}) | -\tfrac{1}{2}\nabla^2 | G^{py}(\alpha_2, \underset{\sim}{r}-\underset{\sim}{B}) \rangle = \lambda^3\Delta\zeta\overline{AB}_x\overline{AB}_y(2\lambda\overline{AB}^2-7)/\alpha_1\alpha_2 ,$$

$$\langle G^{s}(\alpha_1, \underset{\sim}{r}-\underset{\sim}{A}) | \cos(\underset{\sim}{K}_\nu\cdot\underset{\sim}{r}_C) | G^{s}(\alpha_2, \underset{\sim}{r}-\underset{\sim}{B}) \rangle = \Delta\delta\zeta\cos(\underset{\sim}{K}_\nu\cdot\underset{\sim}{r}_{CD}) ,$$

$$\langle G^{px}(\alpha_1, \underset{\sim}{r}-\underset{\sim}{A}) | \cos(\underset{\sim}{K}_\nu\cdot\underset{\sim}{r}) | G^{s}(\alpha_2, \underset{\sim}{r}-\underset{\sim}{B}) \rangle = \Delta\delta\zeta[(\lambda\overline{AB}_x/\alpha_1)\cos(\underset{\sim}{K}_\nu\cdot\underset{\sim}{r}_{CD}) - (\underset{\sim}{K}_\nu)_x\sin(\underset{\sim}{K}_\nu\cdot\underset{\sim}{r}_{CD})/2(\alpha_1+\alpha_2)] ,$$

$$\langle G^{px}(\alpha_1, \underset{\sim}{r}-\underset{\sim}{A}) | \cos(\underset{\sim}{K}_\nu\cdot\underset{\sim}{r}_C) | G^{px}(\alpha_2, \underset{\sim}{r}-\underset{\sim}{B}) \rangle = \Delta\delta\zeta\{(\lambda/\alpha_1\alpha_2)[\tfrac{1}{2}-\lambda\overline{AB}_x^2 - (\lambda/4\alpha_1\alpha_2)(\underset{\sim}{K}_\nu)_x^2]\cos(\underset{\sim}{K}_\nu\cdot\underset{\sim}{r}_{CD}) + (\lambda/2\alpha_1\alpha_2)\overline{AB}_x(\underset{\sim}{K}_\nu)_x(2u-1)\sin(\underset{\sim}{K}_\nu\cdot\underset{\sim}{r}_{CD})\} ,$$

$$\langle G^{px}(\alpha_1, \underset{\sim}{r}-\underset{\sim}{A}) | \cos(\underset{\sim}{K}_\nu\cdot\underset{\sim}{r}_C) | G^{py}(\alpha_2, \underset{\sim}{r}-\underset{\sim}{B}) \rangle = (\lambda/\alpha_1\alpha_2)\Delta\delta\zeta\{\tfrac{1}{2}[u(\underset{\sim}{K}_\nu)_x\overline{AB}_y - (1-u)(\underset{\sim}{K}_\nu)_y\overline{AB}_x]\sin(\underset{\sim}{K}_\nu\cdot\underset{\sim}{r}_{CD}) - \lambda[\overline{AB}_x\overline{AB}_y+(\underset{\sim}{K}_\nu)_x(\underset{\sim}{K}_\nu)_y/4\alpha_1\alpha_2]\cos(\underset{\sim}{K}_\nu\cdot\underset{\sim}{r}_{CD})\} ,$$

where

$$\lambda = \alpha_1\alpha_2/(\alpha_1+\alpha_2),\ \Lambda = [\pi/(\alpha_1+\alpha_2)]^{3/2},\ \zeta = \exp(-\lambda AB^2),$$

$$\delta = \exp[-K_v^2/4(\alpha_1+\alpha_2)],\ u = \alpha_1/(\alpha_1+\alpha_2),$$

and AB_x refers to the x-component of the line joining the points A and B.